Micromechanics for Foamed Asphalt Stabilized Materials

December 2009

Pengcheng Fu

Micromechanics for Foamed Asphalt Stabilized Materials

By

Pengcheng Fu
B.E. (Tsinghua University, Beijing) 2001
M.E. (Tsinghua University, Beijing) 2004

DISSERTATION

Submitted in partial satisfaction of the requirements for the degree of

DOCTOR OF PHILOSOPHY

in

Civil and Environmental Engineering

in the
OFFICE OF GRADUATE STUDIES
of the
UNIVERSITY OF CALIFORNIA
DAVIS

Approved:

_____
Chair: John T. Harvey

_____
Jason T. DeJong

_____
Carl L. Monismith

_____
Bruce L. Kutter

Committee in Charge

2009

Abstract

Micromechanics for Foamed Asphalt Stabilized Materials

by

Pengcheng Fu

Doctor of Philosophy in Civil and Environmental Engineering

University of California, Davis

Professor John T. Harvey, Chair

Full depth reclamation (FDR) of damaged flexible pavements with foamed asphalt stabilization is

a promising pavement rehabilitation strategy. It offers a rapid construction process, potentially

low life cycle cost, and minimal negative impact on the environment. However, as it is a

relatively new technology, it carries a significant risk of providing poor results because of

insufficient engineering and research experience. Many important characteristics of foamed

asphalt treated materials were unknown to practitioners and researchers prior to this study.

Owing to the intrinsic complexities in behavior of this material, conventional research approaches

involving large factorial laboratory experiments intended to indentify all possible interactions

through statistical analyses are not efficient and the conclusions from such studies are often not

reliable.

This doctoral study employed a micromechanical research framework to investigate the behavior of foamed asphalt stabilized materials used in FDR. A Fracture Face Image Analysis (FFIA) technique was developed to quantify the asphalt mastic distribution in foamed asphalt mixes, which is one of the most important microstructural characteristics of this material. FFIA provides opportunities for understanding how mix variables affect material microstructures and in turn how microstructures influence material behavior. This thesis documents a number of important aspects of foamed asphalt mix behavior, including strength, stiffness, curing and mixing.

The study of strength behavior examined the roles of the individual phases in foamed asphalt mixes in determining strength behavior. The effects of granular material gradations, asphalt binder viscosity, compaction effort and water conditioning were investigated separately, and the microstructural mechanisms of these design and construction variables' effects were identified.

The study of stiffness focused on comparing stiffnesses of soaked and unsoaked foamed asphalt mixes measured with a number of different laboratory test methods. The strong dependency of stiffness test results on the applied stress states was quantified. The conclusions highlighted the importance of simulating realistic field stress states in laboratory tests for material evaluation.

The curing mechanisms of foamed asphalt mixes were investigated with several types of laboratory tests as well as direct fracture face inspection. It was found that the development of bonding strength provided by the asphalt mastic is largely dependent on evaporation of

mixing/compaction water.   Important recommendations to engineering practice include allowing

the initial water to evaporate, ensuring adequate drainage, and using active fillers to accelerate

early strength development.   Standard curing procedures for material evaluation were proposed.

This research also, for the first time, discovered that the mixing moisture content in a loose moist

granular material determines the agglomeration states of aggregate particles, and thereby affects

the foamed asphalt distribution patterns in the mix.

Additionally, recommendations are proposed to improve design and construction of FDR-foamed

asphalt projects based on these findings.

Acknowledgements

First, I have to give my deepest thank you to my advisor, Professor John Harvey. It has been my greatest fortune to work with him for almost five years. I was able to constantly learn from him and get his unwavering support. Not only does he offer rigorous training, he also served as a great model for my career development and personal life.

I want to express my sincere appreciation to other members in my dissertation committee, Professor Carl Monismith, Professor Bruce Kutter and Professor Jason DeJong, who have guided and supported my dissertation work, as well as my academic exploration. Additionally, I am also grateful to many other faculty members in the UC Davis Civil and Environmental Engineering Department: Professor Yannis Dafalias, Professor Ross Boulanger, Professor Michael Zhang, Professor Boris Jeremic, Professor John Bolander, and Professor Yueyue Fan, for their guidance and support.

Dr. David Jones and Dr. Bruce Steven deserve my special acknowledgement. Without their help, completing this comprehensive study would have been impossible. The support from Mr. You-Chen Chao, Mr. Syed Bukhari and Mr. Felipe Halles was crucial to the success of this thesis work.

I sincerely thank all my friends and coworkers at the University of California Pavement Research Center. Dr. Bor-Wen Tsai, Dr. Rongzong Wu, Dr. Qing Lu, Dr. Jeremy Lea and Dr. Eung-Jin Jeon have been very nice to me and to my work by providing intellectual and physical help. This thesis work was also made possible by the generous help from the engineers, administrators

and technicians in our laboratory, including Irwin Guada, Mark Troxler, David Rapkin, Maggie Lazar, Oscill Maloney, David Eng, Hector Matha and others.

In closing, I want to express my deep appreciation to my beloved wife, Wei Shen and my little boy, Renyan (Ryan), to whom this dissertation is dedicated.   I owe many thanks to my parents, Wei's family and my sister's family, who have selflessly supported us for so many years.

Pengcheng Fu
Davis, California
April, 2009

Table of Contents

List of Figures

List of Tables

Abbreviations

Caltrans	California Department of Transportation
CMC	Compact Moisture Content
CT	Computed Tomography
ER	Expansion Ratio
FA	Foamed Asphalt
FDR	Full Depth Reclamation or Full Depth Recycling
FFAC	Fracture Face Asphalt Coverage
FFIA	Fracture Face Image Analysis
FFRC	Free-Free Resonant Column
FWD	Falling Weight Deflectometer
HMA	Hot Mix Asphalt
IDT RM	Indirect Tensile Resilient Modulus
ITS	Indirect Tensile Strength
MDD	Multi-Depth Deflectometer
LVDT	Linear Variable Differential Transformer
MMC	Mixing Moisture Content
OMC	Optimum Moisture Content (for compaction)
OMMC	Optimum Mixing Moisture Content
PAP	Pulverized Asphalt Pavement
PG	Performance Grade
RAP	Recycled Asphalt Pavement
RMR	Resilient Modulus Retained
SR	(California) State Route
TSR	Tensile Strength Retained
Tx PD	Triaxial Permanent Deformation
Tx RM	Triaxial Resilient Modulus
UCPRC	The University of California Pavement Research Center
UCS	Unconfined Compressive Strength

Chapter 1 Introduction

1.1   Full Depth Reclamation of Pavement with Foamed Asphalt Stabilization

1.1.1 Pavement rehabilitation and full depth reclamation

Pavement rehabilitation is an important mission of highway agencies, and the choice of pavement rehabilitation techniques and procedures has great financial and environmental impacts on our society.

The asphalt concrete (also known as hot mix asphalt [HMA]) layers usually provide the major portion of the structural capacity of a flexible pavement in the United States, and they inevitably deteriorate under the combined effects of traffic and the environment. The service life of a properly designed and constructed flexible pavement ranges from 10 to 30 years, depending on the materials, structure, construction quality, traffic volume, ambient environment and other factors. Once pavement preservation/maintenance is no longer effective, highway agencies can either perform rehabilitation to extend its service life, or rebuild it when the pavement shows advanced signs of distresses.

Pavement rehabilitation is very costly. According to the California Department of Transportation's (Caltrans) *California State of the Pavement Report, 2007* (Caltrans, 2008), Caltrans spent $462M to rehabilitate 417 lane-miles (or 671 lane-km) of state highways with an average cost of $1.1M per lane-mile (or $0.68M per lane-km) in the fiscal year of 2006/2007. These lanes compose less than one percent of the total length (49,000 lane-miles or 79,000 lane-km) of the state highway system maintained by Caltrans. Apart from the direct financial considerations, road rehabilitation also potentially impacts our society in a number of undesired ways, mainly associated with construction material extraction and transport, as well as highway user delays caused by construction.

In California, directly applying new layers of HMA as overlays on cracked pavements has been the primary rehabilitation strategy for many decades. The new asphalt layer usually fails by reflection of the cracks in the underlying asphalt layers up through the overlay in a relatively short period of time. After multiple overlays have been applied, they will have to be removed to meet the highway profile requirements. Although recycled asphalt pavement (RAP) can be used to partially replace virgin aggregate in manufacturing HMA, considerable effort is needed for transport from the milling sites to HMA plants and to new construction sites, and to process these materials are often associated with undesired environmental impacts.

Full depth reclamation (or recycling) (FDR) of cracked flexible pavement is a promising rehabilitation strategy. The process includes pulverization of the existing asphalt pavement layers together with the upper portion of the underlying aggregate base material, treatment with

stabilization agents (e.g. emulsified asphalt, foamed asphalt, cement, lime, or combinations of these) to improve its engineering properties, followed by compaction to produce a new stabilized base. This process and typical equipment used in California are shown in Figure 1.1. In California the recycling depth is usually about 20 cm, which typically includes 5 cm in the granular base layer below the existing HMA layers. The pulverized material for foamed asphalt treatment is termed "pulverized asphalt pavement" or PAP in this thesis. The FDR procedure is usually performed by a recycling train consisting of a recycler, trucks supplying hot asphalt binder and water, a grader and multiple types of compactors. Such a train proceeds at a speed of several meters per minute, and produces the recycled, stabilized and compacted pavement base material in a continuous fashion. The compacted surface can be opened to traffic (at a controlled low speed) in a few hours. A relatively thin HMA wearing surface is usually applied several days after FDR.

1.1.2 Asphalt foaming

Foamed asphalt is one of the stabilization agents that can be used in FDR. The FDR procedure using foamed asphalt as the primary stabilization agent is termed "FDR-foamed asphalt" in this work, although it is a common practice to add portland cement in conjunction with foamed asphalt to improve certain properties, such as early strength.

Asphalt foaming was originally invented by Dr. Ladis Csanyi at the Engineering Experiment Station, Iowa State University in the 1950s. Mobil Australia acquired Csanyi's patent for this process in the late 1960s and made certain modifications (Jenkins, 2000). The patent expired in

the 1990s, which was one of the reasons why the use of this procedure has accelerated since then.
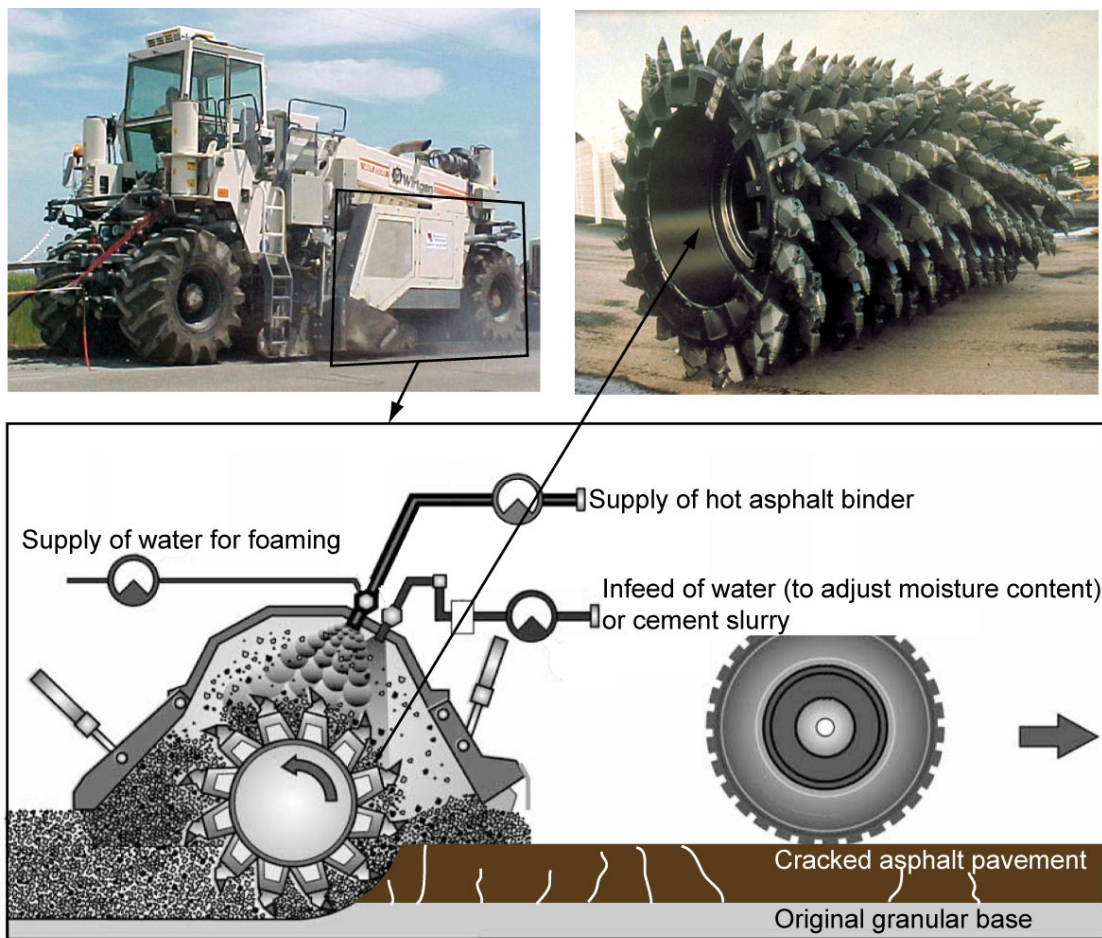
Figure 1.1   FDR-foamed asphalt process and equipment
Note: The upper two photos were provided by Mr. Joseph Peterson (Caltrans) and the lower
figure was redrawn after Wirtgen GmbH (2004)

The basic idea of asphalt foaming is to inject a small quantity of cold water (usually with a mass

ratio of 1% to 5% to the asphalt binder) together with compressed air into hot asphalt (140°C to

170°C) in a specially designed chamber.   The water experiences a sudden temperature increase

and becomes steam.   When the mixture of asphalt cement, steam and compressed air is injected

into the ambient air, asphalt is temporarily expanded into numerous bubbles with greatly reduced

viscosity and increased surface area per unit mass. When being mixed with aggregates at ambient temperature, the asphalt bubbles can be dispersed into the mix fairly uniformly. On the other hand, liquid asphalt binder at high temperature without foaming would immediately become globules when it contact cold aggregates and thus can not be thoroughly dispersed. An analogy to this cold mixing process is to beat an egg white into foam, which can be mixed with dry flour (Raffaelli, 2004). The mixture of foamed asphalt and the treated aggregates (both loose and compacted) is termed a "*foamed asphalt mix*" or a "*foamed asphalt material*" in this thesis, although the asphalt does not exist in a "foamed" state in the mixes.

For a given asphalt binder, the two primary foaming parameters that can be readily adjusted by typical equipment are the binder temperature and the foaming water ratio (to the mass of asphalt). The quality of the yielded asphalt foam is usually quantified by the expansion ratio (ER) and the half-life ($\tau_{1/2}$) as follows (Asphalt Academy, 2002; Wirtgen GmbH, 2004):

- The expansion ratio is calculated as the ratio of the maximum volume of foam relative to the original volume of asphalt binder.
- The half-life is calculated as the time taken in seconds for the foam to collapse to half of its maximum volume.

Intuitively, foam with a higher expansion ratio has a larger surface area per unit mass and lower viscosity due to the thinner asphalt film. Consequently, it is easier for this type of foam to coat more and finer aggregates. The half-life quantifies the stability of the foam. More stable foam

has more effective time to interact with the aggregate, resulting in better coating of the particles. It should be noted this study defined the half-life of an asphalt foam as the time in seconds that the foam takes to dissipate to half of its maximum volume from the time when the foaming nozzle shuts off, not from the moment when it reaches its maximum volume. The reasons for the adoption of this definition were explained in section of 6.4.5 of Jones et al. (2008)

1.1.3 Benefits of FDR-foamed asphalt

FDR, especially FDR-foamed asphalt provides several remarkable benefits in comparison with other alternative flexible pavement rehabilitation strategies.

Compared to HMA overlays, FDR eliminates the potential of reflective cracking by pulverizing the cracked existing HMA layers. Through recycling and reusing in situ granular material, FDR minimizes the needs for extracting and transporting virgin aggregates, as well as the associated environmental impact. The FDR operation only occupies one lane which can be re-opened to traffic in a few hours, and consequently the traffic delay caused by construction is also minimized.

Emulsified asphalt (or asphalt emulsion) is another stabilization agent that can be used in FDR. It has been reported (Jenkins et al., 2004) that foamed asphalt treated and asphalt emulsion treated mixes have comparable strength, stiffness, and water susceptibility. However, the foamed asphalt strategy is often preferred because the asphalt emulsion treatment introduces extra moisture (the continuous phase in the emulsion) into the mix and requires considerably longer curing periods before the road can be opened to traffic. Ramanujam and Jones (2008) reported a direct

comparison between foamed asphalt (with lime) treatment and emulsion treatment (with portland cement) in which the foamed asphalt section showed significantly better performance in terms of handling early traffic and also superior rain resistance before applying the wearing course.

Compared to recycled road base materials treated with portland cement or other cementitious agents, foamed asphalt mixes (may include cement as well) have the additional benefit of improved flexibility or reduced brittleness.

In summary, FDR-foamed asphalt provides a potentially fast, cost-effective and environmentally friendly flexible pavement rehabilitation strategy.

1.2   Challenges to Research on Foamed Asphalt Treated Materials

Since the invention of asphalt foaming in the 1950s, it has been used worldwide to stabilize a great variety of granular materials, from sands, to crushed rocks, and to PAPs. Related research was also actively carried out as reported in the literature. Thorough literature reviews on general aspects of foamed asphalt treated materials concerned in engineering applications were prepared by Jenkins (2000) and Saleh and Herrington (2003). Each following chapter in this thesis focuses on a specific aspect of foamed asphalt mix properties, and a detailed literature review on each topic is presented in each respective chapter. This section does not intend to repeat the comprehensive literature reviews cited above; instead, some observations are made on the literature and a number of additional general issues were identified to guide the scope of this thesis work.

Intrinsic Complexity in Material Behavior

Compared to HMA, foamed asphalt mixes involve more variables, have a less controllable mixing procedure, and exhibit more complex behavior. Aggregates and asphalt cement are the two primary constituents of HMA, while water and, often, active fillers are the additional ingredients of foamed asphalt mixes. The mixing procedure, especially for in situ production, is much less controllable than that of HMA. HMA is usually produced in plants where mixing temperature is accurately controlled and all constituents are allowed to interact for a sufficiently long duration so the homogeneity can almost always be assured. In an FDR operation, the time window in which foamed asphalt can interact with aggregates is usually as short as a few seconds. Thorough mixing is not guaranteed and variability in PAP materials is usually significant even for the same construction section. A number of factors contribute to the variability and complexity

- The existing in situ materials to be reclaimed are usually extremely variable due to the long and complex maintenance history of the roads (e.g. in California);
- Material temperature and moisture content constantly change during the construction; and
- The experience and preference of the recycling machine operators often plays an important role in determining material quality.

Because asphalt only coats a fraction (small or large, depending on many material, environmental, equipment and procedural factors) of fine aggregate particles in foamed asphalt mixes, there exists a mineral filler phase in addition to the aggregate skeleton and the asphalt mastic phase (defined in

Section 3.1), whereas HMA mixes primarily consist of the two latter phases. The mineral filler phase adds more complexities to behavior of foamed asphalt mixes, as will be elaborated in Chapter 3 of this thesis.

"Case Study" Nature of Most Previous Investigations

Most of the studies reported in the literature were associated with certain specific road rehabilitation projects, and are more or less of a "case study" nature. Typically, each of these studies evaluated a series of alternative scenarios of material selection, mix design, or construction procedures for a specific project with laboratory or field testing (or both), which were used as the basis for recommendations for engineering practice. The scopes of these studies were similar to that of an expanded exploratory sensitivity analysis for a project design. Aggregate materials to be treated with foamed asphalt differ remarkably from one place to another in terms of mineralogical characteristics and grading, and behavior of foamed asphalt mixes is greatly dependent on properties of parent materials. Consequently, conclusions from such studies cannot be readily generalized because of the ad hoc structure of the combined results in the literature. This is one of the reasons why comprehensive literature reviews (Jenkins, 2000; Saleh & Herrington, 2003) showed contradictory findings from different researchers regarding almost every aspect of foamed asphalt mix properties .

Some relatively large scale and comprehensive studies were undertaken by South African researchers. One of the studies was initiated and sponsored by the Gauteng Department of

Transport and Public works (Gautrans), South Africa in 1999 and conducted by the Council for

Scientific and Industrial Research (CISR). This study included Heavy Vehicle Simulator (HVS)

testing on FDR-foamed asphalt and FDR-asphalt emulsion sections, each 100 m long (Theyse &

Mancotywa, 2003; Long & Theyse, 2002a) on Road P243/1, and a comprehensive laboratory study

(Long & Theyse, 2002b).

Mix design and structural design frameworks and procedures were established based on this work,

and performance models calibrated against the test data generated in this study, as published in the

Interim Technical Guideline: the Design and Use of Foamed Bitumen Treated Materials or the TG2

(Asphalt Academy, 2002). A similar follow-up study was performed on another road, the N7

(TR11/1) consisting of HVS testing (Theyse, 2004; Long & Brink, 2004) and a laboratory study

(Long & Ventura 2004). The original plan for the N7 study was to validate the conclusions from

the P243/1 study and extend the applicability of the models to a wider spectrum of materials.

However, it was found that some fundamental findings from the P243/1 study were contradicted by

the new results. Rather than confirming and refining the interim design guide, the N7 study raised

more critical questions and identified the need for further investigation.

"Borrowed" Test and Design Methods

Another problem in previous foamed asphalt mix related research is that the design philosophies,

test methods and evaluation criteria for HMA and aggregate base materials have been applied to

foamed asphalt mixes without sufficient validation. Foamed asphalt mixes are mixtures of

aggregates and asphalt with partial asphalt coating, whereas HMA is a mixture with nearly complete asphalt coating. It is intuitively reasonable to assume that the behavior of foamed asphalt mixes is "somewhere between" that of unbound aggregate materials and HMA. However such an assumption could lead to sub-optimum engineering practice since foamed asphalt mixes have some unique characteristics warranting special considerations. The role of water conditioning in material testing and result interpretation is a particularly important example. In most mix and structural design procedures for HMA, mix variables are optimized based on test results for unsoaked mixes. As a safeguard measure, properties of soaked materials are checked against certain minimum requirements. The rationale behind is that HMA mostly works under a largely dry state and complete soaking only occasionally takes place, such as in the event of prolonged raining. On the other hand, classical soil mechanics states that noncohesive soils behave similarly when they are completely dry or completely saturated (in a practical sense as no soil can be completely dry or completely saturated). Consequently, many laboratory tests can be performed either on dry or soaked sands and the results are interpreted as being equal. As will be shown in Section 3.6.2 of this thesis, the situation for foamed asphalt mixes is remarkably different from both of these materials and test results for soaked materials are recommended for design purposes.

In summary, the complex behaviors of foamed asphalt mixes are not well understood, and most previous studies are of an ad hoc nature because they were case studies. The existing design and evaluation methods do not adequately consider the unique characteristics of foamed asphalt mixes.

A credible general framework for analyzing and designing foamed asphalt mixes has not been established.

1.3 Opportunities Provided by Micromechanics

As indicated by Li and Wang (2008), the term "micromechanics" has "multidisciplinary interpretations, and it has been used with different meanings in different contexts." In the context of this thesis work, micromechanics is defined as the analysis and prediction of the properties of multi-phase composite materials at the individual phase level. It is applicable to foamed asphalt mixes due to their multi-phase nature. The application of micromechanical principles and methods offers a number of opportunities to help resolve the aforementioned challenges to research on foamed asphalt materials.

Figure 1.2 shows how a conventional laboratory material study (such as on foamed asphalt mixes) relates mix variables (such as PAP gradation, asphalt type, asphalt content, mixing temperature, etc.) to mix properties (such as strength, stiffness, and their temperature/moisture sensitivity). The main objective of a typical laboratory material study is to investigate how these mix variables affect the mix properties of interest. A common approach is to produce a series of mixes by varying each variable to certain levels, and subsequently observing how mix properties (results of laboratory testing) change accordingly. The challenges to this approach when studying foamed asphalt mixes include the large number of mix variables to be considered, the large number of

mix properties interested, their inevitable and great variability, and potential interactions between the mix variables. To confidently detect all the relationships, the experiment factorial often needs to be unacceptably large. Consequently establishing definitive connections between the mix variables and mix properties for foamed asphalt mixes is extremely difficult in this framework.
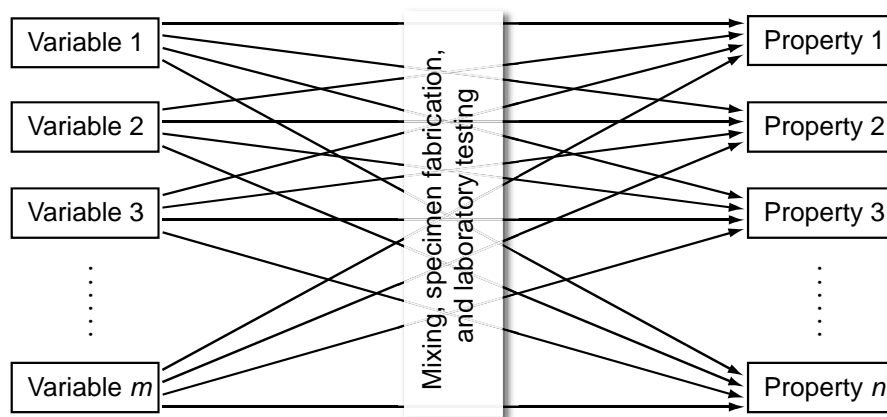
Figure 1.2   A conventional framework for material research

If such a study is performed in the framework of micromechanics, the mix preparation, specimen fabrication, and laboratory testing methods, as well as the experiment factorial design remain largely unchanged. However, the microstructure of each mix is characterized, and serves as the key to interpret test results in terms of mechanical phenomena, rather than relying completely on statistical inference to evaluate hypotheses regarding the effects of the variables on the mechanical properties. A Fracture Face Image Analysis (FFIA) technique was developed for this study to characterize the microstructure of foamed asphalt mixes. Instead of directly relating the change of material properties to the varying mix variables, micromechanics

investigates how the microstructure is influenced by each mix variable and in turn how the microstructure affects material properties. To appreciate the benefits of the micromechanical research framework in terms of simplifying and clarifying laboratory test result analysis, one can compare the number of arrows ($m \times n$ for a conventional study vs. $m+n$ for the corresponding micromechanical study) in Figure 1.2 and Figure 1.3. Each arrow represents a potential relation that needs to be considered and evaluated in the study.
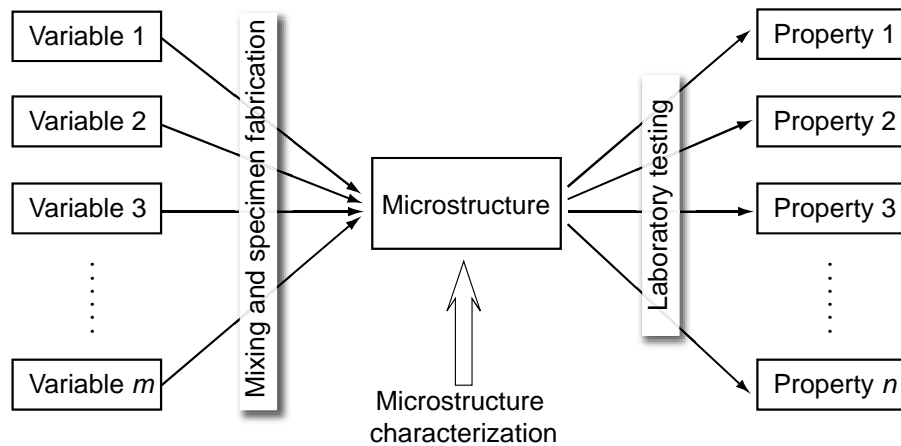
Figure 1.3   The micromechanical framework for material research

1.4   Key Objectives of This Study

The study documented in this thesis employed micromechanics to understand the behavior of foamed asphalt mixes using micromechanical principles in conjunction with conventional laboratory testing. The following objectives were identified in the beginning of the study.

- To identify the key microstructural characteristics of foamed asphalt mixes.

- To develop a simple yet theoretically sound technique for quantifying the microstructure of foamed asphalt mixes.

- To investigate how the main mix variables affect the microstructure of foamed asphalt mixes.

- To investigate how microstructure determines strength behavior of foamed asphalt mixes.

- To investigate how microstructure determines stiffness behavior of foamed asphalt mixes.

- To investigate the curing (or strength development) mechanism of foamed asphalt mixes.

- To investigate the mechanism by which mixing moisture content affects microstructure of foamed asphalt mixes.

- To provide recommendations to engineering practice based on the findings of this study.

1.5   FDR-Foamed Asphalt Research at the UCPRC

The laboratory tests recorded in this thesis were performed as parts of a comprehensive research program on FDR-foamed asphalt undertaken at the University of California Pavement Research Center (UCPRC, Davis and Berkeley) for Caltrans.   This research project is referred to as "the UCPRC study" hereafter in this thesis.   The UCPRC study included extensive laboratory testing and field monitoring.   The laboratory testing program aimed to identify the roles of constituents of foamed asphalt mixes and to select suitable laboratory practices and appropriate test methods, for both advanced research and routine project-level tests.   Field monitoring of FDR-foamed asphalt projects built by Caltrans was performed with the objective of relating laboratory tested

material properties to field tested properties and field performance. That research project was recorded in detail in the final report (Jones et al., 2008).

This thesis work and the UCPRC research project had different goals and scopes although the laboratory test results on which they relied overlap considerably. The primary goal of the UCPRC study was to provide recommendations on mix design methods, structural design procedures and construction guidelines to Caltrans. It therefore had to consider a number of issues specially pertaining to California, especially Caltrans engineering practice. On the other hand, this thesis mainly records the intellectual contributions made by the author during his study with respect to understanding foamed asphalt stabilized material behavior using micromechanical principles. It aims to develop new research methods and to study general material behavior, which will potentially benefit other more specific studies on foamed asphalt mixes as well as studies of other similar materials.

1.6 Organization of the Thesis

Chapter 2 introduces the materials used and the laboratory procedures and test methods used in this study.

Chapter 3 presents a new Fracture Face Image Analysis technique developed for characterizing the asphalt mastic distribution features in foamed asphalt mixes, which is a fundamental microstructural characteristic of this material. The development of FFIA was accompanied by

an investigation of the strength behavior of foamed asphalt mixes.

Chapter 4 investigates stiffness behavior of foamed asphalt mixes. A number of different laboratory test methods were employed. The focus was to study how each constituent phase of foamed asphalt mixes react to different stress states, and to identify laboratory test methods that appropriately represent field stress states experienced by foamed asphalt treated road base.

Chapter 5 studies the curing mechanism of foamed asphalt mixes by a variety of laboratory test methods as well as direct microstructure observation.

Chapter 6 investigates how mixing moisture content affects foamed asphalt distribution in the mix, and in turn how mix properties are influenced. Direct microstructure observations on loose moist aggregate and on specimen fracture faces were performed. The observed phenomena were explained based on thermodynamic principles.

Chapter 7 summarized the findings and makes recommendations to engineering practice.

Chapter 2 Materials, Laboratory Procedures and Test Methods

2.1 Laboratory Testing of the UCPRC Study

Each of Chapters 3 to 6 focuses on a specific attribute of foamed asphalt stabilized materials. The laboratory test data that the analyses rely on were mostly obtained from the laboratory work of the UPPRC study. The UCPRC laboratory study lasted three years and was divided into four major phases. The material properties concerned, variables investigated in these phases and their involvement in this dissertation are summarized in Table 2.1. Detailed descriptions of the UCPRC laboratory study can be found in the final report (Jones et al., 2008).

This chapter gives a general description of the materials, specimen fabrication procedures and test methods being used in this thesis. Since the test data from Phase II of the UCPRC laboratory study are extensively used by both Chapter 3 and Chapter 4 of this thesis, the experiment factorial design is given in Chapter 2. Data from Phase I of the UCPRC study are only occasionally used in Chapter 3 and Chapter 5, and the experiment design is also presented in Chapter 2. On the other hand, the investigations documented in Chapter 5 and Chapter 6 were standalone tasks

(Chapter 5 was a special task and Chapter 6 was one of the tasks in UCPRC study Phase IV), and

the laboratory testing has little interaction with other chapters in this thesis.   Consequently, the

experiment factorial designs are presented in Chapters 5 and 6 respectively.

Table 2.1   Phases of the UCPRC laboratory study

Phases	Objective, or properties concerned	Variables tested	Involvement in dissertation[1]
Phase I	Preliminary and preparatory work, team training	- RAP gradation - Asphalt content - Water conditioning	Ch. 3
Phase II	- Strength behavior - Stiffness behavior - Comparing different laboratory test methods	- PAP source-gradation - Asphalt PG grade - Compaction effort - Water conditioning - Test methods	Ch. 3, Ch. 4
Special Task IIA	Effects of mixing moisture content	- PAP source-gradation - Mixing moisture content - Test methods - Water conditioning	Ch. 6
Phase III	Strength behavior, detailed investigation of asphalt binders and PAP gradations	- PAP source-gradation - Asphalt source-grade - Water conditioning	No involvement
Phase IV	Curing and active filler	- PAP gradation - Asphalt content - Active filler type - Active filler content - Curing conditions - Test methods	Ch. 5

Note: [1] Chapter numbers are for this thesis, not the UCPRC research report.

2.2 Granular Materials to be Treated with Foamed Asphalt

Two types of granular materials were used in the UCPRC research project at different phases. A *RAP* (recycled asphalt pavement) material consisting of milled HMA with certain modifications was used in Phase I (see Table 2.1) to develop laboratory procedures for the later phases as well as for personnel training purposes. In the later phases, two *PAP* materials from California in situ pavement recycling projects were employed, which were believed to better represent materials for foamed asphalt stabilization in California than the RAP. Test results for the PAP materials were used in Chapters 3 to 6, whereas the laboratory test results for the RAP material was only concerned in Section 3.5.1and Section 5.6.

The RAP material was sourced from a hot mix asphalt (HMA) plant owned by Granite Construction Inc. in Sacramento, California. This milled RAP material was plant processed to provide a controlled gradation, and is used in some HMA products as a substitute for more expensive virgin aggregates. The gradation as supplied was somewhat fine (Figure 2.1, RAP-1), as is typical of HMA that has been milled with a diamond encrusted rotating drum rather than pulverized like PAP (Figure 1.1) and was modified with crushed aggregate (100 percent passing a 19 mm sieve) sourced from the GraniteRock A.R. Wilson Quarry near Aromas, California, to obtain a coarser gradation (Figure 2.1, RAP-3). A finer gradation (Figure 2.1, RAP-2) was also produced by modifying RAP-3 with additional baghouse dust (chemically inert, nonplastic, 100 percent passing a 0.075 mm sieve), also obtained from the A.R. Wilson Quarry. RAP-1, -2 and -3 have 9.6 percent, 9.3 percent, and 5.3 percent passing a 0.075 mm sieve (#200) by mass

respectively.

The PAP materials were collected from two different California recycling/ pulverization projects, one on State Route 33 (SR33, Ventura County) and the other on SR88 (Amador Country). The materials are referred to as PAP-33 and PAP-88 respectively in this thesis. The materials were collected during pre-pulverization runs (approximately 200 mm deep) with the recyclers prior to the injection of foamed asphalt. Both materials contained approximately 75% RAP and about 25% granular base and other materials in the original pavement layers by mass, which is typical of FDR projects in California.
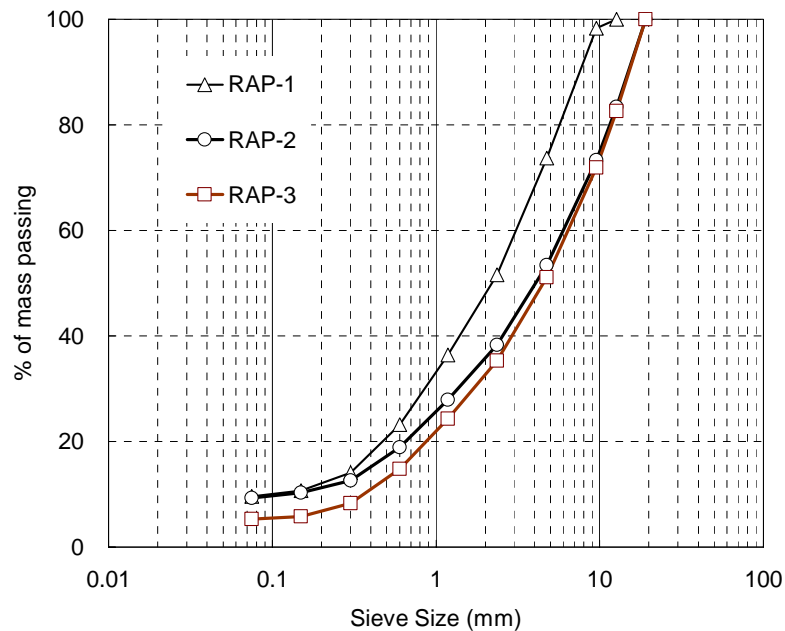
Figure 2.1   Gradation of the original RAP material and the modified gradations

Three gradations (denoted as gradations A, B and C) as shown in Figure 2.2 were constituted from each PAP source by sieving the PAP into four fractions with three sieve sizes (19 mm, 9.5

mm, and 4.75 mm) and recombining them. Plant pulverized RAP, virgin aggregate, and baghouse dust (same as the baghouse dust added to the RAP material) were added to adjust the gradations as elaborated below. PAP particles retained on the 19 mm (3/4 inch) sieve were discarded. This sieving-batching procedure ensured that consistent materials were used throughout the study.

- The PAP-33-A (or simply 33-A) and 88-A materials represented the average gradations as pulverized on the two roads, containing 8 and 10 percent fines passing a 0.075 mm (#200) sieve by mass, respectively.

- The 33-B and 88-B materials represented coarser gradations with 6.5 percent fines passing the 0.075 mm (#200) sieve.

- The 33-C and 88-C materials were produced by adding baghouse dust to 33-B and 88-B to produce materials with 20 percent passing a 0.075 mm (#200) sieve, thereby allowing assessment of the effects of higher fines contents that occur in typical practice on performance.

In this thesis, "mineral filler" refers to the portion of a granular material that can pass a 0.075 mm sieve. The percentage by mass of mineral filler in a granular material is termed the fines content of this granular material.
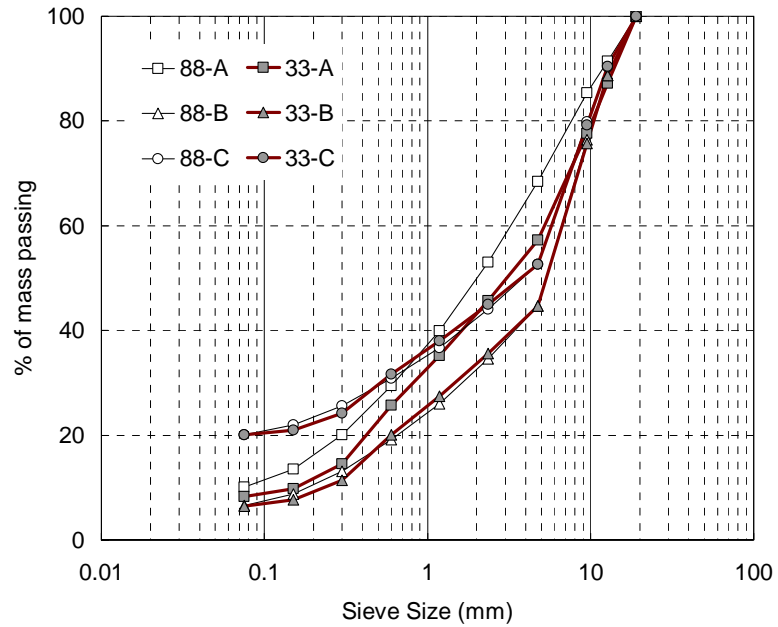
Figure 2.2   Gradation of the original PAP material and the modified gradations

(a) Particles passing 19 mm sieve,
retained on 9.5mm sieve

(b) Particles passing 9.5 mm sieve,
retained on 4.75 mm sieve
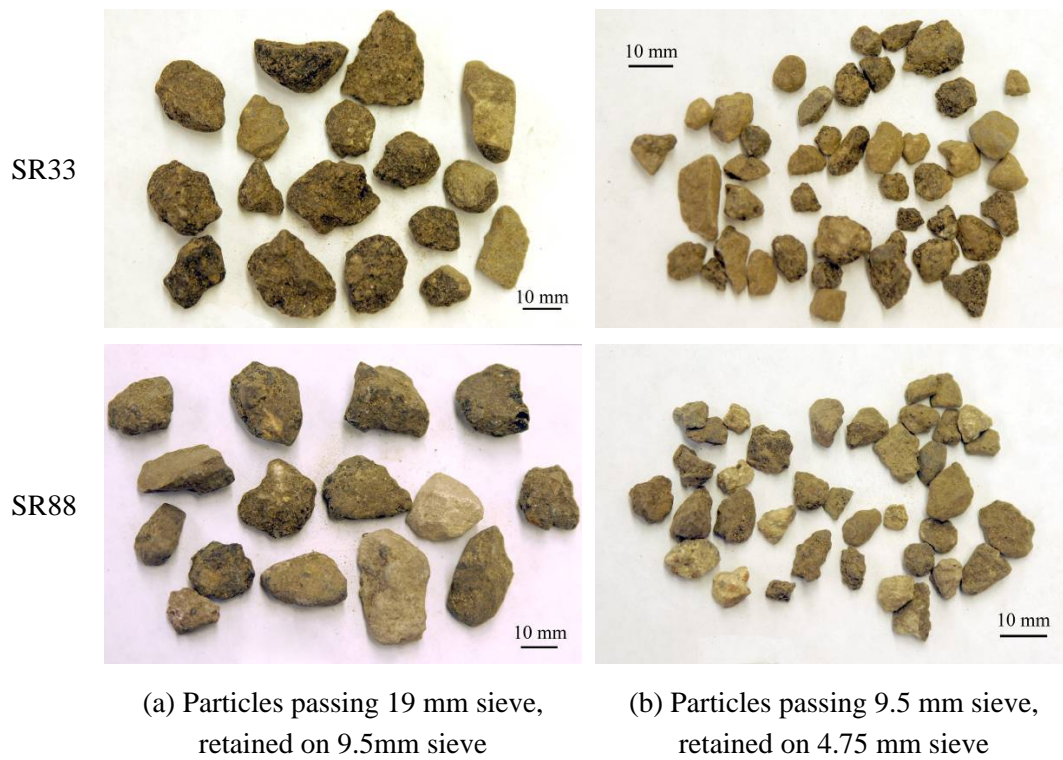
Figure 2.3   Visual properties of aggregate particles from SR33 and SR88

Quantitative morphological analysis was not carried out on the PAP materials collected. A visual inspection showed that the aggregate angularities of the PAPs from SR33 and SR88 were similar as illustrated in Figure 2.3. However, more aggregate particles from SR33 were coated with an oxidized asphalt binder film, compared to those from SR88. Coated aggregate particles had a rougher surface texture than those of the uncoated particles (Figure 2.4), and therefore aggregate particles of PAP-33 have perceivably rougher surface texture.

SR33   SR88

Figure 2.4   Surface texture of typical PAP particles

Some basic properties of the PAP materials are shown in Table 2.2.

2.3   Asphalt Binder

California used the Aged Residue (AR) system from the 1970s until Caltrans adopted the Superpave Performance Grade (PG) system for specifying asphalt binders used in pavement in January 2006. During Phase I of the UCPRC study, when the AR system was still being used,

one AR-4000 asphalt binder (approximately equivalent to PG64-16) was obtained from a local refinery and used for the assessment of specimen preparation procedures and test methods. To foam the binder, it was heated to 150°C and 2.0 percent foaming water was added. The expansion ratio of the foam was 12 and the half-life was 10 seconds.

Table 2.2   Basic properties of the PAP materials.

Parameter	Material					
	33-A	33-B	33-C	88-A	88-B	88-C
Plasticity Index	Nonplastic					
Optimum moisture content[1] (%)	5.4	5.0	5.5	7.0	6.7	6.0
Max. Dry Density[1] (kg/m^3)	2,170	2,190	2,170	2,080	2,110	2,140
pH[2] (AASHTO T289)	8.2	NM[3]	NM	6.7	NM	NM

[1] Determined with the Modified Proctor method (AASHTO T180).

[2] Determined with AASHTO T289.

[3] NM, not measured.

For all the later phases of the UCPRC study, a number of PG graded asphalt binders from different sources and with different grades were used. Only two of them: a PG64-16 and a PG64-10 from the same refinery as the AR-4000 binder are relevant to this thesis work. The foaming characteristics are practically the same as each other. The PG64-16 binder has a Brookfield viscosity of 0.300 Pa·s at 135°C, and the PG64-10 binder has a Brookfield viscosity of 0.384 Pa·s at 135°C.

2.4   Active Fillers

Active fillers were not used in the studies documented in Chapters 3, 4 and 6, since the main focus of these studies was the characteristics of the asphalt mastic phase and its contribution to properties of foamed asphalt stabilized materials.   If active fillers, such as portland cement are present in the mixes, it is very difficult to distinguish the effects of foamed asphalt from those of portland cement with most conventional laboratory testing methods.   The effects of portland cement, especially on earlier performance of foamed asphalt stabilized materials are discussed in Chapter 5.   Other active filler types, including hydrated lime, cement kiln dust and fly ash were investigated in the UCPRC study, but not documented in this thesis.

2.5   Mix Preparation

A Wirtgen WLB 10 laboratory foaming unit and a custom-built twin shaft pugmill mixer were used throughout the study for asphalt foaming and material mixing in the laboratory, respectively. During mix production, dry constituents including PAP/RAP, bag house dust for gradation adjustment and active fillers, if applicable, were first mixed in the mixer, and then the prescribed amount of water was added.   Foamed asphalt was then injected directly onto the material as it was being agitated in the mixer.   Control mixes were mixed without adding foamed asphalt. Precise control of the mixing temperature was found impractical.   Instead, the aggregate temperature was controlled within the range of between 25°C and 30°C at the moment foamed

asphalt was being injected, by preheating the materials and equipment to a moderately high temperature, except that no temperature control measure was taken during Phase I of the UCPRC study.   The mixer has a capacity of 20 kg material for each batch.

2.6   Indirect Tensile Strength Test (100 mm)

Specimens with a nominal diameter of 100 mm (4 in.) and a nominal height of 63.5 mm (2.5 in) were compacted following the Marshall compaction method (Asphalt Institute, 1974).   Three compaction effort levels (35, 50, and 75 blows per face) were used for Phase II and the effects of compaction effort on mix strength are discussed in Section 3.6.3.   75 blows per face were the standard compaction effort for other tasks in this work.

The test setup prescribed in AASHTO T322 (*Standard Method of Test for Determining the Creep Compliance and Strength of Hot Mix Asphalt [HMA] Using the Indirect Tensile Test Device*) was followed for tests reported in Chapters 3, 4 and 6, and the loading was displacement controlled and the testing head was moving at a velocity of 12.5 mm per minute.   In Phase III and Phase IV of the UCPRC study, the loading head velocity was changed to 50 mm per minute for some practical considerations, which complied with AASHTO T283 (*Resistance of Compacted Bituminous Mixture to Moisture Induced Damage*), and only the test results reported in Chapter 5 were affected by this modification.   As test results in different chapters are not directly compared, this inconsistency in loading rates does not affect the validity of the conclusions.

2.7   Indirect Tensile Strength Test (152 mm)

Specimens with a nominal diameter of 152 mm (6 in) and a nominal height of 116 mm (4.6 in) were compacted following the modified Proctor method (AASHTO T180 protocol) with prescribed moisture contents.   The original purpose of AASHTO T180 was to obtain the moisture-dry density curve by compacting a material at various moisture contents.   In this study, only one prescribed moisture content was used for each mix and the compacted specimen was retained for ITS testing.   The 152 mm ITS test was displacement controlled in a manner similar to that of the 100 mm ITS test, and the loading head moving velocity was 18.75 mm per minute, which yielded the same strain rate as that of the 100 mm ITS tests (12.5 mm/min).   The 152 mm ITS test was only used in Phase II of the UCPRC study and the results are presented in Chapter 3.

2.8   Triaxial Resilient Modulus and Permanent Deformation Tests

The triaxial resilient modulus (Tx RM) test and triaxial permanent deformation (Tx PD) test for pavement materials (mainly soils and aggregate materials) use a test setup similar to that of a conventional triaxial compression test in soil mechanics.   A confining stress σ_0 is applied through a latex membrane in a pressure chamber, and load is applied in the vertical direction.   In a resilient modulus test, a contact stress $\sigma_{contact}$ is constantly applied, and a cyclic component σ_{cyc} is superimposed in the form of haversine pulses as seen in Figure 2.5.   Each loading pulse (with a duration of t_{pulse}) is followed by a relaxation period lasting t_{relax}.   Typical axial strain responses

under this type of loading are also shown in Figure 2.5. The resilient modulus test concerns the

recoverable component of the axial strain $\varepsilon_{recoverable}$, and resilient modulus (M_r) is calculated using

equation (2.1):

$$M_r = \sigma_{cyc}/\varepsilon_{recoverable} \tag{2.1}$$

Typically, the axial stress level applied in resilient modulus tests is low relative to the shear

strength of the material being tested, and the test is considered nondestructive. The permanent

deformation test concerns the residual (or irrecoverable) strain development or accumulation.

The number of load pulse repetitions for typical resilient modulus tests is on the scale of hundreds,

while it can approach or exceed one million for permanent deformation tests.

In this study, cylindrical specimens with a nominal diameter of 152 mm (6 in) and a height of

305 mm (12 in) were prepared for Tx RM and Tx PD tests. Compaction procedures prescribed

in AASHTO T180 (modified Proctor) and AASHTO T307 (*Standard Method of Test for*

Determining the Resilient Modulus of Soils and Aggregate Materials) were both assessed in

Phase I. A modified version of AASHTO T180 was ultimately selected in which specimens

were compacted in 12 lifts of 25.5 mm thick layers, with the mass of each layer calculated based

on the 100 percent modified AASHTO density obtained from the 152 mm ITS specimens.

Compared to the procedure in AASHTO T307, which recommends compacting the specimen

using a vibratory hammer without kneading action, the method adopted produces specimens with

less segregation, better bonding between lifts, and more accurate density control.
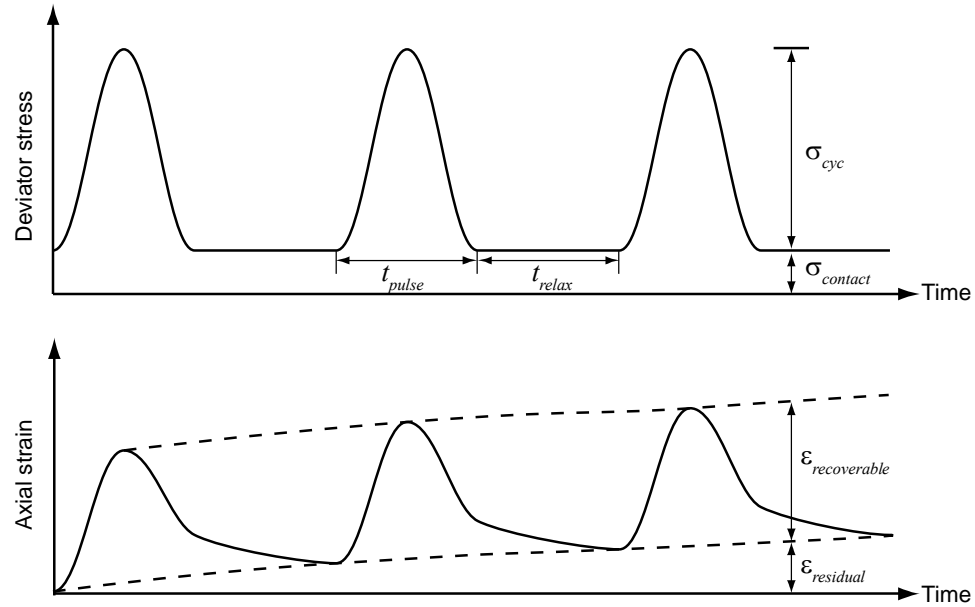
Figure 2.5   Typical axial stress and strain in triaxial resilient modulus tests

The triaxial resilient modulus test procedure was modified from the AASHTO T307 test protocol.

Resilient moduli at various confining stress levels, deviator stress levels, and loading rates were

measured.   The confining stress and deviator stress levels adopted were the same as those of

AASHTO T307, i.e. five confining stress levels, each with three axial stress levels.   For each

combination of confining stress and deviator stress, haversine load pulses at four different loading

rates were successively applied as follows:

- 0.05 second pulse width with 0.45 second relaxation,

- 0.1 second pulse width with 0.4 second relaxation,

- 0.2 second pulse width with 0.8 second relaxation, and

- 0.4 second pulse width with 0.6 second relaxation.

Since the triaxial resilient modulus test is largely nondestructive, some specimens were tested

multiple times, mostly to evaluate the effects of curing or moisture conditioning on the same specimen.

As will be discussed in Chapter 4, foamed asphalt mixes show apparent stress dependent behavior. Equation (2.2), which is modified from Uzan's (1985) general resilient modulus model for granular materials with additional consideration of the effects of loading pulse durations, was used to fit the Tx RM test data.   The average R^2 value was always greater than 0.98.

$$M_r = k_1 p_a \left(\frac{T}{0.1 \text{ second}} \right)^{k_T} \left(\frac{\theta}{p_a} \right)^{k_2} \left(\frac{\tau_{oct}}{p_a} \right)^{k_3} \tag{2.2}$$

where p_a= atmospheric pressure used to nondimensionalize stresses; T= duration of the haversine load pulses; σ_0 = confining stress; σ_d = deviator stress; $\theta = 3\sigma_0 + \sigma_d$ = bulk stress; τ_{oct} =octahedral shear stress, and in the triaxial stress state $\tau_{oct}= \sqrt{2}\sigma_d/3$; k_T, k_1, k_2, and k_3 are material related constants.   Note that the definition of bulk stress in equation (2.2) follows the convention in pavement material related research, and is different from that of the mean stress in soil mechanics.

The resilient modulus of a foamed asphalt mix in triaxial tests is primarily a function of the confining stress (σ_0), the deviator stress (σ_d) and the loading rate (characterized by the haversine load pulse duration T), i.e. $M_r = M_r (\sigma_0, \sigma_d, T)$.   For each triaxial resilient modulus test task, resilient modulus values at two reference stress states, $M_{r1}=M_r(20.7 \text{ kPa, } 62.1 \text{ kPa, } 0.1 \text{ second})$ and $M_{r2}=M_r(137.9 \text{ kPa, } 103.4 \text{ kPa, } 0.1 \text{ second})$ were calculated and reported based on the model

fitting results. M_{r1} represents stiffness at low confining pressure and relatively high deviator stress levels, while M_{r2} represents stiffness at high confining stress and relatively low deviator stress levels. Both stress states were used in the testing sequence of AASHTO T307, and the values reported were calculated on the basis of model fitting results, not test results in the corresponding stress states.

In the study described in Chapter 5, a limited series of triaxial permanent deformation tests were performed on selected specimens. Most of these specimens had already been subjected to Tx RM tests before the permanent deformation tests took place. The objective was to compare the permanent deformation resistance of different mixes under different curing conditions. One confining stress level (68.9 kPa) was used for the permanent deformation tests, which is the median confining stress level for the Tx RM test procedure. During a permanent deformation test, 20,000 load repetitions were first applied at a deviator stress level (σ_d) of 300 kPa, followed by another 20,000 load repetitions at 500 kPa, and then up to 210,000 load repetitions applied at 700 kPa. The duration of each haversine loading pulse was 0.1 seconds and the relaxation time was 0.2 seconds.

2.9   Flexural Beam Test

A new flexural beam strength (monotonic loading until beam fails) test procedure was developed in this study. The nominal dimensions of the beam specimens were 560 mm×152 mm×80 mm.

The quantity of moist material required to fabricate one beam was calculated based on the 100 percent modified AASHTO density determined during the 152 mm ITS test specimen preparation. The material was then compacted in a steel mold to the target volume by alternately applying two steel compaction heads (one flat and one curved, both with dimensions of 150 mm x 150 mm) as shown in Figure 2.6. The compaction heads were driven by a Hilti® TE-76P Combihammer with vibration force. Specimens were tested as extruded from the mold, with no cutting to the nominal dimensions.

The flexural beam test configuration was similar to that of AASHTO T97, but the beam thickness was 80 mm instead of 150 mm, and loading was displacement rate controlled rather than stress rate controlled. The span length was 450 mm and loads were applied monotonically at the two third-points with a constant displacement rate of 25 mm/min. Two metal plates were glued at the mid span of the beam, with a linear variable differential transformer (LVDT) attached to each metal plate to measure the deflection during testing.

2.10 Unconfined Compressive Strength Test

The Unconfined (or Uniaxial) Compressive Strength (UCS) test was performed on the same cylindrical specimens as the triaxial resilient modulus test, which was assumed to be nondestructive. The loading was displacement controlled at a rate of 15 mm/min.
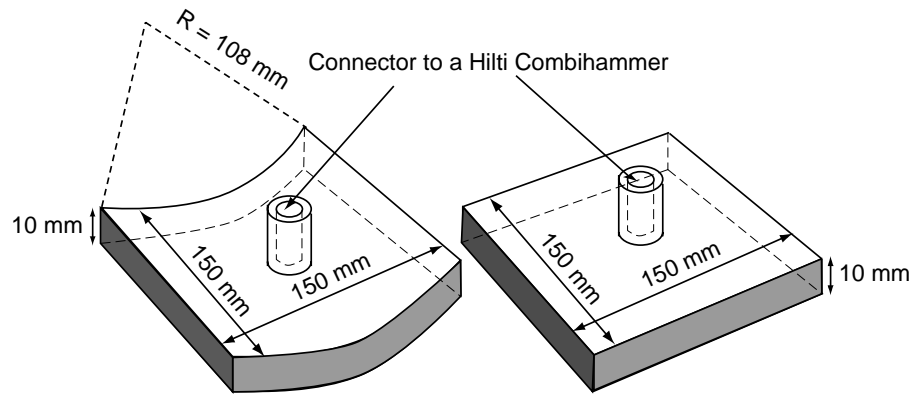
(a) Compaction heads
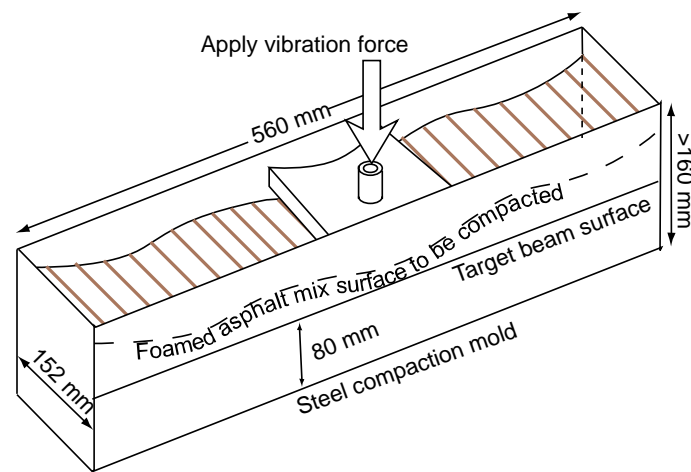
(b) Specimen compaction
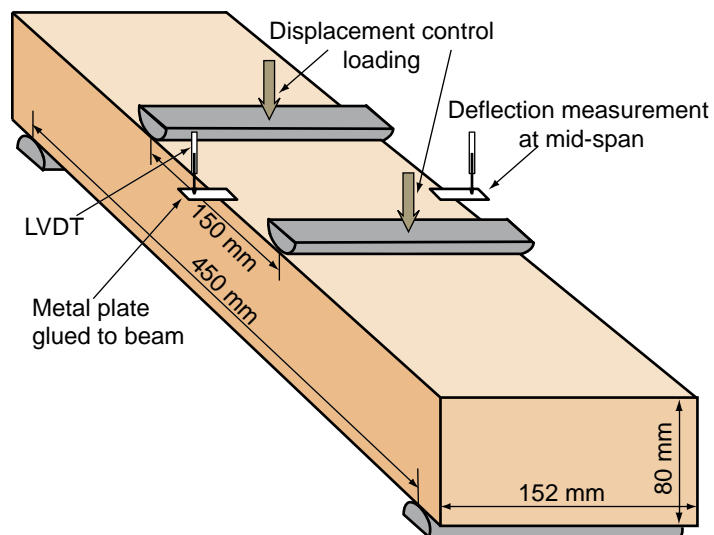
(c) Testing configuration

Figure 2.6   Flexural beam specimen preparation and test configuration

2.11 Free-Free Resonant Column Test

The free-free resonant column (FFRC) test was carried out on cylindrical (triaxial) and beam specimens prior to destructive testing. The test setup is shown in Figure 2.7. The specimen (a cylindrical specimen is shown in this example) is standing on a relatively soft base. A special accelerometer is glued on the top surface of the specimen. In a test, the operator uses a specially instrumented hammer to hit the top surface of the specimen, and the impact force is measured by the load cell on the hammer. The shock wave generated propagates along the specimen, is reflected back from the bottom surface, and is then picked by the accelerometer. Both the accelerometer and the load cell are connected to the same signal processing and data acquisition system, which calculates resilient modulus of the material from the wave propagation speed in the specimen with elastic wave theories. This test normally utilizes cylindrical specimens with a length-to-diameter ratio of 2 (same as the triaxial test specimens), but beam specimens (ratio of 4.5 to 1) were also tested in this study to obtain a larger data set. Since this test is nondestructive, all cylindrical and beam specimens were subjected to this test before the triaxial and flexural beam tests. The specimens were only tested in an unsoaked condition, as efforts to mount the accelerometer on soaked specimens failed.

This test is very inexpensive to perform, in terms of both equipment investment and the effort taken for each test. Additionally this test is nondestructive, so it can utilize specimens that were fabricated for other types of tests.
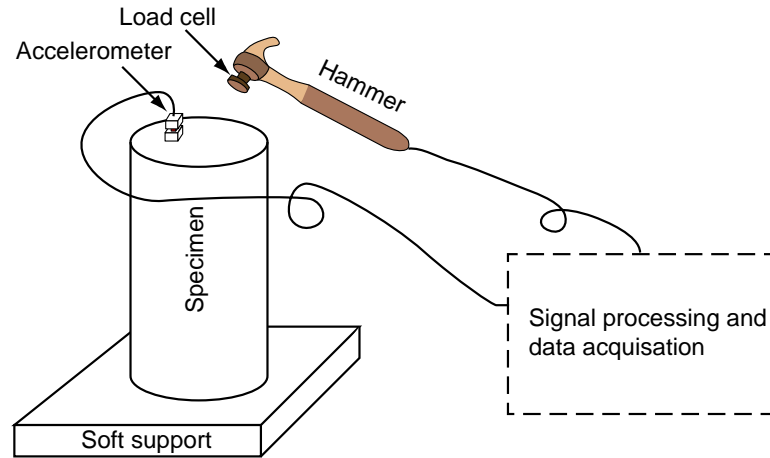
Figure 2.7   Typical setup for the FFRC test

2.12 Mixing Moisture Content

The mixing moisture content (MMC) of a foamed asphalt mix is defined as the moisture content in the granular material when foamed asphalt is injected.   The effects of mixing moisture content on mix properties and the microscopic mechanism were investigated in Special Task IIA (see Table 2.2) of the UCPRC study and documented in Chapter 6 of this thesis.   In the tasks recorded in Chapters 3 to 5 of this thesis, the target mixing moisture content was set to be one percent lower than the optimum moisture content (OMC) for compaction determined with the modified Proctor method (AASHTO T180) for each mix.   This value was tentatively determined based on the findings of the literature review and experience of the UCPRC research team.   As elaborated in Chapter 6, this turned out to be a reasonable choice for MMC to balance the effects of moisture on asphalt dispersion and compaction/density.   Also, as seen in the test results presented in Chapter 6, the effects of MMC on mix properties (strength and stiffness) are less

significant compared to those of other variables considered in Chapters 3 to 5 (such as density, asphalt content, and curing methods).

2.13 Curing

The strategy for selecting curing conditions was similar to that used to select MMC. The working hypothesis for Phase II and Phase III of the UCPRC study as well as the analysis in Chapter 3, 4 and 6 was based on the curing mechanism proposed by Bowering (1970): foamed asphalt specimens do not develop full strength until most of the mixing moisture has evaporated, which implies that moisture evaporation is a significant factor, and possibly the most important factor in curing of foamed asphalt mixes. Experience gained in Phase I of the UCPRC study confirmed this hypothesis. Consequently, the main objective of the curing process was to allow the original mixing and compaction moisture to evaporate at a reasonable temperature so that the mix reached a relative stable and uniformly distributed moisture content throughout the specimen. In the laboratory work presented in this thesis, the curing procedure, unless otherwise indicated, was to cure specimens at 40°C in a forced draft oven with specimens open to air. The curing durations varied from three days to seven days depending on the specimen dimensions as elaborated in the experiment description of each task.

A detailed investigation of curing mechanisms of foamed asphalt mixes was conducted in Phase IV of the UCPRC study as documented in Chapter 5 of this thesis. Two curing procedures were

followed to simulate different field conditions. As they are irrelevant to the work in other chapters, these procedures are described in Chapter 5 to avoid confusion.

2.14 Water Conditioning

The effects of water conditioning on foamed asphalt mix properties are discussed in Section 3.6.2. Specimens subjected to water conditioning were soaked in a water bath at 20°C for 72 hours (or other durations for selected specimens in Chapter 5) with water levels maintained at 100 mm above the top surface of the specimens. The prolonged soaking durations were designed to represent critical field conditions, and to reduce the effects of different specimen sizes on water infiltration.

2.15 Experiment Design of Phase I of the UCPRC Laboratory Study

Phase I of the UCPRC laboratory study was primarily carried out to familiarize the research team with equipment, procedures, and test methods, and to obtain a basic understanding of the attributes of typical California foamed asphalt mixes, before more detailed testing was carried out in the later phases. This phase was thus of a preparatory and exploratory nature to determine specimen preparation and testing procedures for succeeding phases. The test procedures and methods as described in Sections 2.5 to 2.14 were gradually and incrementally established during Phase I, and they were not necessarily implemented from the beginning of Phase I.

The parent materials for the foamed asphalt mixes produced in this phase were the RAP materials (Section 2.2) and the AR-4000 asphalt (Section 2.3). The mix preparation procedure was similar to that was depicted in Section 2.5, except that no temperature control measure was adopted, thus resulting in inconsistent asphalt dispersion. The experiment factorial design is shown in Table 2.3.

Table 2.3   Experiment factorial design for Phase I of the UCPRC study

Variable	Values
Granular material	- RAP-1 - RAP-2 - RAP-3 (gradations shown in Figure 2.1)
Asphalt	- AR-4000
Asphalt content[1]	- 0 - 1.5% - 3.0% - 4.5%
Test method[2]	- ITS, 100mm
Curing	- 40ºC in a force draft oven for seven days, specimens open to air
Water conditioning	- 72 hours soaking (referred to as "soaked") - No conditioning (referred to as "unsoaked")
Replicates per mix	- Four specimens per mix: two soaked + two unsoaked

[1] Asphalt content is percentage by mass of dry aggregate, and aged binder in the original RAP is included in the aggregate mass.

[2] Other types of tests, such as flexural beam tests were also performed but not used in this thesis work.

2.16 Experiment Design of Phase II of the UCPRC Laboratory Study

Unless otherwise noted, all test data in Chapters 3 and 4 were from Phase II of the UCPRC study. The basic idea of Fracture Face Image Analysis was initialized and preliminarily tested in Phase I, and it was further verified and finalized in Phase II. The objectives of Phase II of the UCPRC laboratory study included:

- An investigation into the effects of asphalt binder properties, PAP sources, and PAP gradations on foamed asphalt mix properties measured by different laboratory test methods.
- Comparison of different laboratory test methods for assessing the strength characteristics of foamed asphalt mixes.
- Comparison of different laboratory test methods for assessing the stiffness (or resilient modulus) characteristics of foamed asphalt mixes.

The experiment factorial design of the Phase II UCPRC laboratory study is shown in Table 2.4. The two asphalts types were both foamed at 165ºC with 4 percent foaming water added by mass. The measured expansion ratio and half-life for the PG64-16 binder were 23 and 19.5 seconds, respectively, and 22 and 22 seconds for the PG64-10 binder. For each mix type, one batch of loose mix (65 kg total) was prepared to fabricate the different types of specimens for laboratory testing. A 152 mm ITS specimen was first compacted with the modified Proctor procedure for each batch of loose mix, and the 100% modified Proctor wet density was calculated, based on which the quantities of material for the cylindrical and beam specimens were calculated.

Table 2.4   Experiment factorial design of Phase II for the UCPRC study

Variable	Values
Granular material	Two PAP sources × three gradations for each source. Gradations are shown in Figure 2.2
	- 33-A - 88-A - 33-B - 88-B - 33-C - 88-C
Asphalt	- PG64-16 - PG64-10
Asphalt content	- 0 - 3.0%
Test methods and associated specimen fabrication methods	- ITS (100 mm), see Section 2.6 - ITS (152 mm), see Section 2.7 - Flexural beam, see Section 2.9 - Triaxial resilient modulus, see Section 2.8 - UCS, see Section 2.8 - Free-free resonant column (FFRC), see Section2.11
Compaction effort for ITS-100 mm	- 35 blows on each face - 50 blows on each face - 75 blows on each face
Curing	- 40ºC in a force draft oven for seven days, specimens open to air
Water conditioning	- 72 hours soaking (referred to as "soaked")[2] - No conditioning (referred to as "unsoaked")

Replicates	Two replicate batches for each mix
	For each batch of mix:
	- 9 × 100 mm ITS specimens
	  (3 compaction levels,
	  2 soaked + 1 unsoaked for each compaction level)
	- 2 × 152 mm ITS specimens (soaked only)
	- 2 × beam specimens (1 soaked + 1 unsoaked)
	- 1 × cylinder (multiple Tx RM tests and soaked UCS)

Each cylindrical specimen was subjected to multiple tests. Typically, a Tx RM test was first performed on the unsoaked specimen. Then the specimen was water conditioned and another Tx RM test was performed on the soaked specimen. Finally a UCS test was undertaken on the same soaked specimen. Beam specimens were not prepared for the control mix because the untreated beams were too weak to handle. The 152 mm ITS tests were carried out on soaked specimens only.

Chapter 3 Foamed Asphalt Mix Microstructure Characterization and Micromechanical Interpretation of Strength Behavior

3.1 Foamed Asphalt Mix Microstructure, a Qualitative Description

The term "microstructure of a material" generally refers to the microscopic description of the individual constituents. The term "microstructure" itself is rather generic, and its interpretation is dependent on the material to be studied and the nature of the problems/phenomena concerned. The scale of material microstructure ranges from 10 μm (crystal grains in steel) to 10 mm (aggregate particles in portland cement concrete).

Even for the same material, the scale of microstructure concerned is also dependent on the nature of the material behavior that is being investigated. For instance, the asphalt mastic phase in foamed asphalt mixes is regarded as a homogeneous phase in this thesis work, while asphalt mastic has its own microstructure consisting of asphalt film, fine aggregate particles and air voids. Nevertheless, the internal microstructure of asphalt mastic has little relevance to the problems concerned in this thesis work. Hereafter, foamed asphalt mix "microstructure" mainly refers to the spatial or geometrical configurations of the individual phases in the mix at the scale between 0.5 mm and 20 mm.

To give a general and qualitative description of the microstructure of foamed asphalt mixes, the process forming the microstructure needs to be reviewed. Section 1.1.2 has described the process of asphalt foaming. After asphalt is foamed into numerous bubbles with thin asphalt films, it is injected onto the agitated moist aggregates, either in a laboratory mixer or in a recycler in the field. As the asphalt bubbles are not stable when contacting cold aggregate, they burst, disperse into the aggregate, and finally cool down.

It was described in the literature (Jenkins, 2000) and also observed in this study that if finer and coarser aggregate particles coexist in an untreated mix, foamed asphalt tends to partially coat and bond the fine fraction (termed mineral filler) together to form the asphalt mastic phase. In uncompacted foamed asphalt mixes, the asphalt mastic phase exists in the form of isolated droplets with various sizes. Since the workable duration (before asphalt bubbles burst and lose workability) of this mixing process is as short as a few seconds, only a fraction of the mineral fillers can be coated by asphalt, while a considerable amount of mineral filler remains "free" and eventually forms the mineral filler phase. This procedure is affected by many factors including (Jenkins, 2000) the characteristics of the asphalt foam, the gradation of the aggregate, the mixing technique adopted, and the moisture content and the temperature of the aggregate.

After compaction and curing, a structure similar to that conceptually illustrated in Figure 3.1 is formed, where partially coated large aggregates are "spot welded" with fines mortar (Jenkins, 2000). In Jenkins (2000), the term "mortar" refers to the mix of asphalt mastic (mixture of mineral filler and asphalt cement) and the sand fraction which is partially coated. In this thesis,

sands coated by asphalt are included in the asphalt mastic phase whereas sands without asphalt coating are treated as mineral fillers for simplicity. In such a structure, three major phases can be identified: 1) the aggregate skeleton formed by large aggregate particles, 2) the asphalt mastic phase existing in the form of droplets bonding the aggregate skeleton together, and 3) the mineral filler phase partially filling the voids in the skeleton. In this study, air voids are considered as inclusions in the asphalt mastic and the mineral filler phases, but not considered as a separate phase. This study primarily characterizes the distribution of asphalt mastic in foamed asphalt stabilized materials, and investigates its effects on material properties. The distribution of air voids is not explicitly considered.
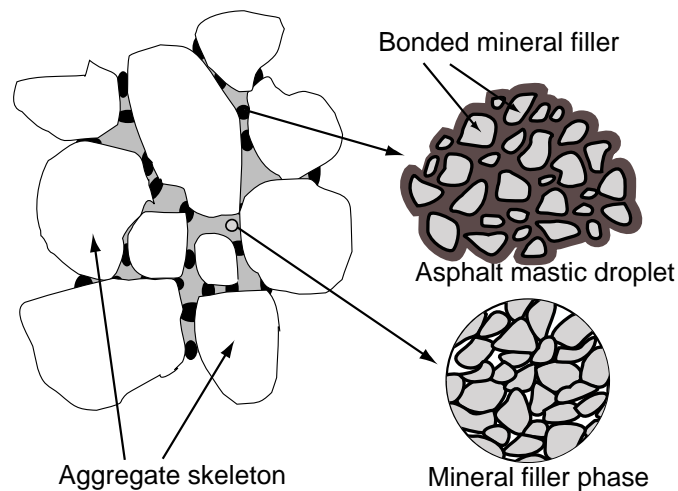
Figure 3.1   A conceptual illustration of microstructure of foamed asphalt mixes

For a given foamed asphalt mix, the sizes and shapes of the large aggregate particles in the parent PAP material are generally easy (at least from a qualitative perspective) to characterize. It is intuitively reasonable to assume that the large aggregate particles forming the skeleton are randomly distributed in the foamed asphalt mix. The action of gravity and compaction might

have certain effects on the orientation of elongated particles, but this is not considered in this study. Segregation was minimized by thoroughly mixing the materials before specimen preparation. It is therefore rational to assume that the asphalt mastic phase and the mineral filler phase are randomly distributed in the voids in the aggregate skeleton.

Consequently, if the microstructure of a foamed asphalt mix is to be quantified, the two most significant variables controlling mix properties should be 1) the volumetric characteristics of the asphalt mastic phase, i.e. how much mineral filler is converted into asphalt mastic when being mixed with foamed asphalt, and 2) the size distribution of asphalt mastic droplets. These two characteristics cannot be directly deduced from basic characteristics of the parent materials. The volumetric characteristics of the mineral filler phase are also of interest, but it is not an independent variable: if more original mineral filler in the PAP material is converted to asphalt mastic, then there is less mineral filler left to form the mineral filler phase.

3.2 Existing Methods for Characterizing Microstructure of Asphaltic Pavement Materials

Efforts to quantify the microstructure of foamed asphalt mixes have been occasionally reported in the literature. Empirical visual criteria for asphalt distribution in treated mixes were proposed by Ruckel et al. (1983) for checking the quality of laboratory and field mixes. Jenkins (2000) performed a statistical analysis of the size distribution of asphalt droplets in foamed asphalt

treated loose mixes to demonstrate how foamability of asphalt affects its dispersion. These two approaches were proposed for uncompacted loose mixes, and literature searches for techniques characterizing microstructure of compacted foamed asphalt mixes did not yield useful information.

On the other hand, research on quantifying the microstructure of HMA has been much more active. These techniques can be classified into three general categories.

2D image analysis on cross sections of HMA specimens

To employ approaches in this category, a compacted HMA specimen is first cut to obtain a smooth cross section or a thin section. Various procedures for sectioning HMA specimens were discussed in Kose et al. (2000). A high-resolution (typically <50 μm per pixel) digital image of the cross section is obtained for image analysis. Since the different phases (mainly asphalt mastic and aggregate) usually have distinct colors, they can be easily differentiated with certain image processing techniques. Air voids can also be identified with some special techniques, such as using a fluorescent dye epoxy with UV light illumination. Such applications were reported as early as 1993 (Eriksen & Wegan). In one of the earliest applications, Yue et al. (1996) used this approach to study the area gradation of aggregate cross sections, the particle orientations, and differences in microstructure induced by different compaction patterns. HMA microstructure studies by Masad and his group were summarized in Masad et al. (1999). Some more recent work (eg. Elseifi et al. 2008) focused on phenomena at a smaller scale (1-100 μm),

such as the internal structure of asphalt mastic using the scanning electron microcopy technology.

3D HMA microstructure characterization with X-ray CT scanning

X-ray computed tomography (CT) is another tool that researchers have employed to characterize the microstructure of HMA. CT scanning directly obtains a 2D map of density (or more accurately, X-ray attenuation) for a thin section of a specimen. As CT scanning is a nondestructive procedure, a series of parallel density maps can be obtained for a specimen. At the current level of the technology, the resolution of the 2D maps (lateral) is typically in the vicinity of 0.1 mm/pixel, while the resolution in the longitudinal direction is several times lower (typically 1 mm/pixel). By combining these 2D images, one can construct the 3D internal structure of the specimen, although this is not a trivial task (eg. Wang et al., 2004). Use of X-ray CT techniques for asphaltic mix research was reported as early as 1999 (Braz et al.) to track the crack development in a cyclic indirect tensile fatigue test. More recently, it has been used to investigate a great variety of problems for HMA research, and a list of such applications is provided by Masad (2004).

Morphological analysis of constituents (aggregate) in HMA

Instead of directly characterizing the internal microstructure of HMA, methods in this category quantify certain morphological features (form, angularity, surface texture, etc.) of aggregates. These methods aim to relate these characteristics to mechanical behavior of the mixes, such as resilient behavior (Pan et al. 2001). Some techniques in this category analyze the 2D projections

of the aggregate particles on to a plane (or multiple orthogonal planes) (eg. Al-Rousan et al. 2007), while others directly work with 3D images obtained by CT scanning (eg. Taylor et al. 2006).

Discussion of microstructure characterization methods for foamed asphalt mixes

None of these existing techniques meet the needs of this thesis study.

For 2D image analysis on cross sections, a smooth cross section or thin section has to be prepared for image acquisition. Foamed asphalt mixes contain a considerable amount of unbound mineral filler, which makes certain areas on a cross section extremely brittle and fragile. Cutting using conventional techniques inevitably destroys the microstructure.

CT scanning relies on the difference in densities between material constituents to distinguish different phases in a composite material. In foamed asphalt mixes, the asphalt mastic phase, the mineral filler phase, and the aged asphalt mastic in the recycled HMA have similar densities, and they are therefore difficult to differentiate by CT scanning.

Another problem is the cost. In the UCPRC study, more than 3,000 specimens were fabricated and tested. The image acquisition method to be used in parallel to the conventional laboratory study has to be economical to perform. It is possible that certain sectioning techniques are able to generate smooth and undisturbed thin sections of foamed asphalt mixes, and it is also possible that CT scanning can produce some insights into the microstructure of this material, but they are both unaffordable for a study of this scale.

The techniques in the third category, namely morphological analysis of constituents, have little relevance to the key microstructural features concerned in this study, namely the volumetric characteristics of the asphalt mastic phase, and its distribution in foamed asphalt mixes. Certainly, the morphological characteristics of the PAP particles have some effect on strength and stiffness of foamed asphalt mixes. However, compared to the role of asphalt mastic, they are of a secondary importance.

3.3   Fundamentals of Foamed Asphalt Mix Fracture Face Image Analysis

3.3.1 Initiation of the idea of FFIA

The basic idea of Fracture Face Image Analysis (FFIC), the image acquisition and analysis method developed for this thesis, was initiated from empirical observations on the fracture faces of tested ITS specimens in Phase I of the UCPRC study (Section 2.15).   Figure 3.2(a) shows a tested ITS specimen, split into two half-pieces.   Figure 3.2(b) shows the appearance of the two fracture faces, on which a number of asphalt mastic spots of various sizes can be seen.   The visible asphalt mastic phase can be identified using image processing techniques as elaborated later.

The following general tendencies were observed during Phase I of the UCPRC study.   First, mixes with higher asphalt contents usually have fracture faces with more asphalt mastic coverage. Second, specimens with more asphalt mastic coverage on the fracture faces generally have higher

strength.　Based on these observations, a question was raised: how do the visual features of the asphalt mastic coverage on fracture faces reflect characteristics of the internal distribution of the asphalt mastic phase?

<div align="center">(a)　　　　　　　　　　　　　(b)　　　　　　　　　　　(c)</div>
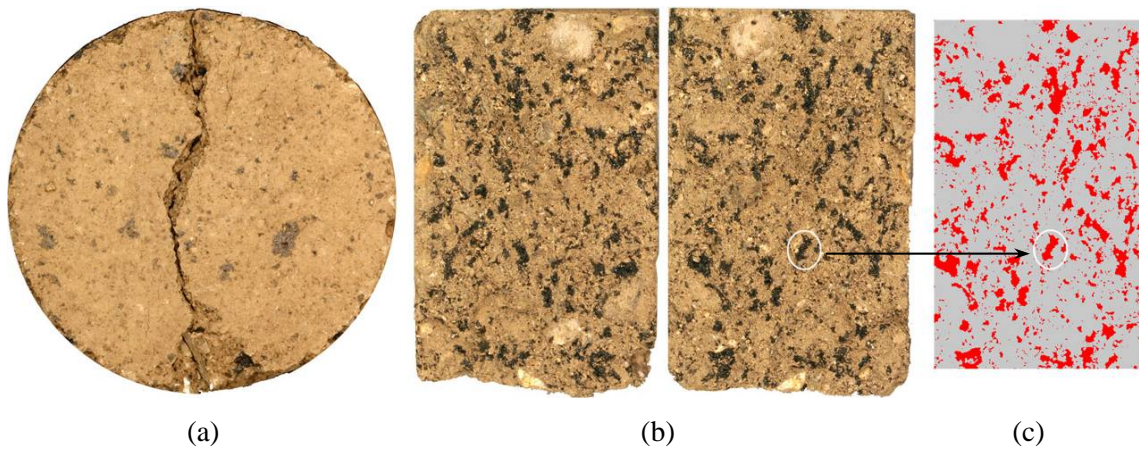
Figure 3.2　A tested ITS specimen and its fracture faces
(a) A tested ITS specimen; (b) the two fracture faces generated; (c) visible asphalt mastic spots on one fracture face identified by digital image processing.

3.3.2 Mapping 2D fracture face asphalt coverage to 3D asphalt mastic distribution

To establish the mapping rules between the 3D asphalt mastic distribution inside the specimens and the 2D distribution of visible asphalt mastic on the fracture faces, the process in which fracture faces are created during fracturing of a laboratory specimen needs to be considered. The conceptual microstructure shown in Figure 3.3(a) is the same as that in Figure 3.1.　In a laboratory strength test, such as an ITS test or a flexural beam test, a fracture is initiated and then propagates through the specimen.　The fracture splits the specimen into two pieces, and each has a visible fracture face.　On the fracture faces, asphalt mastic (dark color) is seen where the fracture has propagated through and split asphalt mastic droplets.　Where the fracture has

propagated through the mineral filler phase, the fracture faces show a significantly lighter color,

depending on the constituents in the original PAP.   It should be noted that Figure 3.3 is a planar

analogy to a 3D phenomenon for illustration purposes.
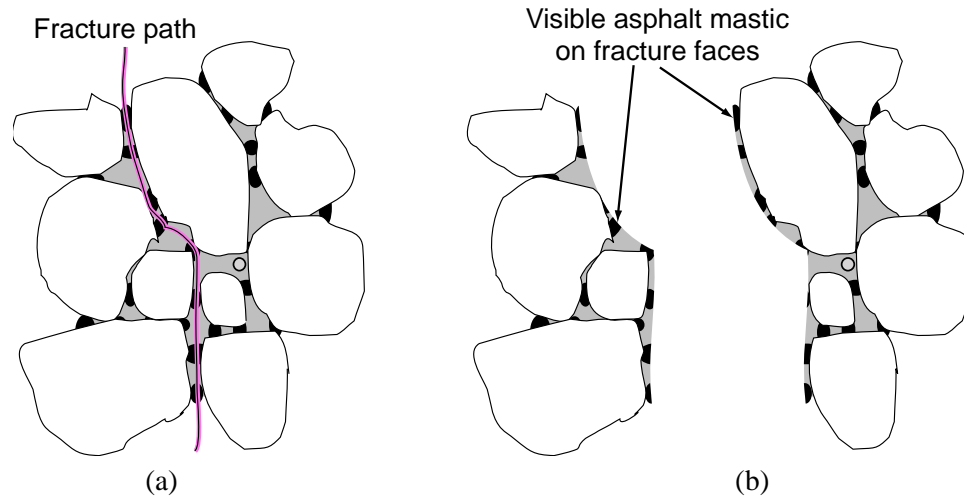
Figure 3.3   Mechanism by which 3D asphalt mastic distribution affects the 2D distribution of
asphalt mastic on fracture faces
(a) Microstructure of a foamed asphalt mix and a fracture path propagating through the specimen;
(b) the specimen is split into two pieces and the fracture faces are visible.

Directly establishing quantitative mapping rules between the 3D asphalt mastic distribution in

foamed asphalt mixes and the 2D visible features of asphalt mastic distribution on fracture faces

is difficult.   A number of general principles can be identified on a semi-quantitative and

comparative basis.   If the mixes subjected to comparison are different in terms of only one

variable (such as original PAP gradation, fines content in the PAP, asphalt content, density, the

specimen fabrication or testing method) and they are otherwise identical, these principles can

predict how the volumetric characteristics of asphalt mastic change with this variable.   Therefore

measuring or calculating exact volume of the asphalt mastic in a unit volume of a foamed asphalt

mix, or the detailed size distribution of asphalt mastic droplets can be avoided.

A new concept termed the "fracture face asphalt coverage" or FFAC is defined as the ratio of the area of the mastic phase visible on a fracture face to the total area of the fracture face, and is considered to be the simplest quantitative characterization of foamed asphalt fracture faces. FFAC is the only quantitative descriptor for fracture face asphalt mastic distribution features used in this thesis, although some other qualitative indicators are also occasionally employed. In digital image analysis, FFAC can be easily calculated by dividing the number of pixels representing the mastic phase, which are significantly darker than the other phases, by the total number of pixels of the entire fracture face on a digital image.

As discussed in Section 3.1, the two most fundamental characteristics of the asphalt mastic phase distribution in a foamed asphalt mix are:

- Its total volume relative to the volume of the mineral filler phase, and

- The size distribution of the asphalt mastic droplets.

If the pattern in which the asphalt mastic phase and the mineral filler phase fill the voids in the aggregate skeleton is random and the mix is homogenous and isotropic in a global sense, the following three mapping rules apply:

- If the size distribution of the asphalt mastic droplets remains constant, then as the volumetric ratio of the asphalt mastic phase to the mineral filler phase increases (implying more mineral filler is coated by asphalt and converted to asphalt mastic during mixing), the FFAC value will be higher.

- Given the same volumetric ratio of the asphalt mastic phase to the mineral filler phase, if the asphalt mastic exists in the form of a large number of small droplets instead of a small number of large droplets, more uniformly distributed small asphalt mastic spots will be visible on the fracture faces as opposed to large concentrated asphalt spots.

- Given the same volumetric ratio of the asphalt mastic phase to the mineral filler phase, the mix where asphalt mastic exists in the form of a large number of small droplets instead of a small number of large droplets should also yield fracture faces with higher FFAC values.

The third mapping rule is not as intuitive or as apparent as the other two rules, and thus requires further explanation. A qualitative analysis of two idealized cases in Figure 3.4 illustrates these effects. Mix-A as shown in Figure 3.4(a) represents a structure with good asphalt dispersion featuring a large number of small asphalt droplets welding the aggregate skeleton together. Mix-B, shown in Figure 3.4 (b) represents a structure with inferior asphalt dispersion, with a few large asphalt droplets. The volumes of the asphalt mastic and mineral filler phases in the two mixes are the same, and the aggregate skeletons are similar. Assuming that the tensile strength of the mineral filler phase is less than that of the mastic phase (which is not always true as will be discussed later), when a crack propagates (from bottom to top) in Mix-A as a result of the action of external forces, it can propagate along either Path-A1 or Path-A2 since the lengths of the two paths and the numbers of asphalt bonds to break are similar. However, in Mix-B, the crack is more likely to propagate along Path-B2, where it encounters fewer asphalt droplets. The fracture faces of Mix-A will show more black spots (broken mastic phase) in terms of both the

number and the total area than those of Mix-B.   At the same time, the tensile strength of Mix-A

should be higher than that of Mix-B.

Fracture Path A2
Fracture Path A1

Fracture Path B2
Fracture Path B1

Large aggregates forming skeleton
Asphalt mastic droplets
Mineral filler phase
A crack propagating through

(a)   (b)
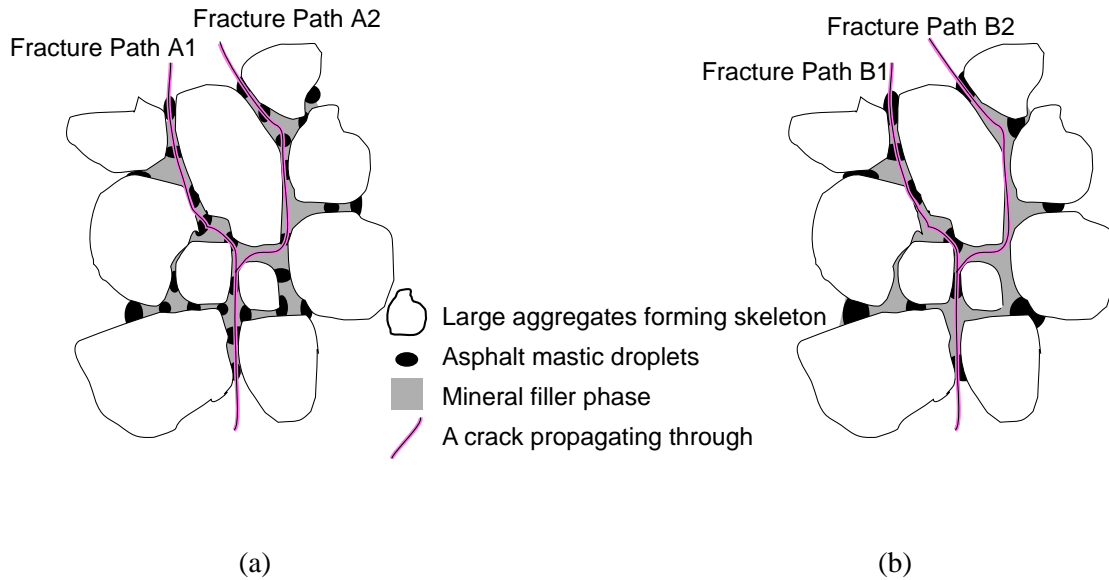
Figure 3.4   Effects of asphalt droplet size on FFAC values
(a) Smaller droplets uniformly distributed; (b) less uniform distribution of large asphalt droplets.

As a simple example, FFAC can be used as a quantitative indicator of the quality of foamed

asphalt distribution for a given recycled material under certain conditions, according to the three

aforementioned mapping rules.   Better quality foam with more preferable mixing conditions

(such as higher temperature and longer interaction time between foam and aggregates) tend to

bond more of the mineral filler to form the mastic phase.   Consequently, the volumetric ratio

between the mastic phase and the mineral filler phase is higher.   Foamed asphalt mixes with

good foam distribution also tend to have a large number of small asphalt mastic droplets.   For a

given PAP and foamed asphalt content, mixes with higher FFAC values are thus preferable.

3.4   Image Acquisition and Processing

3.4.1 Outline of the procedure

The procedure and equipment used to quantify FFAC on fracture faces are simple.   The process

is outlined as follows:

1) Acquire images of laboratory strength test specimen fracture faces using a digital camera.

2) Normalize the brightness of the digital images.

3) Identify those pixels representing the asphalt mastic on the fracture faces.

4) Identify and eliminate glare.

5) Count the pixels representing the asphalt mastic on the fracture face.

6) Calculate the FFAC value.

Digital image analysis software (Foamed Asphalt Fracture Face Image Analysis [FAFFIA]) was

developed by the author at the UCPRC to perform steps 2 through 6.

3.4.2 Image acquisition

ITS and flexural beam tests both yield relatively flat fracture faces that are ideal for image

acquisition and analysis.   A digital single-lens reflex (DSLR) camera with a standard 50 mm

focal length auto focus lens was used to acquire images of fracture faces.   The image resolution

was approximately 0.1 mm of the fracture faces per pixel.   Although color images were acquired,

only the red channel in the RGB color space was used in this study because the mineral filler

phase of the PAP material tested is brown and the contrast between the filler and the asphalt is most distinct in the red channel.

3.4.3 Lighting considerations

The lighting configuration for FFIA needs some special consideration. Fracture faces of tested ITS and flexural beam specimens are uneven, and the characteristic dimensions (wavelengths, depth, et.) of the unevenness and the dimensions of the features (asphalt mastic spots) to characterize are both in the scale of several milimeters. If parallel incident light is cast on a fracture face as shown in Figure 3.5(a), brightness of any small area will be proportional to $\cos\theta$, when θ is the local incident angle for this small area. Consequently, even if the colors of the mineral filler phase and the asphalt mastic phase are homogeneous respectively, brightness of each phase on the images can be highly non-uniform due the surface irregularity. This effect makes identifying asphalt mastic spots in digital images more difficult, as mineral filler can appear quite dark where the incident angle of the light is small. On the other hand, this is not an issue for image acquisition of smooth faces, such as for sawn cross sections of HMA. Scanners are often used to acquire digital images of smooth cross sections of HMA (Kose et al. 2000), and the illumination light in a scanner is nearly parallel.

Parallel incident light

Convergent incident light

θ

Uneven fracture face

Brightness of mineral filler phase

Brightness of mineral filler phase

Brightness of asphalt mastic phase

Brightness of asphalt mastic phase
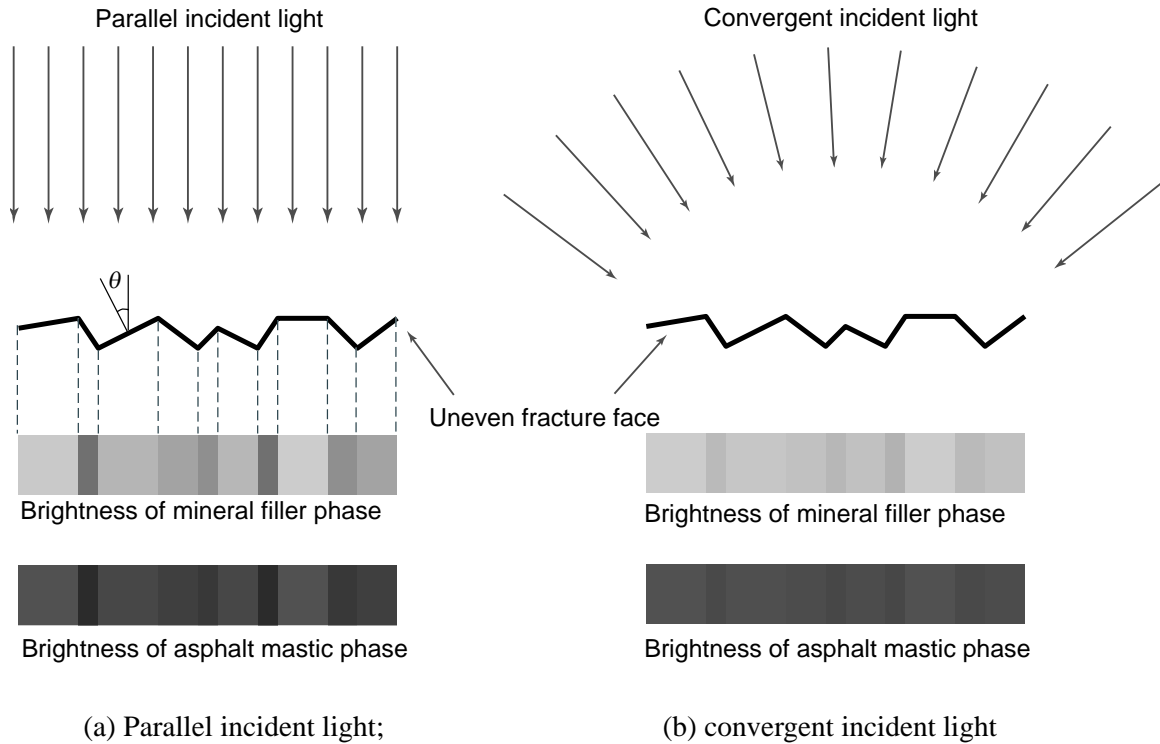
(a) Parallel incident light;   (b) convergent incident light

Figure 3.5   Non-uniform brightness on fracture faces induced by uneven surface

A solution is to have convergent light casting on the fracture faces as shown in Figure 3.5(b), which can effectively homogenize brightness on uneven faces, thereby improving the contrast between the mineral filler phase and the asphalt mastic phase.   This light configuration can be easily achieved by using four to eight lights around the object to be photographed.

3.4.4 Threshold brightness selection

The choice of an appropriate threshold brightness value is also important.   Once selected, pixels darker than the threshold value will be identified as representing asphalt mastic, while brighter pixels will be identified as mineral filler.   On digital images, the boundary between the two phases is rarely distinct and the threshold brightness value is usually determined by a trial and error procedure until satisfactory differentiation between the two phases is achieved on a number

of benchmark images. Some subjectivity is inevitable, but is minimized through the use of a

photographic gray card, which is placed next to the specimen and included in the image to serve

as a reference for normalizing the exposure. Since the colors of the asphalt mastic phase and the

mineral filler phase are highly dependent on the parent materials, a universal threshold value

applicable to all mixes does not exist. Consistency in exposure normalization and threshold

determination is important when comparing a number of specimens. Care must also be taken

when assessing materials containing dark colored minerals such as biotite, garnets, and

tourmalines.

3.4.5 Glare Elimination

Glare on the asphalt mastic phase, caused by specular reflection of light from asphalt cement,

requires special treatment. The glare brightness is normally much higher than the threshold

brightness and can therefore hide asphalt mastic areas. An iterative moving-average type

algorithm was developed to eliminate this problem. In this process, the pixels surrounding each

pixel that is brighter than the threshold brightness are checked. The radius of this area is

determined according to the resolution of the image and typical sizes of glare spots. In this

study, it was set at three pixels (equivalent to 0.3 mm to 0.5 mm). If more than 65 percent of the

pixels in this check area are identified as mastic, then this bright pixel is counted as asphalt mastic.

Each iteration performs this check on every pixel and after several iterations most of the glare

areas are satisfactorily eliminated (Figure 3.6).

(a)   (b)   (c)   (d)   (e)
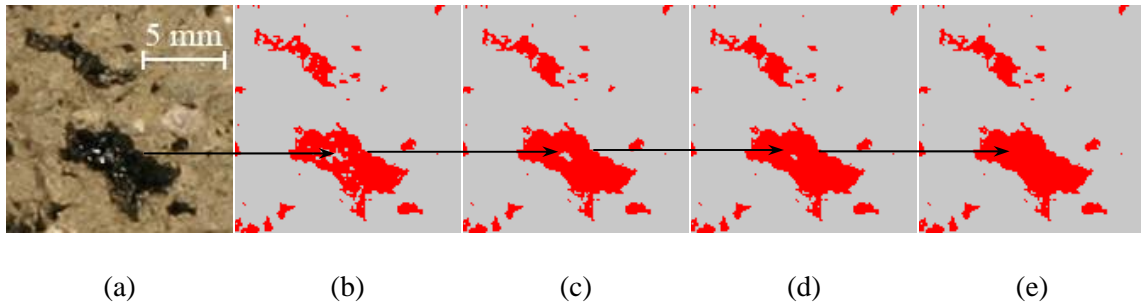
Figure 3.6   Glare elimination on mastic on fracture face images
(a) Original image; (b) initial pixel identification; (c) iteration 1; (d) iteration 2; (e) iteration 3.

3.5   Non-Structural Factors Affecting FFAC Values

FFAC is desired to be an indicator of microstructure - mainly the internal asphalt mastic distribution of foamed asphalt mixes. However, some non-structural factors, i.e. the factors other than the spatial configuration of the individual phases, can also affect FFAC values.   These factors need to be well understood and their effects have to be minimized or controlled to build clear and simple relations between FFAC and mix microstructure.

3.5.1 Strengths of asphalt mastic and mineral filler

For a given foamed asphalt mix, the strengths of the asphalt mastic phase and the mineral filer phase, or their ratio, significantly influences the asphalt mastic distribution on fracture faces.   As shown in Figure 3.4, the appearance of the fracture faces is partially determined by the path along which the fracture "chooses" to propagate.   The propagation path of a fracture in a composite material such as foamed asphalt mixes is determined by both the microstructure and the relative strength of the individual phases.   It was assumed in the example discussed in Section 3.3.2 and

Figure 3.4 that the tensile strength of the asphalt mastic phase is higher than that of the mineral filler phase, which is not always true. If, under certain circumstances the mineral filler phase is stronger than the asphalt mastic phase, the crack in Figure 3.4(b) is more likely to propagate along Path B1 instead of Path B2. The fracture faces yielded by Path B1 would have even higher FFAC values than those by Path A1 or A2. This situation is undesirable from a fracture face image analysis point of view because FFAC is expected to be an indicator of foamed asphalt distribution in the mix with higher values representing better and more uniform dispersion.

The strengths of the mineral filler phase and the asphalt mastic phase in foamed asphalt mixes are controlled by different mechanisms. The tensile strength of the mineral filler phase is mostly attributed to weak chemical cementation and suction from the residual water. Carbonates, iron oxide, alumina and organic matter contained in the PAP may precipitate at inter-particle contacts and act as cementing agents (Mitchell & Soga, 2005). The small amount of residual water provides matric suction and osmotic suction enabling the material to resist tensile stress (Fredlund & Rahardjo, 1993). Introducing water by soaking the specimen dramatically impairs both of these two mechanisms. On the other hand, the tensile strength of the asphalt mastic phase is generally attributed to adhesion of asphalt cement. It is well known that the adhesive strength of asphalt cement is temperature and loading rate dependent: it is higher at a lower temperature and a higher loading rate, and vice versa. The strength of asphalt mastic is also negatively affected by moisture, but its sensitivity is less than that of the mineral filler. This will be quantitatively evaluated in Section 3.6.1.

The effects of the relative strengths of the asphalt mastic phase and the mineral filler phase on FFAC values are demonstrated by the following two cases. The loading temperature/rate and water conditioning are the external factors affecting strengths of individual phases in the following two examples.

The effects of loading rates and temperature are illustrated by two extreme combinations of loading rate and temperature applied to one beam specimen. This beam specimen was fabricated in Phase II of the UCPRC laboratory study (Section 2.16). PAP 33-C was treated with 3% foamed PG64-10 asphalt. No cement or other active fillers were added. Mix preparation and specimen compaction followed the procedures described in Sections 2.5 and 2.9. The beam was not subjected to the flexural strength test as described in Section 2.9. Instead, special procedures were followed to generate the two pairs of fracture faces shown in Figure 3.7 (only one face of each pair is shown).

First, after being cured for seven days at 40°C, the beam was supported at both ends in a forced draft oven at 40°C, and it broke under its own weight yielding fracture faces as shown in Figure 3.7(a). The second pair of fracture faces shown in Figure 3.7 (b) was obtained by splitting one of the broken pieces with a hammer blow after it had cooled to 20°C. The first loading condition represents a slow loading rate at an elevated temperature. The second loading condition represents the opposite condition of fast loading at a lower temperature, and the asphalt mastic strength was significantly higher under the hammer blow than it was under the first loading condition. The strength of the mineral filler phase is largely independent of temperature,

and much less sensitive to loading rate than is the asphalt mastic phase. It is apparent that the

FFAC value for the fracture face shown in Figure 3.7(a) is much higher than that in Figure 3.7(b)

for the reasons as discussed previously.
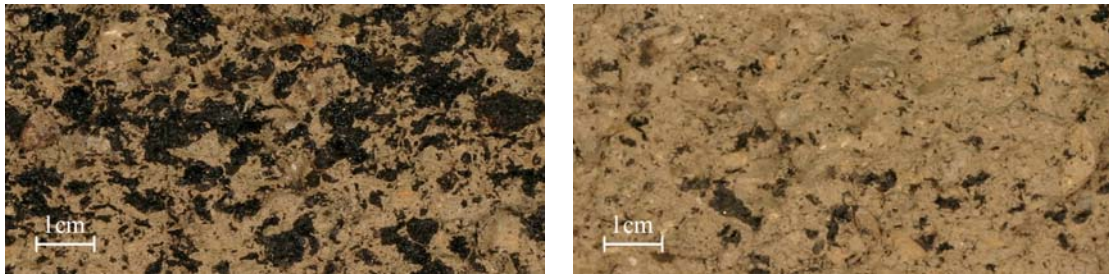
(a) Slow loading rate at high temperature;   (b) fast loading rate at low temperature
Figure 3.7   Fracture faces of the same beam yielded by different loading rate-temperature combinations

Figure 3.8 shows the comparison of FFAC values between the 100mm ITS specimens tested after

curing without water soaking (unsoaked), and their replicate specimens tested after 72 hours of

soaking.   The test data shown in Figure 3.8 were from Phase II of the UCPRC laboratory study.

In both figures, each data point represents one PAP type treated with one type of asphalt

compacted with one compaction effort level (six PAP types, two asphalt types, three compaction

levels, totaling 36 combinations as shown in Table 2.4), and the results shown are average values

for replicate batches and replicate specimens.

On average, FFAC values for unsoaked specimens are 48% higher than for soaked specimens of

the same mix types.   Apparently, the strength ratio between asphalt mastic and mineral filler

increased after water soaking (strength reduction for mineral filler is more significant), and

fractures showed a stronger tendency to propagate through the mineral filler phase and avoid the

asphalt mastic phase wherever possible.
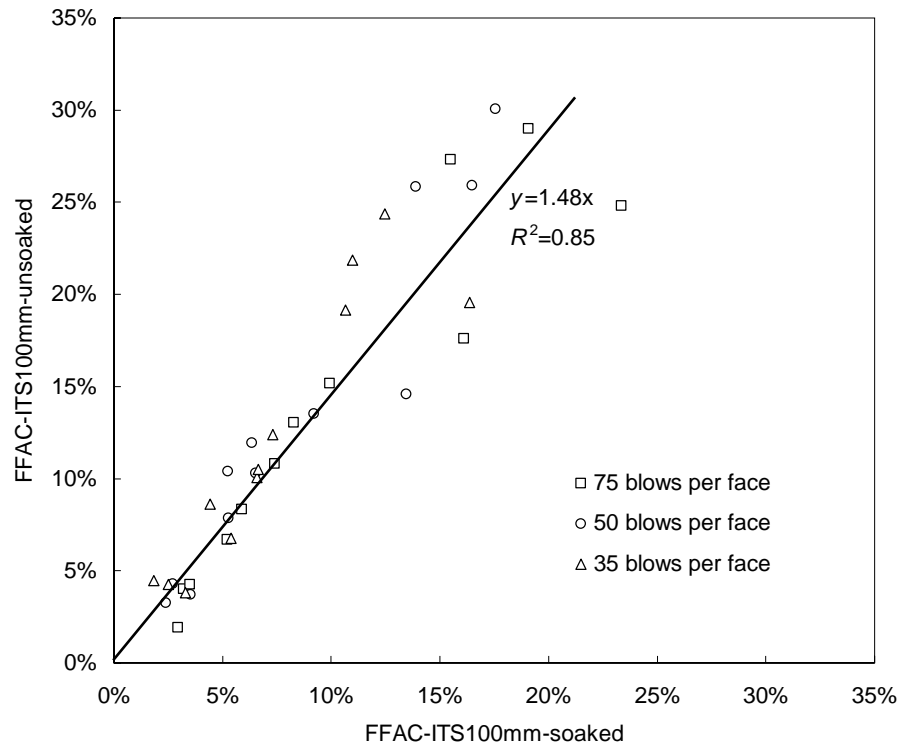
Figure 3.8   Comparison of FFAC values between soaked and unsoaked ITS specimens

3.5.2 Specimen fabrication methods and testing boundary conditions

The compaction method used to fabricate specimens and the test methods (or the associated test

boundary conditions) also have significant effects on FFAC values for foamed asphalt mixes.

Although the distribution of the asphalt mastic phase (i.e. asphalt mastic droplets) in a loose mix

is determined at the mixing stage, the specimen fabrication and compaction methods affect how

the asphalt mastic phase is distributed in laboratory specimens.   Moreover, the test method (or

the test boundary condition) determines where the fractures initiate and how they propagate

through the specimens, thus affecting FFAC.   Figure 3.9 compares FFAC values of soaked

specimens from the same batches of mixes between 100mm and 152mm ITS tests, and between

100mm ITS and flexural beam tests.   All the results shown are for soaked specimens, and the

ITS-100 mm results were for the high compaction effort level (75 hammer blows per face) only.

Most data points are above the 1:1 reference line, which implies that 152mm ITS and flexural

beam specimens tend to have higher FFAC values than do 100mm ITS specimens.
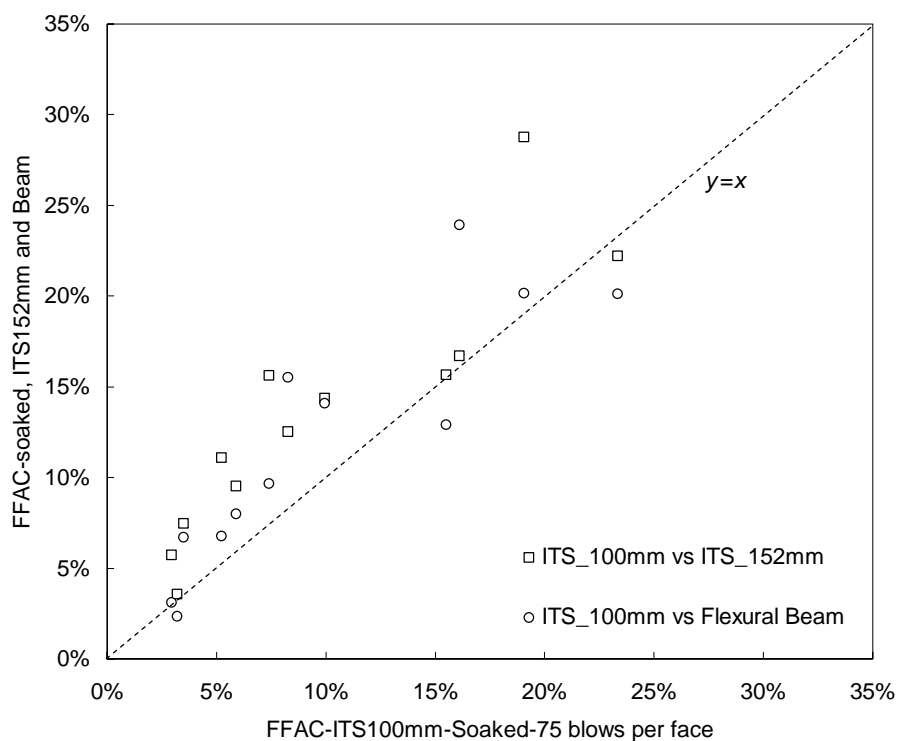
Figure 3.9   Comparison of FFAC values between different test methods

3.5.3 Preferable test condition for fracture face image analysis (FFIA)

As shown in the above qualitative analysis, FFAC is primarily an indicator of the asphalt mastic

phase distribution in foamed asphalt mixes.   It is also affected by other controllable factors,

namely the relative strengths of different phases in the mixes, the specimen fabrication and

conditioning methods, and the test boundary conditions. FFAC should therefore only be used to assess specimens that were fabricated using the same method and were tested with the same test configuration (e.g. testing temperature and loading rate). To make FFAC a positive indicator of asphalt mastic dispersion (i.e. higher values indicating more preferable dispersion patterns), it is desirable that the strength of the asphalt mastic phase is greater than that of the mineral phase. Therefore, soaked specimens in the absence of active fillers should be employed. FFAC is suited for comparing asphalt mastic distributions as a function of mix parameters such as asphalt type, asphalt content, mixing temperature, mixing moisture content, etc. Preferably when the effects of one of these variables are investigated, values of all other mix variables should be the same for all mixes to be compared. All the principles mentioned in Section 3.3.2 are of a comparative nature, and they are strictly valid if the mixes to be compared are based on the same PAP material. Comparisons of FFAC values for mixes with different gradations are also occasionally made in this thesis, but caution should be taken when interpreting results in those situations.

3.6   Interpretation of Strength Behavior Based on Fracture Face Image Analysis

This section discusses strength behavior of foamed asphalt mixes based on FFIA results. These examples demonstrate how FFIA can help us understand of the effects of mix variables on strength of foamed asphalt materials. On the other hand, through these cases, more understanding into the Fracture Face Image Analysis method can be gained.

3.6.1 Tensile strengths of asphalt mastic and mineral filler

In this example, the effects of dispersed foamed asphalt on tensile strength of foamed asphalt mixes are discussed. By using FFIA, the contributions to mix strength from the asphalt mastic phase and the mineral filler phase can be individually estimated. The data were from Phase I of the UCPRC laboratory study (Section 2.15). Attributes of the (plant processed) RAP materials being treated and properties of the asphalt binder (AR-4000) used were elaborated in Sections 2.2 and 2.3, respectively. 100 mm ITS specimens were prepared at a compaction effort level of 75 hammer blows per face. The mix preparation, specimen fabrication, curing, conditioning and test procedures are similar to those discussed in Sections 2.5, 2.13, 2.14, and 2.6, respectively, except that the mixing temperature was not well controlled, resulting in variable asphalt dispersion quality.

Figure 3.10(a) and (b) show the correlations between FFAC and ITS values under the soaked and unsoaked conditions, respectively. In Figure 3.10(a), a linear correlation exists between FFAC and soaked ITS with the R^2 (coefficient of determination) value as high as 0.87. As mentioned in Section 3.5.3, caution should be taken when directly comparing FFAC values of materials with different gradations, but the correlation shown in Figure 3.10(a) appears to be largely independent of gradations and asphalt contents. However, this should not be taken as a universal rule or common phenomenon. The three gradations (RAP-1, -2 and -3) as shown in Figure 2.1 are more or less similar to each other. In Figure 3.10(b), a similar but less distinct correlation exists.
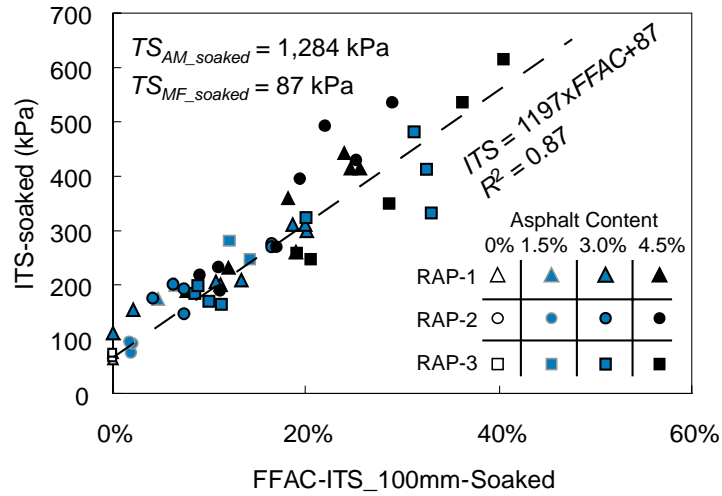
(a) Soaked test results
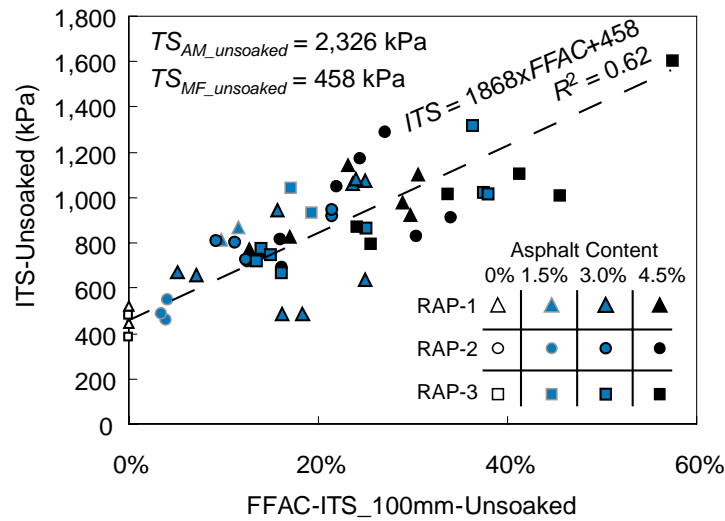
(b) Unsoaked test results

Figure 3.10 Correlation between FFAC and ITS for various mix designs

It is assumed that the overall tensile strength (soaked and unsoaked) of a foamed asphalt mix (TS_{FA}) is a function of the tensile strength of the mineral filler phase (TS_{MF}) and strength of the asphalt mastic phase (TS_{AM}), as expressed in equation (3.1).

$$TS_{FA} = TS_{MF} + (TS_{AM} - TS_{MF}) \times FFAC \tag{3.1}$$

where TS_{FA}, TS_{MF}, and TS_{AM} are the tensile strengths of the foamed asphalt mix, the mineral filler phase and the asphalt mastic phase, respectively.

The tensile strength of the two phases under the soaked and unsoaked conditions can be determined by comparing equation (3.1) to the linear regression results shown in Figure 3.10(a) and (b), respectively.   When the foamed asphalt mixes are soaked, the mineral filler phase loses approximately 81% of its tensile strength (from 458 kPa to 87 kPa) and the asphalt mastic phase loses 45% of its tensile strength (from 2,326 kPa to 1,284 kPa).   This indicates that the tensile strength of the mineral filler phase is much more water sensitive (or less water resistant) than that of the asphalt mastic phase.

3.6.2 Soaked vs. unsoaked strength tests

This section discusses the choice of soaked versus unsoaked strength tests for mix evaluation based on the water sensitivities of the different phases.

Asphalt cement in foamed asphalt mixes only partially coats aggregates, unlike HMA materials, where most aggregates are completely coated.   The voids ratio and permeability of foamed asphalt mixes are typically high allowing water to infiltrate into them from outside the pavement or from wet subgrade, and thus the mix properties in the field are sensitive to moisture conditioning.   The foamed asphalt treated base layer is usually built on top of a thin existing granular subbase layer or directly on the subgrade and is therefore susceptible to seasonal moisture fluctuations.   In farming areas, the situation is often aggravated by irrigation and land

preparation practices that impact roadside drainage. Understanding the effects of water conditioning on foamed asphalt strength behavior is important for adopting appropriate design philosophies and effective test methods.

Most laboratory test studies on foamed asphalt mixes reported in the literature were based on strength testing, primarily using the ITS test, under both unsoaked and soaked conditions. However, two different approaches have been employed in the literature for interpreting unsoaked and soaked test results:

- In the mix design and structural design procedures presented in the South African guidelines (Asphalt Academy, 2002) and the Wirtgen Cold Recycling Manual (Wirtgen GmbH, 2004), unsoaked strengths (both ITS and UCS) are recommended as the primary properties to be maximized, and the maximum moisture susceptibility in terms of Tensile Strength Retained (TSR) is specified. The minimum allowable TSR value, which is the ratio of soaked strength to unsoaked strength, varies between 50 percent and 75 percent depending on local climate.

- Muthen (1998) proposed that foamed asphalt specimens should be tested at the most severe possible working environment (i.e. under soaked conditions). Romanoschi et al. (2004), Marquis et al. (2003) and Kim and Lee (2006) followed Muthen's philosophy to optimize mix design variables solely according to soaked strength values.

The different mechanisms that contribute to foamed asphalt mix strength need to be considered

when studying the implications of unsoaked versus soaked laboratory testing. Cured, unsoaked, untreated PAP specimens (control mixes) normally have measurable tensile strength, which can be generally attributed to the following three mechanisms:

- Weak chemical bonding. The aggregates and fines in the HMA and granular base materials in the original pavement being recycled may contain carbonates, oxides, silicates, organic matter, and other reactive components, which could precipitate at inter-particle contacts and act as cementing agents (Mitchell & Soga, 2005).

- Suction from the residual water. Specimens that have been subjected to oven curing at 40°C still retain some residual moisture after removal from the oven. According to Jenkins (2000), the moisture content of these specimens is generally between zero and 1.5 percent, but always lower than 4.0 percent. According to Lu et al.'s (2007) calculation for an idealized spherical particle model, the tensile strength contributed by capillary suction in silts is typically several tens of kPa. Osmotic suction, which also contributes to the total suction, is often of the same magnitude as capillary suction.

- Adhesion of the old oxidized asphalt binder. Although the residual binder in RAP has been partially oxidized, it can still develop cohesion during compaction, with the level dependent on the extent of oxidization and the temperature at which the material is compacted and cured. Compared to the other two mechanisms discussed above, this mechanism is considered to be of a lesser importance, and therefore is ignored in the following discussion.

These mechanisms are also applicable to foamed asphalt treated materials. In addition, asphalt

mastic contributes to the overall tensile strength by bonding aggregate particles together. During this study, observations of the fracture faces of tested ITS and flexural beam specimens revealed that fractures seldom (if ever) initiate in and propagate through aggregate particles due to the much lower strength of the other phases in the mix.

If foamed asphalt specimens are tested for tensile strength in the unsoaked state, three of the mechanisms discussed above (weak chemical bonding, suction, and foamed asphalt bonding) all contribute to the measured strength. However, when foamed asphalt specimens are soaked in water, most of the voids are fully or partially filled with water. The weak chemical bonds between aggregates are significantly weakened and suction is greatly reduced. The bonds provided by asphalt mastic are also negatively affected by soaking, but to a lesser extent. As seen in the example of Section 3.6.1, after soaking the mineral filler phase of the RAP lost 81% of its tensile strength, whereas the strength reduction for the asphalt mastic phase was 45%. Therefore, under soaked conditions and in the absence of active fillers, the tensile strength of foamed asphalt mixes is primarily provided by asphalt mastic, the bonding effects of which are readily measurable.

Table 3.1 and Figure 3.11 provide a summary of the strength test results using three different test methods (100 mm ITS, 152 mm ITS and flexural beam), two different moisture conditions (unsoaked and soaked), two PAP sources (SR33 and SR88), and three gradations (in place [-A], coarse [-B], and fine [-C]). The results from the untreated mixes are also included, and identified as "control". Each strength value shown for the treated specimens are the average of

the two binder types (PG64-16 and PG64-10 both with an asphalt content of 3.0 percent) and

averaged over all the replicate specimens tested.
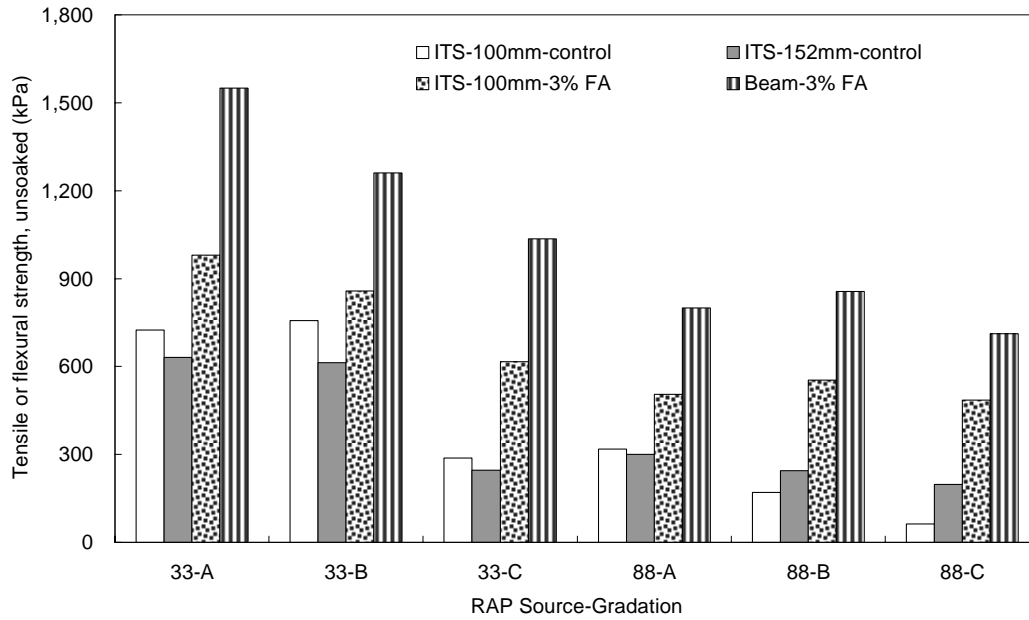
(a) Unsoaked test results
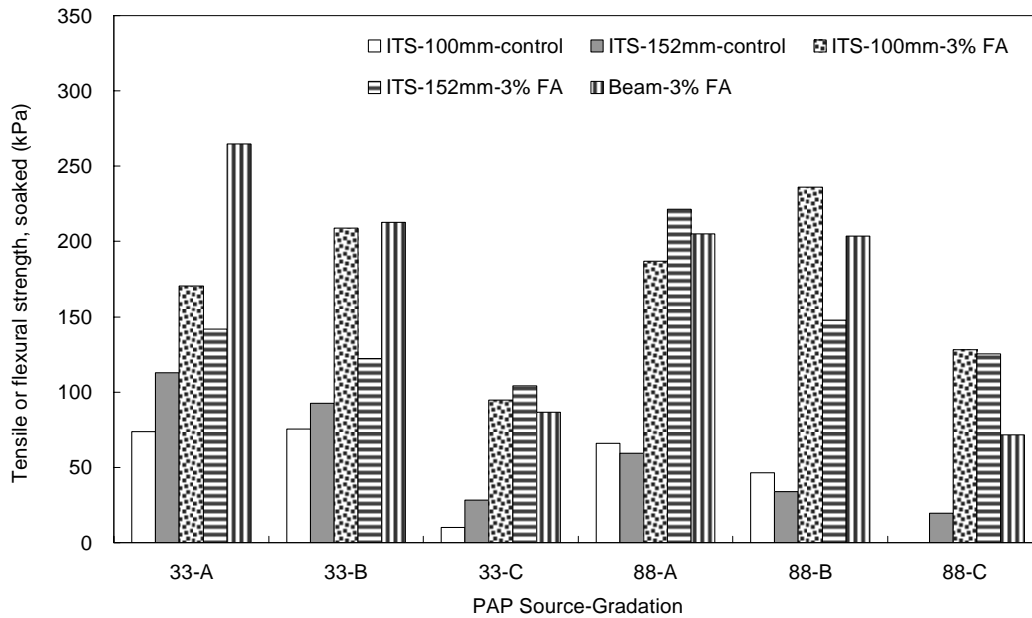
(b) Soaked test results

Figure 3.11 Comparison of unsoaked and soaked strength test results

Table 3.1   Indirect tensile strength and flexural strength of various foamed asphalt mixes under soaked and unsoaked conditions

| PAP Type | Unsoaked | | | | Soaked | | | | |
| | Control | | 3% Foam Asphalt | | Control[1] | | 3% Foam Asphalt | | |
	ITS 100 mm[1]	ITS 152 mm	ITS 100 mm[2]	Beam	ITS 100 mm[1]	ITS 152 mm	ITS 100 mm[1]	ITS 152 mm	Beam
33-A	725[3]	632	979	1,550	74	113	170	142	265
33-B	756	613	857	1,261	76	92	209	122	213
33-C	287	246	616	1,036	10	28	95	104	87
88-A	318	300	505	800	66	60	187	222	205
88-B	172	244	555	856	46	34	236	148	204
88-C	64	198	486	711	0	20	128	125	72

[1]   Untreated mixes.

[2]   Only average of results for compaction with 75 blows shown.

[3]   All strength values shown are in kPa.

The results indicate that the unsoaked control mixes of the SR33-A and SR33-B materials had much higher tensile strengths than the other control mix types.   The higher strengths were attributed to a weak chemical reaction between the fines, given that the addition of 15 percent baghouse dust (which diluted the existing fines) to the SR33-C mix resulted in significantly lower strength.   The added baghouse dust thus appeared to dominate the unsoaked strength of the SR33-C material.   The weak cementation and suction were mostly eliminated after the specimens were subjected to water conditioning, with the SR33-A and SR33-B control mixes losing 80 to 90 percent of their unsoaked strength.

The foamed asphalt treated mixes showed similar trends.   Although the ITS and flexural beam

strength values increased with the addition of foamed asphalt, the unsoaked strengths still appeared to be dominated by the properties of the PAP materials. The unsoaked ITS values of the treated SR33-A and SR33-B materials were between 44 and 120 percent higher than those of the other four PAP materials. In contrast, the soaked tensile strengths of the SR33-A and SR33-B materials were similar to, or less (depending on the test method) than, those of other treated PAP materials. This indicates that the properties (chemical bonding and suction) dominating the unsoaked strengths are not significant when the materials are soaked prior to testing. These results clearly indicate that the stabilizing effects of foamed asphalt are best observed under the soaked condition, which is desirable for mix evaluation purposes.

3.6.3 Effects of density on microstructure and strength

In Phase II of the UCPRC study, three levels of compaction effort (35, 50, and 75 blows per face, or high, medium and low) were used to compact the 100 mm-ITS specimens as seen in Table 2.4. The bulk specific gravity, soaked ITS test results, and FFAC values of the ITS specimens are summarized in Table 3.2. The results shown in Table 3.2 are averages of the values for two binder grades, replicate batches of mixes, and replicate specimens for each batch. Data shown in Figure 3.12 and Figure 3.13 are average values for replicate batches of mixes, but results for the two grades of asphalt are shown separately. Due to the large number of specimens to measure and the limited available resources, the standard procedures for measuring bulk specific gravity of hot mix asphalt were not followed to measure the densities of these specimens. Instead, the diameter and height of each ITS specimen were measured, from which the bulk

volume was estimated. Since the surfaces of the specimens after curing were not perfectly

smooth, a high variance was observed. However, the overall comparison of bulk specific

gravities between different compaction effort levels should be valid, given that a consistent

procedure was followed.

Table 3.2   Effects of compaction effort on density, soaked strength and FFAC

PAP	75 blows/face			50 blows/face			35 blows/face		
	BSG[1]	ITS (kPa)	FFAC	BSG[1]	ITS (kPa)	FFAC	BSG[1]	ITS (kPa)	FFAC
33-A	2.12	170	12.7%	2.07	131	11.5%	2.03	89	9.2%
33-B	2.11	209	21.2%	2.06	131	17.0%	1.98	92	14.4%
33-C	2.15	95	4.2%	2.14	89	4.0%	2.10	75	4.0%
88-A	2.06	187	5.5%	1.99	143	5.0%	1.95	103	5.0%
88-B	2.11	236	12.2%	2.09	176	9.9%	2.03	121	8.6%
88-C	2.11	128	4.4%	2.07	110	3.8%	2.02	81	3.1%

[1]BSG = bulk specific gravity

On average, the resulting bulk densities of the specimens compacted with the medium

compaction effort were two percent lower than the bulk densities of the specimens compacted

with the higher effort, and soaked ITS values were 26 percent lower as shown in Figure 3.12.

Similarly, the density and strength reduction for the specimens compacted with the low

compaction effort were 4 percent and 48 percent lower, respectively, compared to the high

compaction effort specimens. The effects of compaction on strength of foamed asphalt mixes

are very significant, and the highest practically possible density should be strived for during

construction.
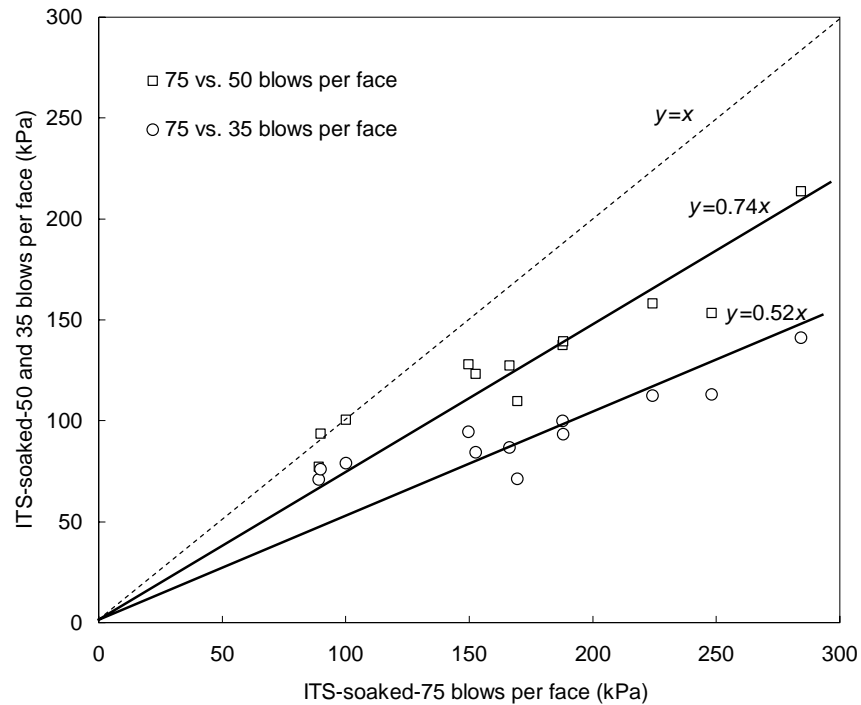
Figure 3.12 The effects of compaction effort on ITS

The comparison of FFAC values between specimens compacted with different effort levels is shown in Figure 3.13.   On average, specimens compacted with the medium and low compaction effort levels also showed lower FFAC values, by 17% and 29% respectively compared to those for high compaction effort specimens of the same mixes.   As discussed in Section 3.3.2, volumetric characteristics of the asphalt mastic phase in a foamed asphalt mix, for example the volumetric ratio between asphalt mastic and mineral filler, and the size distribution of asphalt mastic droplets primarily determine FFAC values.   As these characteristics are the same for specimens fabricated from the same batch of mix and independent of the compaction effort level, compaction must affect FFAC values through a different mechanism that was not discussed in previous sections.   One possible mechanism is illustrated in Figure 3.14.   As compaction effort increases, the two adjacent aggregate particle becomes closer.   The asphalt mastic droplet

between the two particles is squeezed and forced to extend along the gap between them.   The

contact area between the asphalt mastic droplet and each aggregate particle also becomes larger

as the density increases, resulting in greater bonding strength after curing.   Apparently, mixes

with higher density should have higher strength and yield fracture faces with higher asphalt

mastic coverage according to this mechanism, although other mechanisms might also apply.
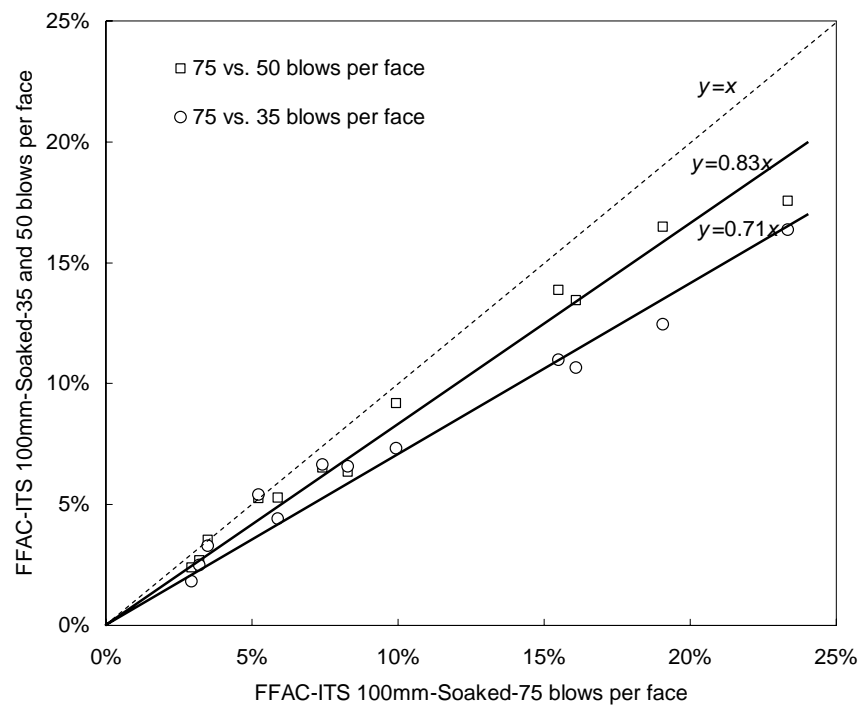
Figure 3.13 The effects of compaction effort on FFAC

Aggregate particles   Asphalt mastic droplet

(a)   (b)   (c)
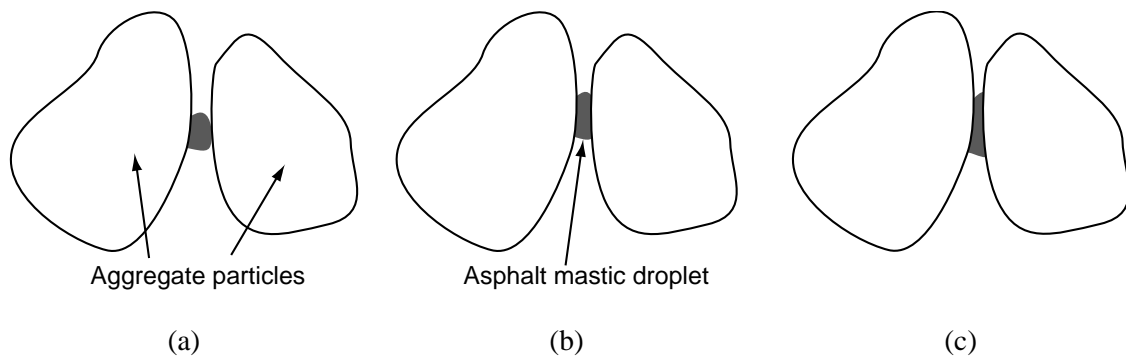
Figure 3.14 One possible mechanism by which compaction affects FFAC
(a) Low compaction effort; (b) medidum compaction effort; and (c) high compaction effort.

3.6.4 Effects of asphalt binder properties on strength

As shown in the experiment factorial design in Table 2.4, two asphalt binder types (or grades), PG64-16 and PG64-10 from the same refinery were tested in Phase II of the UCPRC laboratory study. Some basic characteristics of the asphalt binders are described in Section 2.3, and their foaming characteristics as measured in Phase II of the UCPRC study are described in Section 2.16. The effects of binder grades on the soaked strength of 100 mm and 152 mm ITS specimens are summarized in Figure 3.15. The mixes treated with the softer (less viscous) PG 64-16 asphalt generally had higher tensile strengths and better asphalt distribution represented by higher fracture face asphalt coverage (FFAC) values than the PG64-10 binder. One exception was the 100 mm ITS tests for PAP 33-B, for which the mix treated with the PG64-10 binder had both better asphalt dispersion (higher FFAC value) and higher strength. Another exception was the 152 mm ITS tests for PAP 33-A, for which the mix treated with the PG64-16 binder had better asphalt dispersion but lower strength. For some PAP-asphalt binder combinations, only one batch of mix was made due to material, equipment and schedule limitations, and high variation in test results were observed. These two exceptions are attributed to such variation.

Two characteristics of an asphalt binder primarily determine the capacity of foamed asphalt (after being foamed and mixed) to improve the tensile strength of granular materials:

- The level of dispersion of the asphalt in the mix, and

- The strength of bonding provided by the dispersed asphalt.
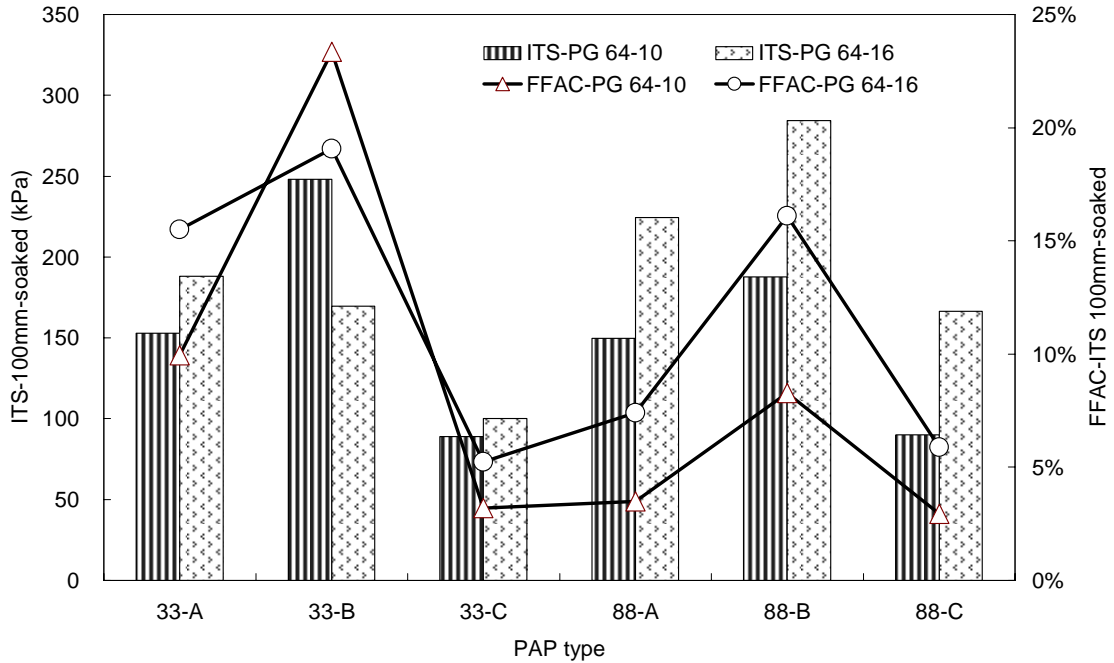
(a) Results for 100 mm ITS tests
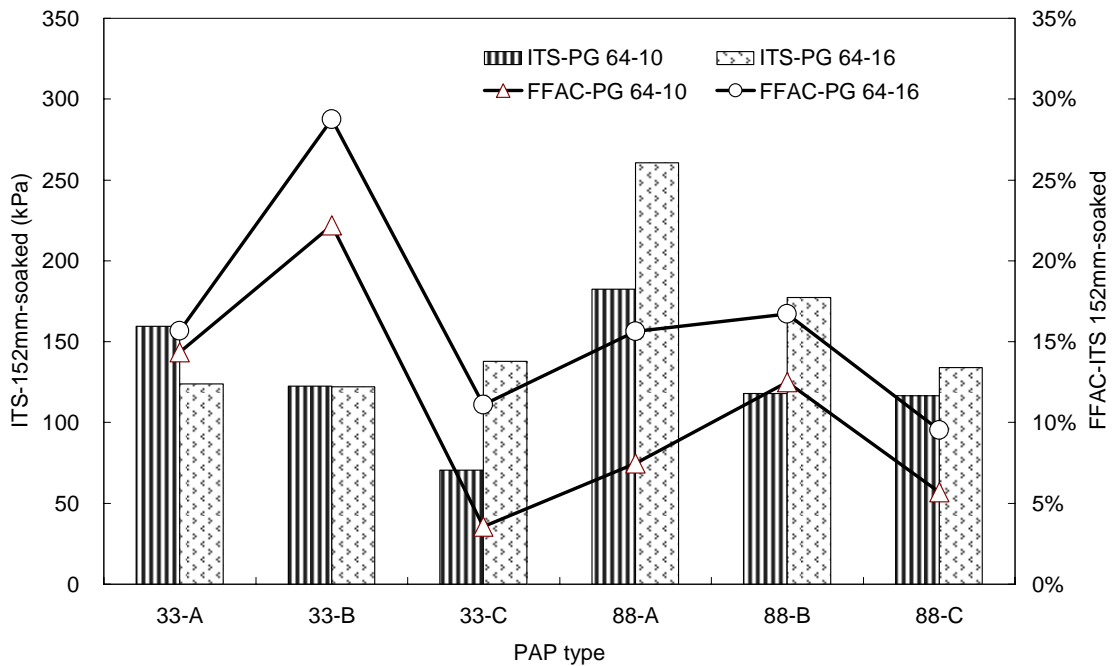
(b) Results for 152 mm ITS tests

Figure 3.15 Effects of asphalt binder grade on strength and FFAC

The grade of asphalt influences these characteristics in opposing ways. Test results indicate that

the softer (or less viscous) asphalt (PG64-16) has better dispersion. Although the two grades

used in this study have similar foaming characteristics in terms of the expansion ratio and half-life (Section 2.16), Fracture Face Image Analysis results clearly show that the softer grade has significantly better dispersion.   The softer asphalt has lower viscosity than the harder asphalt at the same temperature and same expansion ratio.   It is considered likely that when the asphalt bubbles collapses, the softer asphalt film adheres to more of the finer aggregate particles.

It is intuitive to assume that the bonding provided by the harder asphalt should have higher strengths at the same temperature and loading rate.   However, the test data clearly show that asphalt mastic dispersion, as quantified by FFAC values, has a dominant influence on strength.

The direct implication of this phenomenon to engineering practice is that when different asphalt binders with similar foaming characteristics (expansion ratio and half-life) are available, the softer (or less viscous) binder should be chosen.

3.6.5 Effects of PAP gradations

The three simple rules for mapping 2D asphalt mastic distribution on fracture faces to 3D asphalt mastic distribution in mixes as elaborated in Section 3.3.2 are all valid on a comparative basis for comparing mixes made of the same PAP material (i.e. PAP source and gradation).   Examples in Sections 3.5.1–3.6.4 only involve comparison of FFAC values of mixes with similar (Section 3.6.1) or exactly the same (all other sections) PAP source-gradation combinations.   The effects of PAP source and gradation are more complex than the effects of other factors investigated in this chapter.

The correlations between FFAC and strength for soaked 100 mm ITS, 152 mm ITS, and flexural beam tests are shown in Figure 3.16. Each data point represents one combination of PAP type and asphalt type, and the value shown is the average of replicate batches of mixes and replicate specimens. All the mixes shown had an asphalt content of 3%, and for 100 mm ITS tests only the results for specimens compacted with the high compaction effort level (75 hammer blows per face) are shown. The correlations are not as distinct as that shown in Figure 3.10 owing to the wide spectrum of gradations used. However, some general trends common to all of the three test methods can be observed.

For PAPs with a large quantity of mineral fillers (passing a 0.075 mm sieve), such as PAPs 33-C and 88-C, the FFAC and strength values are usually low. For a given foamed asphalt content, as the fines content of a PAP increases, the fraction of mineral fillers that is bonded by foamed asphalt decreases, and fines that remain free of bonding increase. Therefore, for PAPs with a higher fines content, the volumetric ratio of the asphalt mastic phase to the mineral filler phase is smaller. A possible corresponding microstructure is illustrated in Figure 3.17(a), where excessive mineral filler forms a continuous mineral filler phase and prevents asphalt mastic droplets from effectively bonding large aggregate particles together. The soaked strength of this type of foamed asphalt mix is limited by the soaked strength of the mineral fill phase, which is typically low. Fracture faces are mostly covered by mineral filler and strength improvement from asphalt mastic is limited.

On the other hand, for PAPs with a small quantity of fines (PAPs 33-A, 33-B and 88-B), a

microstructure as shown in Figure 3.17(c) is possible. The volumetric ratio of asphalt mastic to mineral filler is high, and an "open" microstructure is likely to form. Many asphalt mastic droplets visible on fracture faces actually do not participate in bonding large aggregate particles and thus the contribution to tensile strength is low. Consequently, although a large portion of the fracture faces is covered by asphalt mastic (high FFAC values), the strength is not proportionally high.

Figure 3.17(b) shows microstructural features somewhere between the two aforementioned extreme cases. FFAC values for such a microstructure are not as high as those of the microstructure shown in Figure 3.17(c), but strength might be comparable.
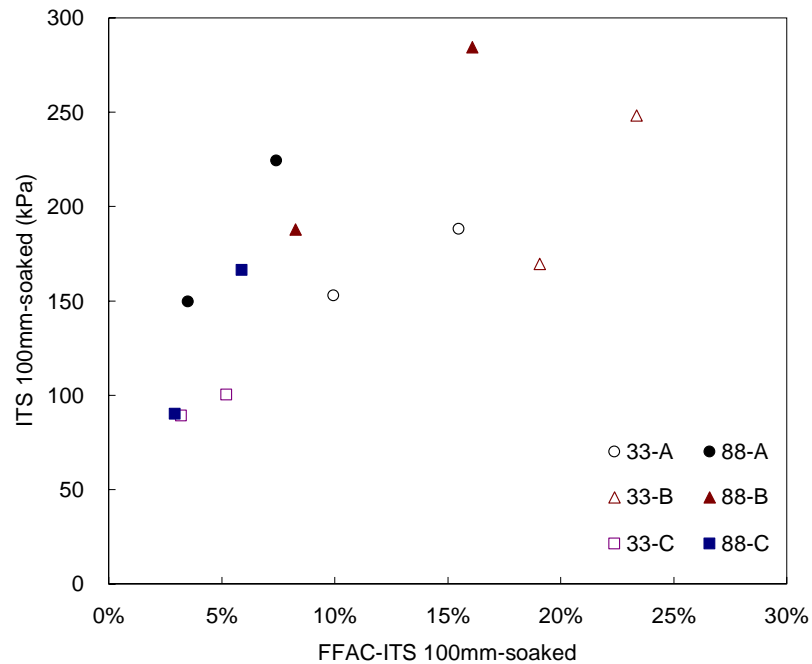
(a) Soaked 100 mm ITS tests
Figure 3.16 Correlation between FFAC and soaked strength for different test methods
(to be continued)
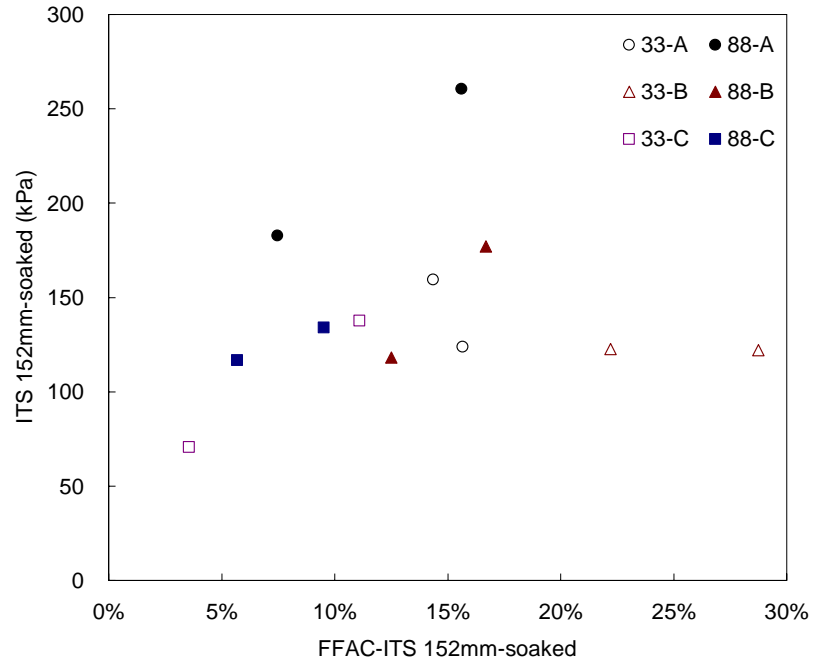
(b) Soaked 152 mm ITS tests
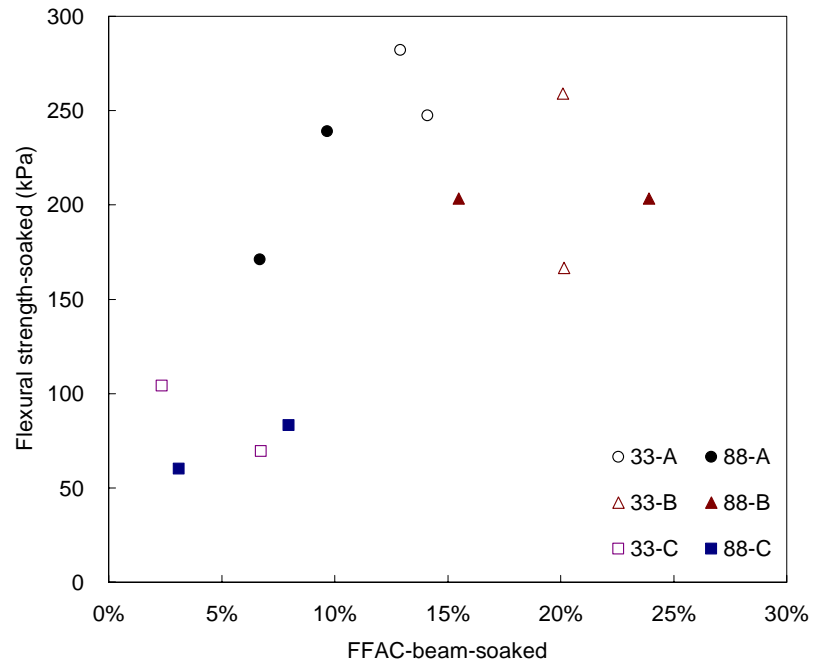
(c) Soaked flexural beam tests

Figure 3.16 Correlation between FFAC and soaked strength for different test methods
(continued)
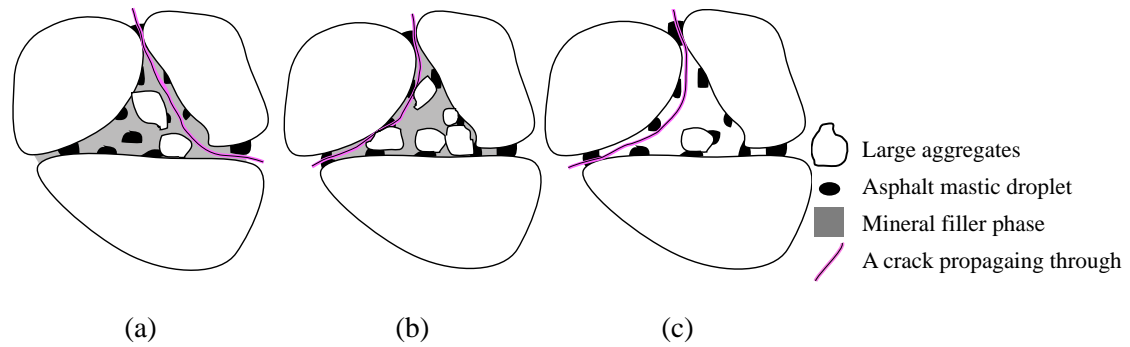
Figure 3.17 Conceptual microstructures corresponding to different PAP gradations
(a) Material with a high fines content; (b) with a intermediate fines content; (c) with a low fines content.

It is apparent that FFAC values of foamed asphalt mixes with significantly different PAP gradations should not be directly compared to predict strength behavior. Mixes yielding higher FFAC values do not necessarily result in higher strength. Even for mixes with similar PAP gradations, such direct comparison should be treated with caution. As seen in Figure 2.2 and Table 3.2, PAPs 33-B and 88-B have similar gradations. When they are treated with three percent foamed asphalt, 33-B mixes yield significantly higher FFAC values than do 88-B mixes, but strengths of treated 33-B mixes are only slightly lower than those of 88-B mixes. Although the two PAP materials have the same proportion by mass passing a 0.075 mm sieve, particle size distributions for particles smaller than 0.075 mm might be significantly different, which cannot be measured by conventional sieve analysis. The constituents of these two PAPs might be slightly different as suggested by the different pH values (Table 2.2). These factors may have contributed to this phenomenon, but were not further investigated in this study.

3.7   Diagnosing Mix Problems with Qualitative Fracture Face Inspection

Qualitative and empirical fracture face inspection in conjunction with conventional strength testing can help identify problems in foamed asphalt mixes for project level mix evaluation/ design.   This visual inspection can be undertaken by experienced engineers, and does not require special digital image analysis hardware or computer software.

Although the appearance of foamed asphalt mix fracture faces is highly dependent on the granular material (PAP in most cases) being treated, some general guidelines are provided.

On fracture faces of ideal good quality foamed asphalt mixes, asphalt mastic spots should be uniformly distributed.   For soaked ITS specimens, Fracture Face Asphalt Coverage (FFAC) values should be close to or greater than 15%.   Large asphalt mastic spots with diameters greater than 10 mm should be rare, and large areas without asphalt coverage should be rare as well. Such a fracture face is shown in Figure 3.18(a).

On the fracture face shown in Figure 3.18(b), a concentrated asphalt mastic distribution with large asphalt mastic spots (or "patches") is visible.   The FFAC value for this specimen might be high, but that for its replicate specimens might be low, resulting in high variation.   This situation often indicates inferior and non-uniform asphalt distribution.   Possible reasons include: 1) the asphalt binder has poor foaming characteristics, 2) the temperature of the aggregate being treated is too low, and/or 3) the mix was too wet and large agglomerations of fine aggregates are formed as will be discussed in Chapter 6 .
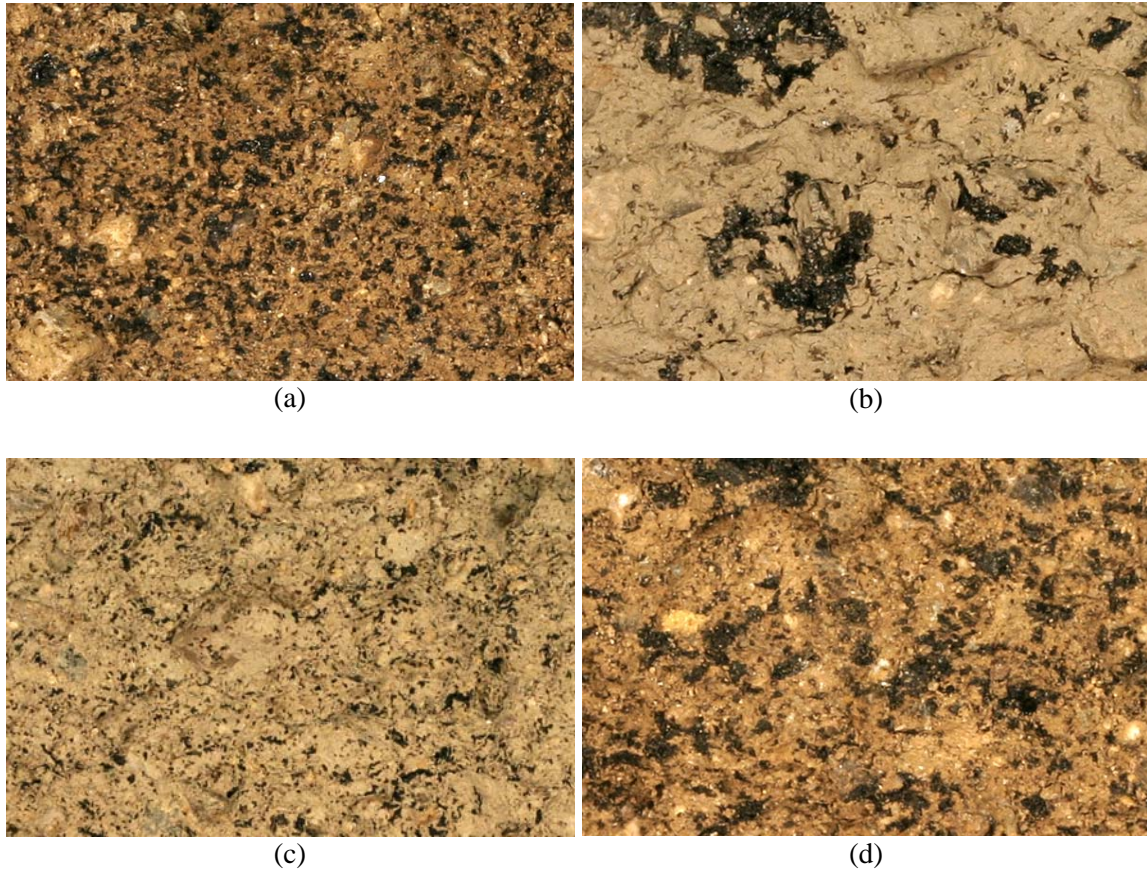
Figure 3.18 Typical fracture faces showing different asphalt distribution features
Note: Approximately 80% of the fracture surface area [~80 mm × 50 mm] is shown in each
photo.

The fracture face shown in Figure 3.18(c) has a uniform asphalt mastic spot distribution with small spot sizes. However, the asphalt coverage ratio is low. This might indicate that the fines content of the aggregate is too high. Although foamed asphalt has satisfactory dispersion in these mixes, there is still a large quantity of free mineral filler forming a largely continuous and weak mineral filler phase. Soaked indirect tensile strengths of such mixes are typically lower than 100 kPa. Measures to improve the effectiveness of foamed asphalt stabilization for these mixes include: 1) introducing coarser aggregate to reduce the fines content, 2) increasing asphalt content, and 3) changing the pulverization procedure to reduce fines produced.

The fracture face shown in Figure 3.18(d), on the other hand, has a high asphalt coverage ratio but shows numerous large asphalt spots. This might indicate that the quantity of fines is small, and the corresponding microstructure might be similar to that shown in Figure 3.17(c). However, as long as the soaked tensile strength is acceptable, no special measures are recommended to modify the gradation.

3.8   Summary and Conclusions

The primary task of this chapter was to develop a microstructure characterization method to quantify asphalt mastic phase distribution in foamed asphalt mixes. A literature survey found that a number of methods, mainly via image analysis of specimen cross sections (including thin sections) and X-ray CT scanning were previously developed for quantifying hot mix asphalt (HMA) microstructures. However, none of these can be applied to foamed asphalt materials due to difficulties in obtaining smooth cross sections or the complex constituents unsuitable for CT scanning and analysis. Based on observations on fracture faces of tested ITS specimens, the idea was initiated to imply 3D asphalt mastic distributions in foamed asphalt mixes from 2D asphalt mastic distributions on fracture faces. Such a method is termed Fracture Face Image Analysis, or FFIA.

In an ITS test or flexural beam test, two fracture faces are generated when a crack propagates through a specimen. The asphalt mastic distribution features visible on fracture faces are

primarily determined by volumetric characteristics of the asphalt mastic phase and other phases. Starting with a well established conceptual microstructure model for foamed asphalt materials, three basic principles for relating 2D fracture face asphalt mastic distributions to 3D asphalt mastic distributions were established. The Fracture Face Asphalt Coverage (FFAC), which is the ratio of the area of the mastic phase visible on a fracture face to the total area of the fracture face, was found to be a simple and effective indicator of asphalt mastic dispersion in a foamed asphalt mixes under certain conditions as demonstrated by the examples in this thesis. The effects of the main non-structural factors, including the relative strength between the asphalt mastic phase and the mineral filler phase, and specimen fabrication and testing methods were analyzed and the preferred test conditions for comparing FFAC values of different mixes were established. A standard procedure of acquiring, processing and analyzing digital images of fracture images was also developed.

Fracture Face Image Analysis was undertaken in parallel to conventional strength tests of a variety of foamed asphalt mixes. A number of insights into the microstructural mechanisms of foamed asphalt mixes strength behavior were obtained and are summarized as follows:

- Fracture Face Image Analysis results in conjunction with soaked and unsoaked ITS tests were used to calculate strengths of the asphalt mastic phase and the mineral filler phase. Results show that the tensile strength of the mineral phase is extremely sensitive to water conditioning, whereas moderate strength reduction of the asphalt mastic phase is expected when the specimens are soaked.

- Laboratory test results indicate that under unsoaked conditions, weak chemical cementation and suction from residual water in the mineral filler phase can dominate tensile/flexural strength of foamed asphalt mixes, and thus obscure the stabilization effects of the foamed asphalt. Since one of the main objectives of a mix design process is to evaluate and optimize the stabilization effects of foamed asphalt, this situation is undesirable. On the other hand, under soaked conditions the efficacy of foamed asphalt treatment can be readily distinguished. Additionally, as soaked conditions are more critical to pavement performance and are inevitable in most field locations, strength tests under soaked conditions are recommended to evaluate the stabilization effects of foamed asphalt in project level mix design.

- Compaction effort or density was found to have remarkable effects on tensile strength of foamed asphalt mixes. Specimens subjected to higher compaction efforts have slightly higher densities, but significantly higher strengths. The FFAC values were higher as well. A microstructural mechanism to explain the observed phenomena was proposed, and it implies that higher compaction effort helps strengthen bonding between asphalt mastic and the aggregate skeleton.

- If two asphalt binders with similar foaming characteristics are compared, the softer or less viscous binder was found to have better stabilization effects. Fracture Face Image Analysis results suggested that the softer asphalt binder is better dispersed in PAP mixes.

- Finally, the effects of PAP gradations were quantitatively analyzed. It was found that FFAC values of foamed asphalt mixes with significantly different PAP gradations should

not be directly compared to predict strength behavior. Mixes yielding higher FFAC values do not necessarily result in higher strength.

Apart from quantitative image analysis for research purposes, Fracture Face Image Analysis can also be empirically undertaken by experienced engineers to diagnose foamed asphalt mix problems. Some basic guidelines were suggested.

Chapter 4 Stiffness Behavior of Foamed Asphalt Mixes

4.1   Introduction

This chapter discusses resilient modulus (or stiffness) behavior of foamed asphalt stabilized mixes as measured by various laboratory test methods, emphasizing the effects of water conditioning and different test boundary conditions on test results.   This chapter also aims to investigate the microstructural mechanisms governing the observed phenomena.

4.1.1 Resilient modulus of foamed asphalt stabilized materials

Resilient modulus (denoted as "M_r" in this chapter), or stiffness of a foamed asphalt treated material characterizes its resistance to resilient deformation under applied loads.   It is defined as the ratio of the amplitude of the applied stress to the amplitude of the resultant recoverable strain, as shown in equation (2.1).   Although the definition points to measuring "recoverable" deformation under cyclic loading, the initial elastic modulus measured in monotonically loaded tests is also often taken as the resilient modulus.   In a typical full-depth recycled pavement structure, the resilient modulus of the foamed asphalt stabilized base layer has a significant influence on both the bending deformation and fatigue life of the HMA surfacing, and the distribution of the traffic load by the HMA layer and the foamed asphalt stabilized base layer to

reduce stresses in the weaker underlying layers.

As elaborated in Section 3.1, the microstructure of foamed asphalt mixes is different from that of HMA and unbound aggregate materials. If the active filler (e.g. portland cement) content is low, a foamed asphalt stabilized material is considered to be a weakly asphalt-bound material with behaviors different from that of the other two categories of materials. It is well known that the strength, resilient modulus and permanent deformation resistance of foamed asphalt mixes are dependent on stress states (e.g. Ebels & Jenkins, 2006; Fu & Harvey, 2007; Jenkins et al., 2007), which is a typical behavior of unbound or weakly bound granular materials. On the other hand, foamed asphalt mixes can bear tensile or bending deformation, and even show some fatigue resistance, which is a typical characteristic of bound materials. This has been demonstrated by indirect tensile strength tests (e.g. Nataatmadja, 2001), monotonic flexural beam tests (Long & Theyse, 2002b; Long & Ventura, 2004) and cyclic flexural beam tests (Twagira et al., 2006; Ramanujam & Jones, 2007).

4.1.2 Laboratory test stress states vs. field stress states

Laboratory resilient modulus test methods and procedures currently used for foamed asphalt mixes by researchers and practitioners were all originally developed for other pavement materials. For instance, the indirect tensile resilient modulus (referred to in this thesis as "IDT RM") test (AASHTO TP31 [deleted in 2002], ASTM D4123 [withdrawn without replacement in 2003] and LTPP P07) and the cyclic flexural beam test for dynamic modulus and fatigue (AASHTO T321)

were both originally developed for HMA materials. The triaxial resilient modulus (referred to in this thesis as "Tx RM") test (AASHTO T307) is a conventional test method for unbound granular materials. The Tx RM test and the frequency sweep with cyclic flexural beam test were specifically designed to measure resilient modulus, whereas resilient modulus is a "byproduct" of some other tests, such as the triaxial permanent deformation (Tx PD) test and the cyclic flexural beam test for fatigue.

Although these tests all quantify stiffnesses of materials, the boundary conditions applied and the resultant stress states are significantly different. The flexural beam test to some degree simulates the stress state of the HMA pavement surface layer subjected to loading of a tire, with tensile stress at the bottom and compressive stress at the top of a beam specimen. However, it does not include the horizontal confinement stresses present in the pavement. In contrast, the Tx RM test applies various combinations of compressive confining stresses and deviator stresses, but no tensile stress can be induced within the specimen in typical test setups. The stress state in a specimen subjected to the IDT RM test is more complicated. According to elastic theories for a homogenous continuum, horizontal tensile strain and stress are induced within the cylindrical specimen subjected to narrow vertical strip loads. However, the applicability of such theories to foamed asphalt mixes, which present typical characteristics of granular materials, is questionable.

The stress state in a foamed asphalt stabilized base layer in a real world pavement subjected to traffic loading cannot be represented by any one of these laboratory tests alone. The stress state at certain locations in the foamed asphalt stabilized base layer is similar to that of a triaxial test; at

some other locations, for instance at the bottom of the foamed asphalt layer, tensile strain is induced which is similar to the stress state at the bottom of a flexural beam specimen. Therefore, laboratory test results should be interpreted with caution and should not be assumed to be completely representative of the properties in the pavement structure for design.

4.1.3 Problems with the IDT RM test

The IDT RM test was the most widely used test method for foamed asphalt mixes found in the literature (Nataatmadja, 2001; Chiu & Lewis, 2003; Marquis et al., 2003; Collings et al., 2004; Ramanujam & Jones, 2007; Khweir, 2007), mainly due to the ready availability and low cost of the equipment. However, unrealistically high resilient modulus values (higher than 5,000 MPa) were reported by most of the above researchers. On the other hand, researchers who used other test methods, namely the Tx RM test (Jenkins et al., 2002; Jenkins et al., 2004; Fu & Harvey, 2007; Jenkins et al., 2007), the Tx PD test (Long & Theyse, 2002b; Long & Ventura, 2004; Jenkins et al., 2007), the monotonic flexural beam test (Long & Theyse, 2002b; Long & Ventura, 2004), the cyclic flexural beam fatigue test (Twagira et al., 2006; Ramanujam & Jones, 2007), and the temperature- frequency sweep with cyclic flexural beam test (Twarira et al., 2006) generally reported values within a range of between 500 and 3,000 MPa, which is consistent with the back-calculation results from field deflection measurements, including Falling Weight Deflectometer (FWD) tests (Lane & Kazmierowski 2003; Ramanujam & Jones, 2007) and multi-depth deflectometer (MDD) tests (Long & Theyse, 2004). This discrepancy between resilient modulus determined using the IDT RM test and other test methods is especially evident

in studies where multiple test methods were carried out for the same materials. These studies

have shown that the IDT test yields much higher resilient modulus values than other test methods

(Ramanujam & Jones, 2007), while triaxial tests, beam tests and field deflection back-calculation

all yield values within a similar range (Long & Theyse, 2002b; Long & Ventura, 2004; Long &

Theyse, 2004).

A preliminary observation from the literature reveals that the IDT RM test might overestimate

resilient modulus of foamed asphalt mixes and thus should not be used in mix evaluation and

structural design. On the other hand, resilient moduli tested with triaxial type or beam type tests

are more credible indicators and their test conditions are more relevant to field stress states.

Two potential reasons for this discrepancy are suggested below, but further investigation with

theories and models capable of capturing the semi-granular nature of foamed asphalt mixes, such

as the discrete element method (Ullidtz, 2001) is needed to better understand the IDT test, which

is beyond the scope of this thesis work.

The calculation of stress in the IDT test relies more heavily on the assumptions of continuum

mechanics than is the case for the triaxial and beam tests. In IDT tests, loads are applied

vertically through two narrow loading strips, and calculation of horizontal tensile stress relies on

continuum mechanics, whose applicability to foamed asphalt mixes is questionable. In triaxial

tests, confining stress and deviator stress are applied uniformly, and in a global sense the

calculation of resultant stresses only relies on the assumption that the internal stress should

balance the applied external load. The situation for the internal stress of bending beam

specimens is similar because on any transversal cross section, the normal stress has to balance the applied bending moment. This fundamental difference between the IDT test and the other two types of tests is further evidenced by noting that the Poisson's ratio is used in calculating stress of the IDT test while no material-specific constant is used in the stress calculation for the other two test types. Furthermore, the concept of the Poisson's ratio itself relies on continuum mechanics assumptions.

In IDT tests, the width of the loading strips (13 mm) and the distance (25 mm) between the two gages measuring deformation is smaller than or close to the dimensions of large aggregate particles. The specimen sizes and deformation gage lengths for triaxial tests and flexural beam tests are much larger and stress distribution is more uniform.

Based on these observations in the literature, the IDT RM test was not employed in the current study of resilient modulus behavior of foamed asphalt mixes.

4.1.4 Water conditioning

The effects of water soaking on strength behavior of foamed asphalt stabilized materials have been discussed in Section 3.6.2. The microstructural mechanisms governing strength behavior of foamed asphalt treated materials also influence stiffness behavior, which is further investigated in this chapter. Resilient modulus measurements of water soaked foamed asphalt mixes were only occasionally reported by Australian researchers (Nataatmadja, 2001; Ramanujam & Jones, 2007), but they were all carried out with the IDT RM test. Literature searches for resilient

modulus measurements for soaked foamed asphalt mixes with triaxial or beam type tests were unsuccessful. Evaluating resilient modulus of water soaked foamed asphalt mixes with the Tx RM test and the monotonic flexural beam test is a main focus of this chapter.

4.1.5 Temperature and loading rate

Because of the presence of asphalt (in the form of both newly introduced foamed asphalt and partially oxidized asphalt from the original HMA), resilient modulus of foamed asphalt mixes shows temperature and loading rate dependency. Fu & Harvey (2007) studied the temperature dependency of foamed asphalt mix resilient modulus as well as its interaction with stress dependency under triaxial test boundary conditions. Temperature sensitivity coefficients (a dimensionless parameter) from 0.0065 to 0.013 were measured. Limited FWD back-calculation results also showed similar temperature sensitivity coefficient values.

Flexural beam frequency sweep tests were reported by Twagira et al. (2006). The materials tested contained between 2.4 and 3.6% foamed asphalt and 0 to 1.0% portland cement. It was found that generally a 10 fold increase in loading frequency increases the measured resilient modulus by approximately 25%.

Compared to the effects of water conditioning and stress states, the effects of temperature and loading rates are of a less complicated and more predictable nature, and thus are not the main focus of this study.

4.1.6 Summary of the experiment design

The study documented in this chapter was performed in Phase II of the UCPRC study. The detailed experiment design is elaborated in Table 2.4. Six PAP materials (two PAP sources and three manufactured gradations for each source) were treated with two types of asphalt binder (PG64-16 and PG64-10). Two asphalt content levels (zero for the control mixes and three percent) were tested and no active filler was used. Three test methods, namely the free-free resonant column (FFRC) test (Section 2.11), the Tx RM test (Section 2.8) and the flexural beam test (Section 2.9) were performed on both soaked and unsoaked specimens. Detailed procedures for mix preparation, specimen fabrication, curing and water conditioning are elaborated in Chapter 2. It was found that the effects of asphalt binder grades on foamed asphalt mix stiffness behavior were less significant than that of other factors discussed in this chapter. Consequently, tabulated results shown in this chapter are averages of pooled values for mixes treated with the PG64-16 and PG64-10 binders and for replicate specimens.

4.2   Free-Free Resonant Column Test Results

The detailed test procedure for the FFRC test is described in Section 2.11. In this study, the FFRC test was performed on triaxial and beam specimens prior to destructive testing. The specimens were only tested in the unsoaked condition, as it was not possible to mount the accelerometer on soaked specimens.

The repeatability of this test was considered satisfactory.   Figure 4.1 shows a comparison of the results for two replicate beams (denoted as Specimen A and Specimen B) made from the same batch of mix.   The relative difference was generally within five percent.
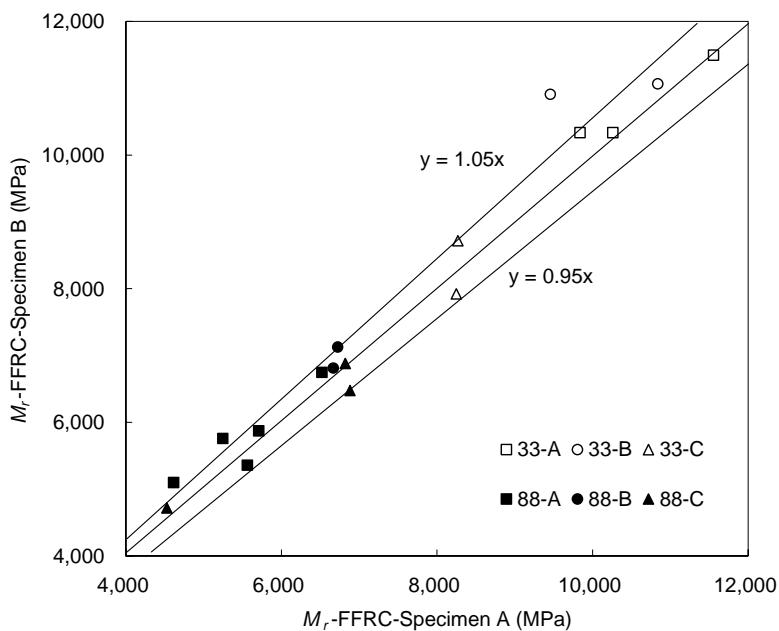
Figure 4.1   Repeatability of the FFRC test

There was a high correlation (Pearson correlation coefficient of 0.97) between the FFRC resilient modulus values for beam specimens and those for triaxial specimens made from the same mix batch (Figure 4.2).   The FFRC resilient modulus values for triaxial specimens were consistently lower (by 13 percent on average) than the FFRC resilient modulus values for beam specimens. This can be potentially attributed in part to the aggregate particle orientation induced by compaction.   During FFRC tests, the wave propagation direction in triaxial specimens is the same as the direction of the compaction action whereas it is perpendicular to the direction of the compaction action in beam specimens.
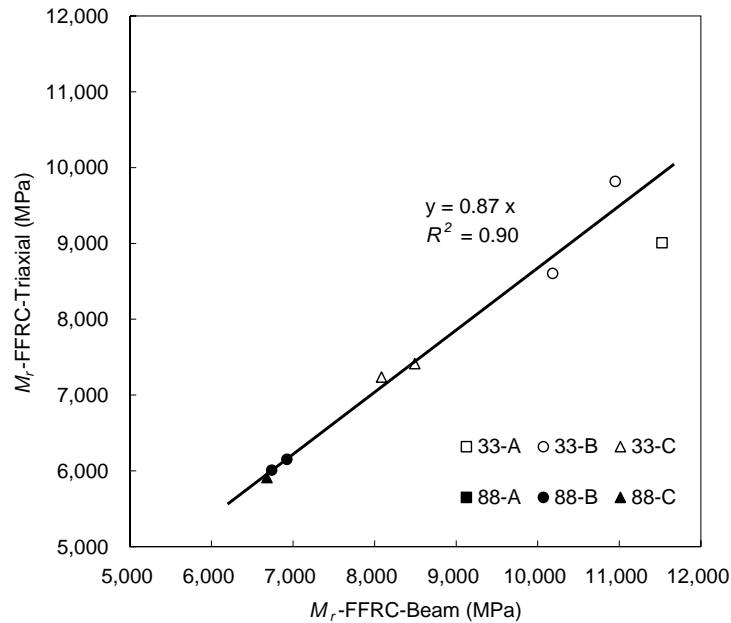
Figure 4.2 Correlation of beam and triaxial specimen FFRC resilient modulus values

Apparently, FFRC tests overestimate resilient modulus of foamed asphalt mixes.   The resilient

modulus values determined from triaxial and flexural beam tests on the same mixes were

generally lower than 2,000 MPa, as will be discussed in Sections 4.3 and 4.4, while typical values

of 4,000 MPa to 12,000 MPa were recorded in the FFRC tests.   Given that the resilient modulus

of foamed asphalt mixes is stress and loading rate dependent (i.e. higher frequencies and smaller

strain amplitudes result in higher stiffness for asphalt bound materials), the stress induced in

FFRC tests is of very small amplitude and high frequency compared to the field condition, and

thus has minimal relevance to the stress state induced by traffic loading on pavement structures.

The FFRC modulus values for unsoaked specimens appeared to be very dependent on PAP

sources.   The specimens prepared from SR33-A and SR33-B PAPs have significantly higher

FFRC moduli than the other PAP sources and gradation.   The same trend was observed in

strength test results (Figure 3.11 and Table 3.1), and is evident in the correlation between FFRC

resilient modulus and flexural strength results of monotonic flexural beam tests (Figure 4.3).

This was attributed to weak natural chemical bonding in the fines matrix of the SR33 PAPs,

which exhibited brittle, but stiff, properties especially at low stress levels, in the unsoaked state,

but which does not influence performance of the material in the soaked state.   Dilution of the

material with additional mineral fines (15 percent baghouse dust) reduced the effect of this

bonding as seen in results for 33-C PAPs compared with those for 33-A and 33-B PAPs in Figure

4.3.
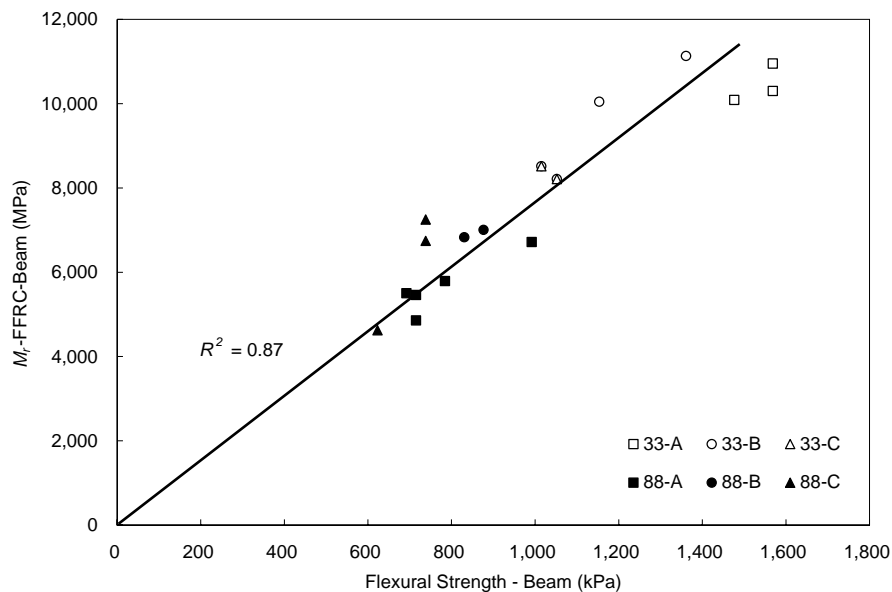
Figure 4.3   Correlation between FFRC resilient modulus and flexural strengh
Note: Tests carried out on the same beam specimens.

In summary, the FFRC test was found to be relatively simple and inexpensive to carry out with

high repeatability.   However, given that the testing stress state is very different from the working

stress state of foamed asphalt mixes in pavement structures, the results are considered to be of a

questionable value for foamed asphalt treated material evaluation and pavement design.

4.3   Triaxial Resilient Modulus Test Results

All triaxial specimens were subjected to resilient modulus tests under unsoaked and then soaked conditions.   Combinations of various load pulse durations, confining stresses, and deviator stresses were applied to each test.   The detailed test setup, test procedure, the model used to fit the test results, and the definition of the two reference stress states are described in Section 2.8. An average R^2 value of 0.983 was obtained when fitting the model (equation [2.2]) to all the test results.   Model fitting results are presented in Table 4.1.

A comparison of test results for untreated control and foamed asphalt treated mixes in both soaked and unsoaked states resulted in the following observations:

Soaked control mixes of the SR33-A and SR33-B PAPs have significantly higher resilient moduli than specimens made with the SR88-A and SR88-B PAPs.   This trend differed from that for strength test results discussed in Section 3.6.2, which indicated that the SR33-A/-B and SR88-A/-B materials have similar performance in terms of soaked strength.   The difference is attributed to the coarser surface texture of the SR33 aggregate (Figure 2.3), which may influence stiffness behavior by affecting aggregate particles repositioning/reorientation under triaxial loading but have minimal effects on tensile strength.

Table 4.1   Triaxial resilient modulus test results

PAP	Unsoaked						Soaked						
	k_1	k_T	k_2	k_3	M_{r1} (MPa)	M_{r2} (MPa)	k_1	k_T	k_2	k_3	M_{r1}[1] (MPa)	M_{r2}[1] (MPa)	RMR[2] (%)
Foamed Asphalt Treated Specimens													
33-A	10,433	-0.06	0.19	-0.03	1,131	1,467	7,406	-0.09	0.17	-0.06	833	1,026	72
33-B	9,794	-0.04	0.16	-0.01	1,038	1,298	8,153	-0.11	0.15	-0.06	916	1,106	87
33-C	9,450	-0.04	0.15	-0.03	1,015	1,235	5,469	-0.09	0.27	-0.10	664	920	70
88-A	8,467	-0.04	0.18	-0.05	941	1,188	7,864	-0.09	0.21	-0.05	881	1,163	96
88-B	8,560	-0.05	0.19	-0.03	938	1,205	6,672	-0.09	0.22	-0.06	763	1,006	82
88-C	7,528	-0.03	0.19	-0.05	842	1,078	4,600	-0.08	0.31	-0.10	564	837	72
Untreated Control Specimens													
33-A	10,901	-0.03	0.16	-0.05	1,211	1,484	8,004	-0.06	0.24	-0.05	908	1,239	79
33-B	9,240	-0.04	0.24	-0.04	1,031	1,420	6,953	-0.07	0.25	-0.10	833	1,131	80
33-C	6,469	-0.01	0.29	-0.19	880	1,199	NR[3]	NR	NR	NR	NR	NR	NR
88-A	8,369	-0.04	0.25	-0.07	967	1,332	3,693	-0.05	0.40	-0.16	495	807	56
88-B	9,278	-0.03	0.26	-0.10	1,116	1,548	3,553	-0.06	0.45	-0.17	487	845	49
88-C	8,447	-0.03	0.23	-0.08	983	1,322	NR	NR	NR	NR	NR	NR	NR

[1] M_{r1} and M_{r2} are defined in Section 2.8.

[2] RMR = Resilient Modulus Retained. In this case $$RMR = \frac{1}{2}\left(\frac{Mr_{1-soaked}}{Mr_{1-unsoaked}} + \frac{Mr_{2-soaked}}{Mr_{2-unsoaked}} \right)$$

[3] NR = No Result: specimens disintegrated during water conditioning.

Foamed asphalt treated materials have similar resilient modulus values to the control specimens **in the unsoaked state**, except for the treated SR33-C materials, which had a slightly higher resilient modulus (by approximately 10 percent) than the same untreated specimens at both reference stress levels.

Soaked foam asphalt treated SR88-A and SR88-B materials have significantly higher resilient moduli compared to the untreated materials, especially at low confining stress levels. Untreated SR33-C and SR88-C materials did not withstand soaking and collapsed before testing, whereas the treated specimens of the same materials withstood soaking and retained decent stiffness.

The differences in soaked resilient moduli between SR33 PAPs (-A and -B), and SR88 PAPs (-A and -B) materials are less significant for the foamed asphalt treated mixes than for the untreated control mixes. In the control mixes, the characteristics of the aggregate (e.g. surface texture) probably dominate resilient modulus behavior, while the presence of asphalt binder in the treated mixes is one of the dominant factors for stiffness behavior of foamed asphalt treated mixes.

Figure 4.4 shows correlations between the FFAC values for the soaked 152 mm ITS specimens and the four material constants in equation (2.2) for soaked triaxial tests. Data points with FFAC = 0 correspond to the values for the soaked untreated control materials. The untreated SR33-C and SR88-C material specimens collapsed during soaking and results are therefore not available. It should be noted that the 152 mm ITS specimens were made from the same batches of materials as the triaxial specimens, and similar compaction procedures (equivalent to modified Proctor) were followed. Some observations regarding the effects of foamed asphalt stabilization on material

stiffness can be made by tracking the change of material constants (k_T, k_1, k_2 and k_3) in equation (2.2) with the difference in asphalt dispersion indicated by FFAC values.

The constants k_T, k_2 and k_3 represent the sensitivity of the foamed asphalt mix resilient modulus to loading rates (or load pulse durations), bulk stresses, and deviator stresses, respectively. Constant k_1 is a scalar term and if all the other parameters are the same, increasing k_1 values results in increasing resilient modulus values at low confining stress levels. As the FFAC value increases (generally representing better asphalt dispersion in the mix), the resilient modulus at low confining stress levels also increases (Figure 4.4[a]), the resilient modulus is more sensitive to loading rates (Figure 4.4[b]), but less sensitive to bulk stress values (Figure 4.4[c]) and deviator stress values (Figure 4.4[d]). These effects are more significant for the SR88-A, SR88-B, SR88-C and SR33-C materials compared to the SR33-A and SR33-B materials. As discussed in Section 3.6.5, direct comparisons of FFAC values between mixes made of PAPs with significantly different gradations should be avoided or made with caution. In this light, these observations are only made to provide some general and qualitative insights.

In summary, triaxial resilient modulus test results show that foamed asphalt stabilization does not always increase the absolute values of resilient modulus, under either unsoaked or soaked conditions. Foamed asphalt treatment transforms material behavior from that of typical unbound granular materials towards that of partially asphalt-bound materials, with the resilient modulus more loading rate dependent but less stress dependent. The significance of this transforming effect also appears to be influenced by certain characteristics of the PAP materials.

For example, PAP materials with coarser surface textures appear to be less affected by foamed asphalt stabilization in triaxial stress states, and aggregate particle interlocking and frictional sliding play significant roles in addition to the cohesion provided by the foamed asphalt.
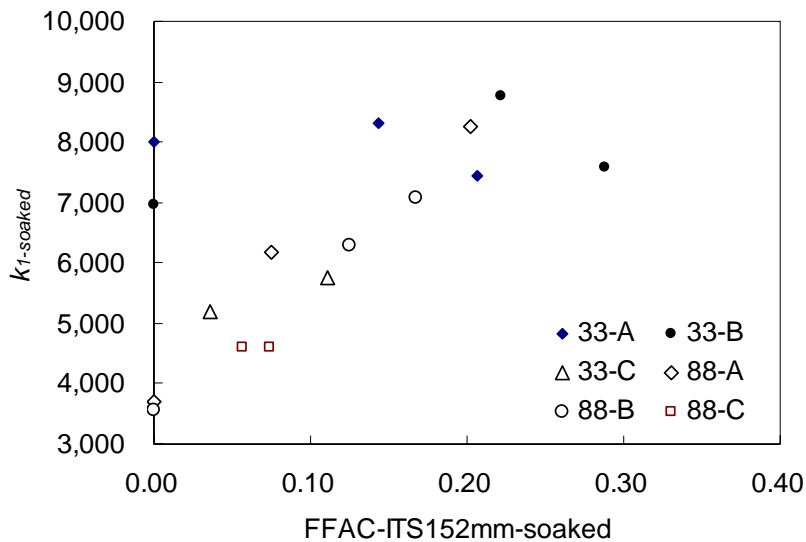
(a) FFAC vs. $k_{1\text{-}soaked}$
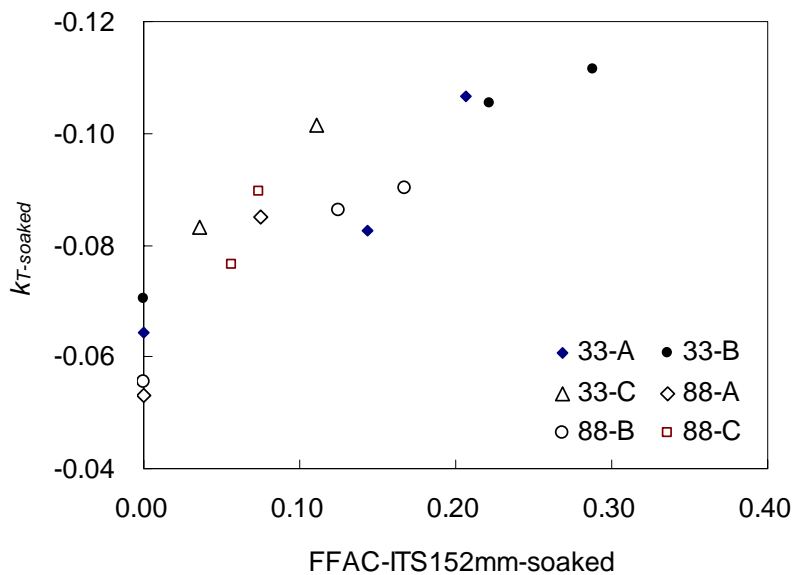
(b) FFAC vs. $k_{T\text{-}soaked}$

Figure 4.4   Correlation between FFAC and resilient modulus constants

(to be continued)
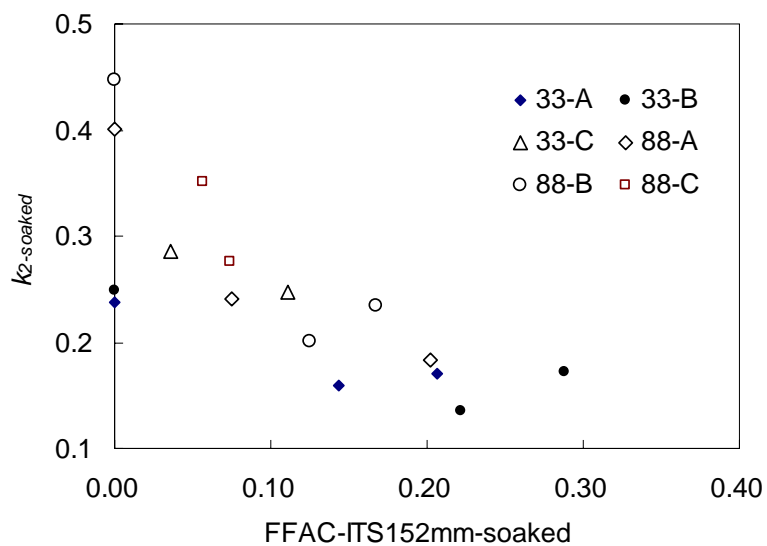
(c) FFAC vs. $k_{2\text{-soaked}}$
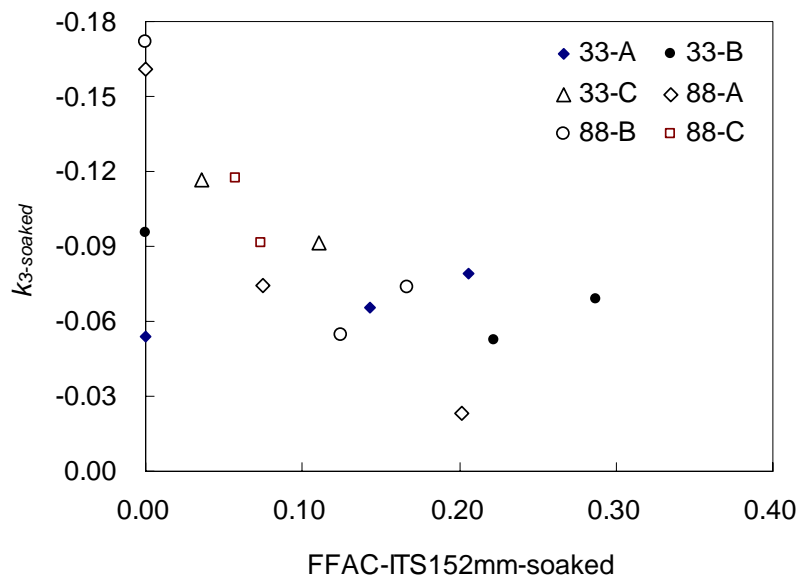
(d) FFAC vs. $k_{3\text{-soaked}}$

Figure 4.4   Correlation between FFAC and resilient modulus constants
(continued)

4.4   Flexural Beam Test Results

4.4.1 Test results

The monotonic flexural beam test results for both unsoaked and soaked specimens are shown in

Table 4.2.   The parameter E^{bend} is the equivalent Young's modulus for bending, or simply termed

"bending stiffness", determined from the initial segments of the stress-strain curves.

Strain-at-break (ε_b) is the tensile strain at the bottom of a beam at the mid-span, computed from the

measured beam deflection when the deflection-load curve reached its peak.   All calculations were

based on the Euler-Bernoulli beam theory.   Many of the metal deflection measurement plates (see

Figure 2.6[c]) detached after soaking and thus only a limited number of successful tests were

completed.   Test results should therefore be interpreted with care as the variance could be large.

Table 4.2   Resilient modulus tested by monotonic flexural beam tests

PAP	Unsoaked			Soaked			$\dfrac{E^{bend}_{soaked}}{E^{bend}_{dry}}$ (%)	$\dfrac{E^{bend}_{soaked}}{M_{r1-soaked}}$ (%)
	N^l	$E^{bend}_{unsoaked}$ (MPa)	ε_b	N^l	E^{bend}_{soaked} (MPa)	ε_b		
33-A	3	1,689	2,632	1	117	4,230	7	14
33-B	2	1,381	2,632	1	249	2,444	18	27
33-C	2	1,673	2,444	1	70	3,760	4	11
88-A	5	855	2,181	5	98	4,230	11	11
88-B	2	1,073	2,820	2	82	4,512	8	11
88-C	3	873	2,444	2	50	4,606	6	9

[1]N = number of specimens that were tested with successful deflection measurement.

The following observations were made:

In the unsoaked state, beams made with the SR33 PAPs have higher bending stiffness than those

made with materials sourced from SR88. The difference in strain-at-break for the two materials sources is small. Interestingly, the amplitudes of the equivalent Young's modulus for bending (E^{bend}) for unsoaked specimens were similar to those of the triaxial resilient modulus (M_{r1}) as shown in Table 4.1.

When the beams are soaked, they lose between 82 and 94 percent of their bending stiffness, while the strain-at-break values have a moderate increase. In contrast, triaxial specimens lose an average of 21 percent of their stiffness when soaked as shown in Table 4.1.

This discrepancy in water sensitivity of stiffness between the Tx RM test results and the flexural beam test results was attributed to the different stress states associated with the two test methods. Foamed asphalt treated materials with no active filler resist applied loading primarily by three mechanisms, namely interlocking and frictional sliding of the aggregate particles, bonding provided by the asphalt mastic phase, and bonding in the mineral filler phase (i.e. weak cementation and suction of residual water). These three mechanisms are respectively insensitive to water conditioning, moderately sensitive to water conditioning, and very sensitive to water conditioning. The first mechanism resists compression and shearing forces under confinement in triaxial stress states, and therefore has a dominant role in the behavior of soaked triaxial specimens when the other two mechanisms diminish with water conditioning. Consequently, water conditioning has a relatively limited effect on the triaxial resilient modulus. On the other hand, the third mechanism, which was relatively strong but brittle, contributes most of the tensile deformation resistance in unsoaked beam specimens. When beams are soaked, the first and

third mechanisms contribute little, and asphalt mastic dominates in resisting tensile deformation, and hence the overall stiffness of beam specimens is highly sensitive to moisture damage. Since the asphalt bonding is more ductile than the bonding in the mineral filler phase, the strain-at-break increased moderately for soaked beams.

4.4.2 Calculation of tensile stiffness

In the above analysis, stiffness of foamed asphalt treated materials is represented by the bending stiffness E^{bend}. When a beam is subjected to bending, the upper portion of its cross section is in compression, and the lower portion in tension. Even the same foamed asphalt material can have significantly different tensile stiffness and compressive stiffness (Young's moduli when the material is in tension and compression, respectively). The difference for unsoaked foamed asphalt materials is generally negligible, as implied by $E^{bend}_{unsoaked} \approx M_{r1-unsoaked}$. However, as suggested by the mechanism analysis presented above, this difference can be very significant when foamed asphalt treated materials are soaked, as different microstructural mechanisms are mobilized to resist tension and compression respectively. Generally, the compressive stiffness is greater than the tensile stiffness, and the bending stiffness E^{bend} is the resilient modulus of an "equivalent beam" which has the same bending resistance as that of the beam being studied, but has the same tensile stiffness and compressive stiffness. In certain situations, the resilient modulus value of foamed asphalt treated material in pure tension is of interest. This section derives the equations used for calculating tensile stiffness (or tensile resilient modulus) of foamed asphalt materials based on the bending stiffness.

The cross section of a beam is shown in Figure 4.5. Assume the tensile and compressive stiffnesses are E^+ and E^- repectively, and the ratio between them is $\alpha^2 = E^+/E^-$. When this cross section is subjected to a bending moment M, the neutral axis is generally not located at the mid-height, but at a height of ch from the bottom of the beam where c is a parameter to determine.
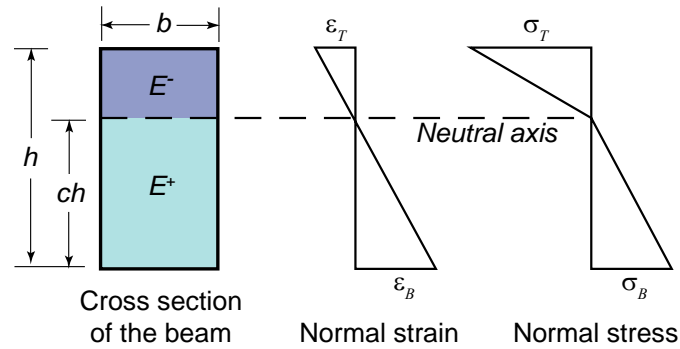
Figure 4.5   Strain and stress distribution on a beam cross section

$$E^+ = \alpha^2 E^- \tag{4.1}$$

$$\frac{\varepsilon^T}{\varepsilon^B} = \frac{h - ch}{ch} = \frac{1 - c}{c} \tag{4.2}$$

$$\sigma^T = E^- \varepsilon^T ; \quad \sigma^B = E^+ \varepsilon^B \tag{4.3}$$

where ε_T and ε_B are the normal strains at the top and the bottom of the beam respectively, and σ_T and σ_B are the corresponding normal stresses.

The tensile (F^+) and compressive (F^-) forces on the cross section should balance each other as shown in equation (4.4). By inserting equations (4.1), (4.2) and (4.3) into (4.4), the relation as shown in equations (4.5) and (4.6) can be obtained, which shows the vertical location of the neutral axis as a function of α.

$$F^+ = 0.5chb\sigma_B = F^- = 0.5(1-c)h\sigma_T \tag{4.4}$$

$$\frac{E^+}{E^-}\frac{\varepsilon_B}{\varepsilon_B} = \alpha^2 \frac{c}{1-c} = \frac{1-c}{c} \tag{4.5}$$

$$c = \frac{1}{1+\alpha} \tag{4.6}$$

The bending stiffness provided by the beam cross section is

$$\sum EI = \frac{1}{3}E^-b(\frac{\alpha h}{1+\alpha})^3 + \frac{1}{3}E^+b(\frac{h}{1+\alpha})^3 = \frac{1}{3}(\frac{\alpha}{1+\alpha})^2 E^- bh^3 \tag{4.7}$$

In Table 4.2, the equivalent tangential Young's modulus for bending E^{bend} was calculated by assuming a homogeneous beam with the same stiffness for compression and tension as shown in Figure 4.6.
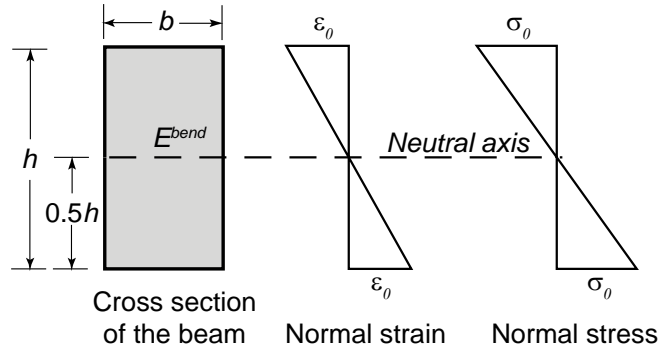
Figure 4.6   Stress and strain distribution on an equivalent homogeneous beam

Assume E^- can be approximated by the resilient modulus values from triaxial tests at low confining stress levels, i.e. M_{r1} in Table 4.1.   For the test performed in this study, the values for λ^2 can be found in the last column of Table 4.2, where:

$$\frac{E^{bend}}{E^-} \approx \frac{E^{bend}}{M_{r1}} = \lambda^2 \tag{4.8}$$

The bending stiffness provided by the equivalent beam should be the same as that of the beam in Figure 4.5, or computed in equation (4.7).

$$E^{bend}I^{equi.} = \frac{1}{12}E^{bend}bh^3 = \frac{1}{3}(\frac{\alpha}{1+\alpha})^2 E^- bh^3 \tag{4.9}$$

The relation between α^2 and λ^2 as shown in equation (4.10) can be obtained.

$$\alpha^2 = (\frac{\lambda}{2-\lambda})^2 \tag{4.10}$$

In Table 4.2, the values of $\lambda^2 = E^{bend}/M_{r1}$ under the soaked condition range between 9% and 27%. According to equation (4.10), the corresponding α^2 values range between 3% and 12%, or when soaked, the stiffnesses of foamed asphalt mixes resisting tension are 88% to 97% lower than of the stiffnesses resisting compression.

4.5   Summary and Conclusions

Resilient modulus or more generally, stiffness is an important property of foamed asphalt stabilized mixes.   Owing to the unique microstructural characteristics, the stiffness behavior of foamed asphalt mixes is expected to be different from that of unbound granular materials and that of typical asphalt bound materials.   This chapter investigates the resilient modulus (or stiffness) behavior of foamed asphalt stabilized mixes as measured by various laboratory test methods,

emphasizing the effects of water conditioning and different test boundary conditions on test results. It also aims to reveal the microstructural mechanisms governing the observed behaviors.

Different PAP materials were treated with foamed asphalt and tested with three different test methods (namely the free-free resonant beam test, the triaxial resilient modulus test and the monotonic flexural beam test) under both soaked and unsoaked conditions. Significant findings include:

- The free-free resonant beam test is relatively simple and inexpensive to perform with high repeatability. However, given that the testing stress state is very different from the working stress state of foamed asphalt mixes in pavement structures, the results are considered to be of a questionable value for foamed asphalt material evaluation and pavement design.

- The triaxial resilient modulus test results show that foamed asphalt stabilization does not always increase the absolute values of resilient modulus, under either unsoaked or soaked conditions. Foamed asphalt treatment transforms material behavior from that of typical unbound granular materials towards that of partially asphalt-bound materials, with resilient modulus more loading rate dependent but less stress dependent.

- The monotonic flexural beam test results show that foamed asphalt stabilized mixes lose most of their tension resistant stiffness when soaked. In a pavement structure subjected to traffic loading, a portion of the foamed asphalt stabilized base is in tension, and in most California environments the base material is more or less soaked for a few months each

year. Consequently, the low stiffness in tension has to be considered in design. However typical triaxial resilient modulus tests ignore this problem, which may lead to non-conservative design. A seasonal field monitoring study in California documented in Fu et al. (2009b) found that, compared to the resilient moduli in dry seasons, the stiffness reduction of foamed asphalt stabilized road base attributed to field moisture increases was approximately 35% to 45% depending on the characteristics of the sites. This observation further emphasizes the importance of properly considering the significant stiffness reduction for soaked foamed asphalt stabilized materials in tension.

In summary, the findings documented in this chapter highlight the importance of choosing appropriate laboratory test methods and test conditions that can simulate/represent field stress states and field environments for characterizing field behavior/performance of foamed asphalt stabilized materials, and the importance of understanding the stress states and test conditions when interpreting laboratory test results.

Chapter 5 Curing Mechanism of Foamed Asphalt Mixes

5.1   Introduction

Curing is the process in which a material (foamed asphalt mixes in this thesis work) develops

strength and stiffness with time.   The strength and stiffness of foamed asphalt mixes is relatively

low immediately after mixing and compaction, in both the laboratory and the field, and then

increases through curing.   A number of external conditions/factors play different roles in this

process.   Foamed asphalt mixes are multi-phase materials, and understanding the curing

mechanism requires insight into the strength/stiffness development mechanism of each phase, the

interaction between these phases, and the effects of curing conditions.   Understanding of the

curing mechanism of foamed asphalt mixes is necessary for:

- Developing standard laboratory curing procedures to represent field conditions;
- Developing field construction procedures to accelerate early strength development and at
   the same time optimize long term performance.

The effects of different curing conditions have been documented by many researchers. However,

laboratory curing procedures reported in the literature are far from standardized.   Meanwhile,

construction practice is largely empirical and mostly based on conventional practice for cement

and emulsion stabilization, which may not result in optimal performance for foamed asphalt materials. The main objective of the study documented in this chapter is to investigate the curing mechanism of foamed asphalt mixes. Review of previous research, the results of several laboratory testing methods, as well as direct microstructure observations were used to fulfill this objective.

5.2   Discussion of Curing Conditions

5.2.1 Desired features of laboratory curing conditions

The following general features are desired for a laboratory curing procedure to be adopted in a research program and/or in a project level design process.

Relevance to field conditions.   The primary purpose of most laboratory testing is to evaluate material properties under expected field conditions by testing the same materials under more controllable and convenient laboratory conditions. The laboratory properties need to reflect the field properties being studied.

Adequate consideration of material properties.   Material characteristics differ from one material to another, and also from one phase of a material to another phase. Design of curing conditions should consider all these characteristics. For example, high humidity is often desirable for curing mixes containing portland cement, because the hydration process of cement takes place in

the presence of water. In contrast, if water is irrelevant to the curing of certain materials, or inhibits curing, then creating a humid environment would be unnecessary, and could have negative effects on the evaluation of material properties.

Repeatability and reproducibility. Repeatability and reproducibility characterize the ability to produce the same results if the same material is tested following the same procedure, by the same operator, in the same laboratory (pertaining to repeatability) or by different operators in different laboratories (pertaining to reproducibility). Standardization of procedures is one common means to improve repeatability and reproducibility. However, there are inevitably some factors not directly controlled in a procedure. The effects of these uncontrolled factors should be well understood to ensure they do not significantly bias or dominate the testing results.

Simplicity. Increased complexity increases the chances for operational errors, thereby impairing repeatability and reproducibility. A complex procedure involving expensive equipment is often inappropriate for project level design for cost and schedule reasons as well.

5.2.2 Curing mechanisms for different phases of foamed asphalt mixes

Foamed asphalt stabilized mixes are composite materials. It is important to understand the behaviors of the different phases and how they are affected by curing to understand the curing mechanism of the composite material itself. A conceptual microstructure model for a foamed asphalt mix was presented in Section 3.1 as illustrated in Figure 3.1. The following discussions of some general behaviors of the individual phases pertaining to curing are based on that model.

The *aggregate skeleton* is formed by large aggregate particles. The skeleton itself can withstand applied compressive or shearing load by normal and tangential inter-particle contacts. Strength from this mechanism is available immediately after compaction and is not substantially affected by curing.

The *asphalt mastic phase* exists in the form of numerous droplets bonding the aggregate skeleton together. Asphalt mastic is a mix of asphalt cement and fine aggregate particles bonded by the asphalt binder during the mixing procedure. The bonding between asphalt mastic and the aggregate skeleton develops during curing, and the asphalt mastic phase itself hardens too. The hardening of asphalt mastic during curing should be mostly attributed to moisture evaporation, since short term aging of asphalt binder at a mild temperature is usually minimal. According to Jenkins (2000), "Bowering (1970) stated that laboratory specimens only develop full strength after a large percentage of the mixing moisture has been lost". This observation implies that moisture evaporation is a significant factor, and possibly the most important factor in curing of the asphalt mastic phase. Since the original reference by Bowering (1970) could not be obtained in this study, it is unknown whether this statement was an empirical observation, or a conclusion based on a formal study.

The *mineral filler phase* consists of fine aggregate particles not bonded by asphalt during mixing. The mineral filler phase partially fills the voids in the aggregate skeleton. It has low strength immediately after compaction when it is still wet, but can have a relatively high strength when dry as discussed in Section 3.6.2. This phase normally loses most of its strength when infiltrated

by water, and can regain strength as water evaporates.

Portland cement or other *active fillers* are often added to foamed asphalt mixes to improve certain properties, especially early-age strength and stiffness (Khweir, 2007). Since cement content is often within the range of one to two percent, an independent phase is not formed. Instead, cement powders are mostly dispersed into the mineral filler phase, and potentially contribute to mix strength and stiffness by strengthening the mineral filler phase. It is reasonable to assume that the curing mechanism pertaining to cement in foamed asphalt mixes is no different from that in conventional cement treated granular materials. The strengthening effects of cement on the mineral filler phase are studied in this chapter.

5.2.3 Laboratory vs. field curing conditions

As previously mentioned, a key objective of a laboratory curing procedure is to reflect field conditions. Important environmental conditions for field foamed asphalt mix curing include the ambient air temperature and humidity, and the moisture content and permeability of the underlying pavement layers and subgrade. Ambient air temperature varies during the course of construction and curing, while underlying layers and subgrade moisture conditions vary along the road. These conditions are difficult to precisely replicate or standardize in the laboratory. In California, several distinct climate regions exist (Harvey et al., 2000), including coastal areas that are generally cool and humid during the construction season, inland valley areas that are hot and dry, and mountain areas that are warm and dry. Human activities, such as irrigation and

drainage often alter curing conditions within a region. Simulating all of these distinct conditions in a standard laboratory procedure is not feasible, and developing different procedures for each condition is not realistic.

The laboratory curing procedure proposed in this study simulates two (and potentially more if needed) extreme field conditions for material characterization purposes. Experienced design engineers can then evaluate the test results against the conditions expected for a specific project.

5.2.4 Curing temperature

Three curing temperatures were adopted in most of the studies reported in the literature. Bowering (1970) recommended curing foamed asphalt specimens in an oven at 60ºC for 72 hours. Bowering and Martin (1976), Acott (1980), Lancaster et al. (1994), Maccarrone et al. (1994), Muthen (1998), Lane and Kazmierowski (2005), Hodgkinson and Visser (2004), and others followed this practice. Ruckel et al. (1983) suggested a curing temperature of 40ºC and a curing period of 24 hours to simulate field conditions in the first 7 to 14 days after construction, and 40°C and 72 hours to simulate longer term (>30 days) curing in the field. The curing temperature of 40ºC was adopted by the South African guidelines (Asphalt Academy, 2002), and was followed in several studies in South Africa (Long and Theyse 2002b; Long and Ventura 2004) and the United States (Marquis et al., 2003). Ambient temperatures have also been used by researchers for curing. Ruckel et al. (1983) recommended curing foamed asphalt specimens in the compaction molds at ambient temperature for one day to simulate one day of field curing

under dry, temperate conditions. Saleh (2004), Nataatamadja (2001), Long and Theyse (2002b), Long and Ventura (2004) and other researchers used ambient temperatures for longer durations (7 days to 28 days) to cure their specimens. Bowering and Martin (1976) reported that curing temperature did not significantly affect Marshall or California Bearing Ratio test results, whereas Nataatamadja (2001) found that curing temperature had significant effects on resilient moduli tested using the indirect tensile method.

Curing at 60ºC appears to be inappropriate for foamed asphalt mixes, at least for the prevailing asphalt grades used in California FDR practice. In the UCPRC study, curing at temperatures above 50ºC in exploratory trials resulted in appearance of foamed asphalt mix specimens different from that of specimens cured at 40ºC or lower: apparent asphalt binder flow was observed, implying altered asphalt dispersion patterns induced by the high temperature. Monitoring of four projects in the hot California Central Valley showed that temperatures rarely exceeded 50ºC at the mid depth of the foamed asphalt treated layer (Jones et al. 2008).

Curing at a temperature close to ambient (e.g. 15ºC or 25ºC) potentially impairs the repeatability and reproducibility of the procedure. The effect of relative air humidity is difficult to control at these temperatures. Curing specimens at a moderately elevated temperature can effectively reduce the influence of ambient air humidity. The saturation pressure of water vapor is 2.3 kPa at 20ºC and 7.4 kPa at 40ºC (Fredlund and Rahardjo, 1993). Ten and one hundred percent of the relative humidity at 20ºC corresponds to relative humidity values of three and thirty percent at 40ºC, respectively. The difference in evaporation rates between three and thirty percent

relatively humidities should be much smaller than those between ten and one hundred percent at relative humidities.

Based on these considerations, 40ºC appears to be an appropriate compromise.

5.2.5 Sealed vs. unsealed curing

Jenkins (2000) proposed to seal specimens in plastic bags while curing. The theoretical basis was the concept of equilibrium moisture content in the field. The South African guideline adopted this practice (Asphalt Academy, 2002). However, some subsequent studies in South Africa (Long and Ventura, 2004) found that specimens cured under this condition appeared to be too wet to represent typical field conditions, and thus some modifications to the procedure were explored (Long and Ventura, 2004), but never formalized.

In the current study, specimens were not sealed in experiments that investigated long-term curing conditions in the field. Curing under the sealed condition is not considered to represent the typical conditions in California. Sealing also considerably increases the testing complexity. However, in tasks assessing short-term strength gains (i.e. relating to early opening to traffic) sealing the specimens provides a conservative estimate of curing in the field.

5.3   Laboratory Experiment Program

5.3.1 Experiment design

The experiment design for this curing study is summarized in Table 5.1.   Details about this laboratory experiment study are elaborated in this section.

5.3.2 Materials, mix preparation and specimen fabrication

This study was largely qualitative with a goal of understanding a general phenomenon.   In this light, only one granular material (PAP 88-A) and one asphalt cement type (PG64-16) were tested. The same materials were used in the studies documented in Chapter 3 and Chapter 4 of this thesis. The asphalt was foamed with a Wirtgen WLB10 laboratory plant at 150°C with 3% foaming water by mass added.   The resulting average expansion ratio was in the range of 17 to 20, and the half-life was 23 to 30 seconds.   The mix preparation procedure was described in detail in Section 2.5.   The mixing moisture content (MMC) was empirically selected based on direct observations of the agglomeration states of fine particles and workability, with measured values shown in Table 5.3.   A quantitative study of the effects of MMC on mix properties is reported in Chapter 6 of this thesis.   For each mix type, one batch of loose mix (20 kg total) was prepared to fabricate a triaxial specimen and a series of ITS specimens.

As indicated in Table 5.1, ITS, Tx RM and Tx PD tests were performed in this study.   The same specimen fabrication procedures and test setups as described in Sections 2.6 and 2.8 were

followed.   All tests were carried out at 20ºC.

Table 5.1   Experiment factorial design for the curing study

Variable	Values
Parent material	- PAP 88-A and asphalt PG64-16
Asphalt content	- 0 and 3%
Active filler type	- Portland cement, Type II
Active filler content	- 0, 1% (selected mixes only), and 2%
Test method	- Indirect Tensile Strength (ITS, 100 mm) - Triaxial Resilient Modulus (Tx RM) - Triaxial Permanent Deformation (Tx PD)
Curing condition	- Curing Condition A, sealed, at 20ºC for 24 hours - Curing Condition B, open to air, at 40ºC for 7 days

Soaking condition	- Tested immediately after Curing Condition A
	- For specimens subjected to Curing Condition B
	  ITS: 24 hour soaking
	  Triaxial: soaking duration varied for each test, 1 day to 38 days

Replicates	- Four ITS specimens per mix per test condition - One triaxial specimen per mix per test condition Multiple rounds of Tx RM tests were applied to selected specimens

5.3.3 Curing conditions and water conditioning

Two curing conditions, denoted as Curing Condition A (or Curing A, or Condition A) and Curing

Condition B (or Curing B, or Condition B) respectively were adopted in this study.

For Condition A, each specimen was extruded from the mold immediately after compaction and

sealed in a plastic bag, then cured at 20ºC for 24 hours. Subsequently, the specimen was removed from the bag and tested immediately without further soaking or drying. When tested, the specimens should have moisture contents slightly lower than the mixing moisture contents, as some water inevitably evaporated from the specimens and condensed on the plastic bags.

For Condition B, specimens were extruded from the molds immediately after compaction and placed in a forced draft oven at 40ºC for seven days. Specimens were not sealed during the curing procedure. The curing procedure discussed in Section 2.13 is similar to Condition B.

These two conditions are believed to correspond to two extreme conditions in the field, with Curing A representing a conservative condition for water evaporation and simulating the environment that foamed asphalt treated materials experience in the first few hours after construction. Curing B represents a more optimistic condition for water evaporation. In the California Central Valley, FDR projects are normally constructed in summer and a foamed asphalt treated base would typically have reached the state of Curing B at the end of the dry season (in September or October).

Specimens cured under Condition B were subjected to water conditioning before testing. They were placed in a water tank at 20ºC for prescribed durations with water levels maintained at 100 mm above the top surfaces of the specimens.

5.4   Test Results

5.4.1 ITS test results

The ITS test results are summarized in Table 5.2.

Table 5.2   ITS test results

Curing Condition	Mix Design[2]				
	0C0A	2C0A	0C3A	1C3A	2C3A
Curing A	58[1]	426	66	213	335
Curing B[3]	36	594	353	435	900

[1] Strength results are in kPa.

[2] "*XCYA*" represents the mix design.   For example "2C3A" indicates that the mix contained 2% cement and 3% foamed asphalt.

[3] ITS specimens having been subjected to Curing Condition B were soaked before testing.

The following observations were made:

Mixes containing cement (2C0A, 1C3A and 2C3A) developed considerable strength in the first 24 hours under Curing Condition A regardless of the asphalt content.

The strength of the mix containing only foamed asphalt (0C3A) and cured under Condition A for 24 hours was similar to the strength of the untreated control mixes (0C0A) cured under the same condition.   The tensile strength measured under these conditions can be mostly attributed to matrix suction in the mineral filler phase (Lu et al., 2007).

After curing under Condition B followed by soaking, mixes containing only foamed asphalt (0C3A) developed substantial strength when compared with the control mix (0C0A).   These

results indicate that asphalt mastic, once cured, can provide long term strength even after the relatively light brittle cementation breaks down, as would be expected under longer term traffic loading.   Mixes containing both foamed asphalt and cement showed similar improvements.

5.4.2 Triaxial resilient modulus test results

Nine triaxial specimens were fabricated for this study, and their mix designs and the measured mixing moisture contents (MMC) are listed in Table 5.3.   Selected specimens were subjected to multiple tests after different curing/soaking conditions.

The model used to fit the triaxial results is described in Section 2.8.   An average R^2 value of 0.98 was obtained for model fitting. Mr_1 and Mr_2 are resilient modulus values in two representative stress states based on model fitting results, and their interpretation is also described in Section 2.8.

Selected Tx RM results for mixes tested under various curing-soaking conditions are plotted against the confining stress applied in Figure 5.1.   Only the results for one pulse loading duration of 0.1 second are shown.   Data point scattering at each confining stress for each mix is attributed to the different deviator stress levels applied.

The results of the Tx RM tests are summarized below.

- In terms of the effects of curing conditions and mix designs, similar trends to those observed in ITS test results were recorded for the triaxial resilient modulus tests.

- The measured resilient modulus values of mixes containing foamed asphalt and no cement (Specimen TriA [0C3A]) with 24 hours curing (Condition A) were similar to that of the control mix (Specimen TriH [0C0A]).

Table 5.3   Triaxial resilient modulus test results

Label	Mix design	MMC (%)	Pre-test conditioning	MC[1] (%)	Model Fitting Results					
					k_1	k_T	k_2	k_3	M_{r1}[2] (MPa)	M_{r2}[2] (MPa)
TriA	0C3A	5.3	Curing A	5.3	1,599	-0.05	0.59	-0.23	244	499
			Curing B and 6 day soak	5.7	6,087	-0.08	0.28	-0.10	737	1,042
TriB	0C3A	6.0	Curing B and 7 day soak	5.3	5,503	-0.06	0.31	-0.10	667	996
TriC	2C3A	5.8	Curing A	5.8	8,630	-0.05	0.28	-0.10	1,052	1,496
			Curing B and 1 day soak	3.8	11,112	-0.05	0.24	-0.07	1,281	1,747
			Curing B and 7 day soak	4.4	11,634	-0.05	0.21	-0.08	1,349	1,747
			Curing B and 38 day soak	4.9	11,882	-0.05	0.22	-0.06	1,355	1,797
TriD	2C3A	5.8	Curing B and 1 day soak	3.8	8,832	-0.05	0.35	-0.11	1,095	1,720
			Curing B and 7 day soak	4.4	10,104	-0.05	0.30	-0.08	1,201	1,762
			Curing B and 38 day soak	4.9	9,651	-0.05	0.32	-0.08	1,151	1,737
TriE	2C0A	5.1	Curing A	5.1	10,257	-0.05	0.27	-0.12	1,267	1,742
TriF	2C0A	5.5	Curing B and 5 day soak	4.5	9,083	-0.04	0.36	-0.10	1,114	1,781
TriG	1C3A	4.3	Curing A	4.3	5,846	-0.06	0.29	-0.14	744	1,048
TriH	0C0A	7.1	Curing A	7.1	1,623	-0.01	0.63	-0.17	232	523
TriI	0C3A	5.6	Only for Tx PD test, see Section 5.4.3							

[1] MC = Moisture content when tested

[2] M_{r1} and M_{r2} are defined in Section 2.8

- Resilient modulus of the 0C3A mixes increased substantially after being cured under Condition B and then soaked (Specimen TriB [0C3A] and second test for TriA [0C3A]), even though the moisture content (5.3%) as tested was similar to that measured for

Specimen TriA [0C3A] after Curing Condition A. At the same time, the cured mixes show higher sensitivity to loading rates (with higher absolute values of k_T) and lower sensitivity to stress states (with lower absolute values of k_2 and k_3), implying that after the curing procedure, material behavior was transformed from that of typical unbound granular materials towards that of asphalt bound materials.
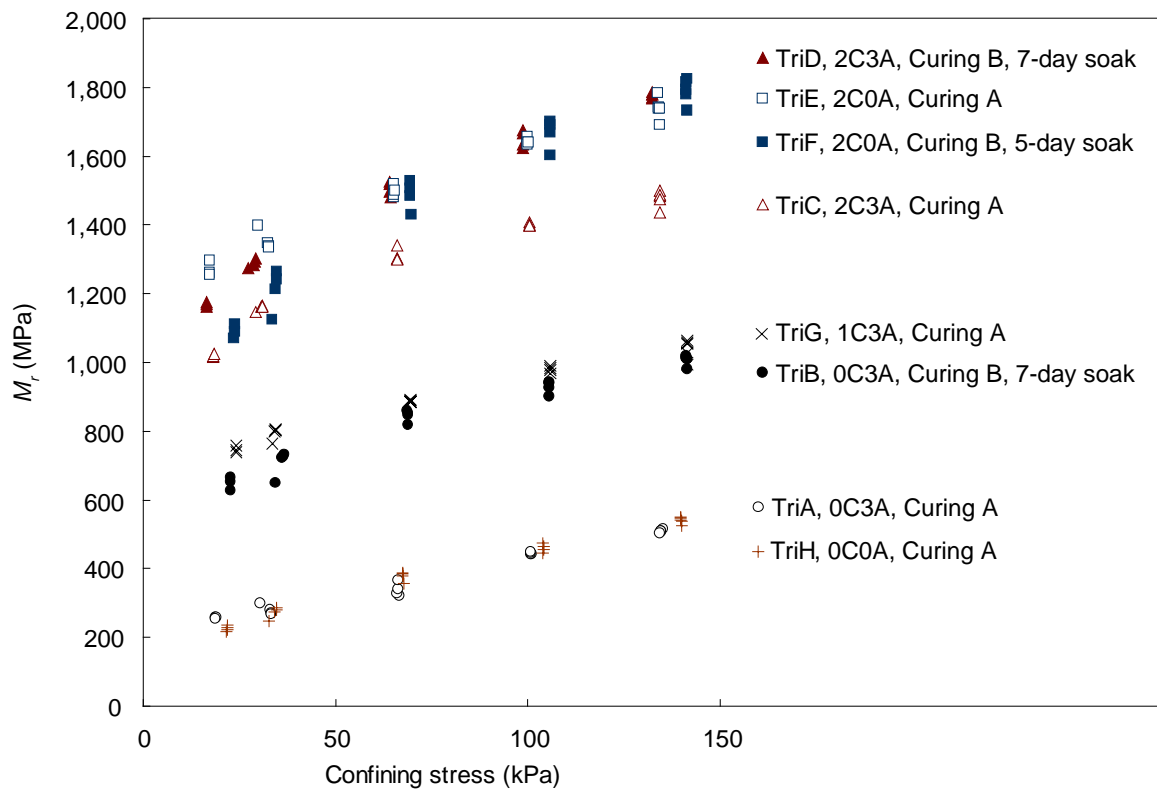
Figure 5.1   Selected Tx RM results for different mix designs and curing conditions

- The ITS and Tx RM test results both indicate that the strength gains of the foamed asphalt only developed after the onset of drying, and that once cured, the mixes with foamed asphalt and no cement (0C3A) showed considerably better properties (i.e. higher strength and stiffness) than the control mix (0C0A), indicating that foamed asphalt provides long

term strength and stiffness which would be retained after the brittle light cementation breaks down under longer term traffic loading.

- Strength gain in cement treated materials showed significant development in the first 24 hours (Curing Condition A), and consequently mixes containing cement (Specimens TriC [2C3A], TriE [2C0A] and TriG [1C3A]) had much higher stiffnesses than those containing no cement (Specimens TriA [0C3A] and TriH [0C0A]) after being cured under Condition A. Stiffnesses increase with increasing cement content, as expected.

- Specimens TriA (0C3A) and TriC (2C3A) had similar resilient modulus values to those of Specimens TriB (0C3A) and TriD (2C3A) respectively after curing (Condition B) and soaking. This indicates that the loading history after Curing Condition A does not alter the post-cured (Condition B) material properties.

- Specimens TriC (2C3A) and TriD (2C3A) were also subjected to triaxial resilient modulus testing after various durations (1 day to 38 days) of soaking. No significant change in material properties was observed during this process, while moisture contents moderately increased. The effects of moisture damage and longer term strength gain under these curing conditions are not apparent.

5.4.3 Triaxial permanent deformation test results

A limited series of triaxial permanent deformation (Tx PD) tests were performed on selected triaxial specimens listed in Table 5.4. Most of these specimens had already been subjected to Tx RM tests before the permanent deformation tests took place.

Table 5.4   Mix design, curing-soaking conditions and test moisture content for specimens subjected to triaxial permanent deformation tests

Specimen	Mix Design	Test Condition	Moisture Content as Tested (%)
TriB	0C3A	Curing Condition B, 7 day soak	5.3
TriC	2C3A	Curing Condition B, 40 day soak	4.9
TriG	1C3A	Curing Condition A	4.3
TriH	0C0A	Curing Condition A	7.1
TriI	0C3A	Curing Condition A	5.6

The axial strain development of the five specimens for the three deviator stresses in the test sequence is shown in Figure 5.2.   Compressive strain is considered positive in the figure.   The mix design, curing condition and soaking condition for each specimen prior to testing are also shown.
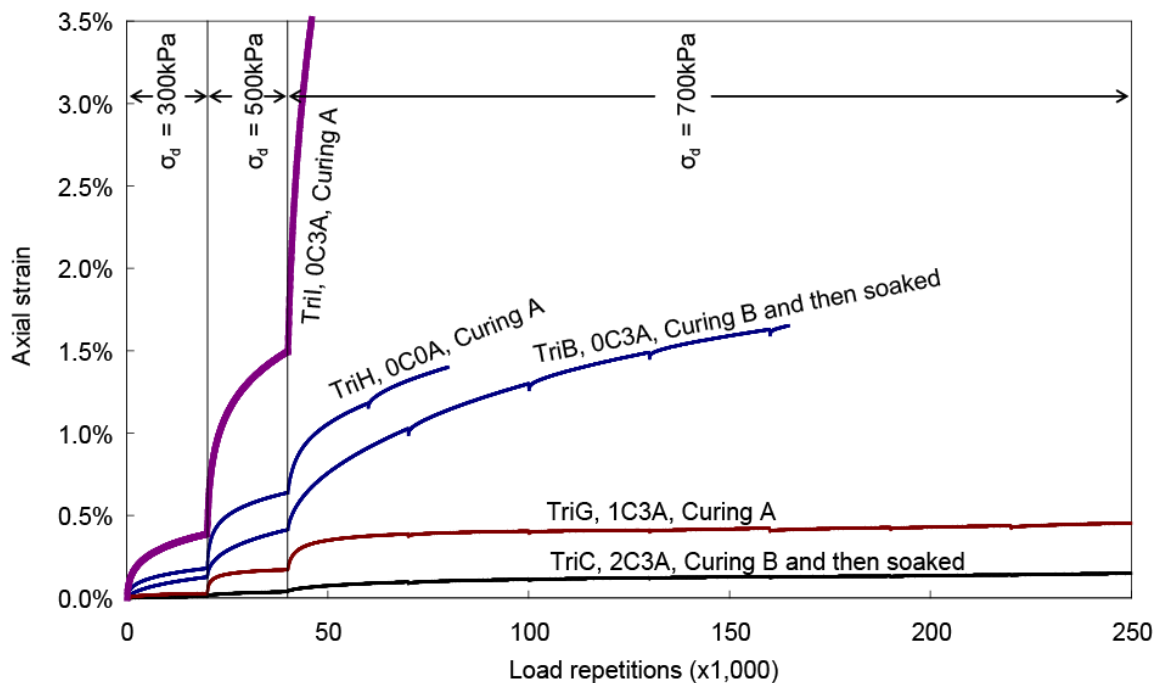
Figure 5.2   Triaxial permanent deformation test results

The following observations were made from these results:

The mix containing three percent foamed asphalt and no cement (Specimen TriI [0C3A]) and cured under Condition A had the poorest permanent deformation resistance, with performance worse than that of the untreated control (Specimen TriH [0C0A]). This was attributed to the asphalt mastic phase behaving as a lubricant reducing the permanent deformation resistance.

After Curing Condition B, the permanent deformation resistance of this mix (0C3A [Specimen TriB]) improved significantly.

The permanent deformation resistance improved significantly when cement was added for mixes that had only been subjected to Curing Condition A (Specimen TriG [1C3A] compared to Specimen TriI [0C3A]). The permanent deformation resistance improved with increasing cement content, as expected.

The results of this limited testing confirm that no significant bonding of foamed asphalt develops if most of the moisture has not evaporated, and that a significant improvement in permanent deformation resistance is obtained from foamed asphalt mixes after dry curing, even after re-soaking. Results also show the role of cement in preventing early permanent deformation in foamed asphalt treated materials.

5.5   Curing Mechanisms of Foamed Asphalt Mixes

A number of insights into the curing mechanism of foamed asphalt treated materials were gained from the test results shown and observations of fractured ITS specimens.

The curing processes of asphalt mastic and active fillers appear to take place independently.   In the tests reported in this chapter and other tests undertaken during this thesis study, there was no evidence or sign showing that foamed asphalt chemically reacted with portland cement or any other active filler used (including cement kiln dust, fly ash, and lime; see [Jones et al. 2008] for details).   Therefore the existing theory, knowledge, and experience pertaining to specific active fillers (e.g. portland cement) also applies to foamed asphalt mixes regarding the contribution of these active fillers.

The curing and strength development mechanisms associated with foamed asphalt (or asphalt mastic in the mix) are illustrated in Figure 5.3.   When foamed asphalt is injected onto agitated moist aggregate (PAP in this case), it partially bonds the fines to form asphalt mastic, visible in the loose mix as small droplets (Figure 5.3 [a]).   Aggregate particles in the loose mix are mostly coated with a water membrane.   After compaction, the asphalt mastic droplets are in tight contact with the aggregate particles (Figure 5.3 [b]), but due to the presence of the water membrane, they do not physically bond to the aggregates until most of the molding moisture has evaporated (Figure 5.3 [c] and [d]).   During the curing process, water in larger voids evaporates first.   It is more difficult for water to evaporate from smaller voids, especially at the asphalt

mastic-aggregate particle interface, due to the lower thermodynamic potential. However, once the bonds between the aggregate particles and asphalt mastic droplets have formed, only partial damage to these bonds will occur if water is re-introduced into the mix (Figure 5.3 [e]). This explains why in the Tx RM tests, specimens TriA (0C3A) (after Curing Condition A) and TriB (0C3A) (after Curing Condition B and soaking) had the same moisture contents as tested, but the stiffness of the latter specimen was much higher and less sensitive to different stress states.
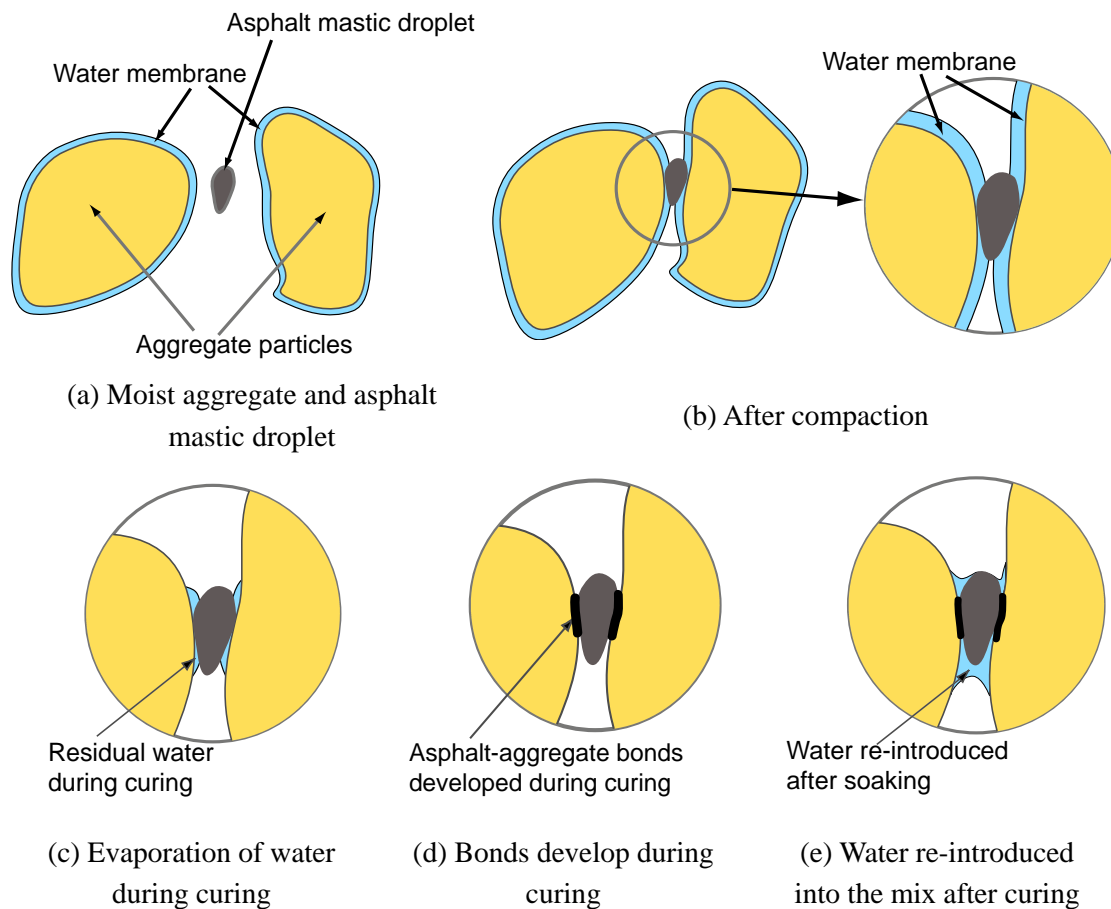
Figure 5.3   Conceptual illustration of the curing process for asphalt mastic
Note: The mineral filler phase and air voids are not explicitly shown.

Figure 5.3 only shows a conceptual illustration of the relations between aggregate particles,

asphalt mastic and molding water, as well as their evolution as water evaporates and as water is reintroduced. The influence of the mineral filler phase was not explicitly considered in the above discussion. This phase is distributed throughout the mix along with the foamed asphalt mastic phase, partially filling the voids in the aggregate skeleton as shown in Figure 3.1. It also develops strength during the curing process, but when water is reintroduced into the mix the strength of the mineral filler phase is significantly reduced. The profiles of water menisci depicted in Figure 5.3 are not necessarily accurate. As virgin aggregates and mineral fillers are hydrophilic while asphalt and asphalt coated PAP are hydrophobic, portraying their interfaces with water is complicated and beyond the scope of this thesis work. Nevertheless, these illustrations adequately describe the proposed model for the fundamental phenomena discussed in this thesis.

This discussion was supported by evidence from specimen fracture face observations. When a fracture encounters asphalt mastic droplets while propagating in a foamed asphalt specimen that has only been subjected to Curing Condition A, it travels primarily through the interface between the foamed asphalt mastic droplets and aggregate particles where the bonds have not fully developed (Figure 5.4[a]). However, in a specimen that has been subjected to Curing Condition B and further soaking, the fracture is more likely to propagate through the asphalt mastic droplet as shown in Figure 5.4(b). It may break the asphalt mastic-aggregate interface, but the chance that the fracture would precisely split asphalt and aggregate is small. The fracture faces of two such ITS specimens (both 0C3A) are shown in Figure 5.5(a) (ITS Specimen A, after being

subjected to Curing A) and Figure 5.5(b) (ITS Specimen B, after Curing B and soaking) respectively. These two specimens were selected from the ITS tests carried out in parallel with triaxial tests TriA (0C3A) and TriB (0C3A) respectively, which had identical mix designs (3% foamed asphalt and no cement). The broken pieces were dried at ambient temperature before the photos were taken. Figure 5.5(a) and (b) each represent approximately 80 percent of the fracture face of a specimen (80 mm x 50 mm). Magnified images (various magnification factors) of these two fracture faces are shown in Figure 5.5(c) through Figure 5.5(f). The asphalt mastic droplets on the fracture face of Specimen A were partially covered by mineral filler, and are thus not visible in Figure 5.5(a), but are clearly visible in Figure 5.5(c) and (e). The fracture face of Specimen B had a notably different appearance, with asphalt mastic droplets split along the fracture.
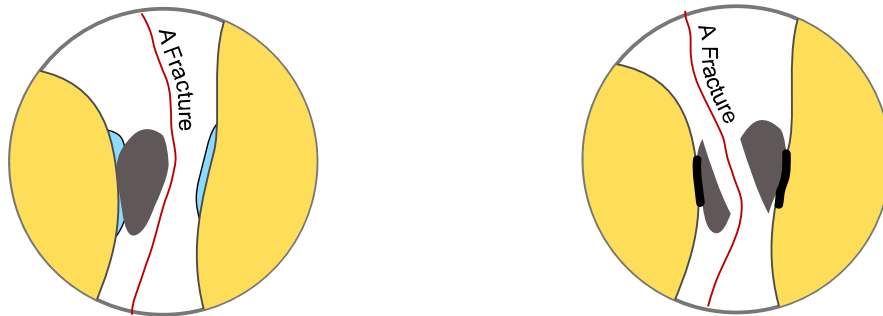
(a) Fracture propagating through Specimen A;   (b) fracture propagating through Specimen B

Figure 5.4   Hypothetical fracture paths for uncured and cured specimens

(a) Fracture face of Specimen A
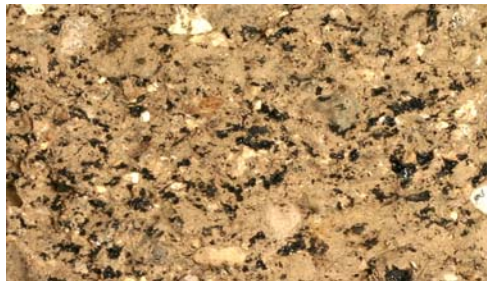
(b) Fracture face of Specimen B
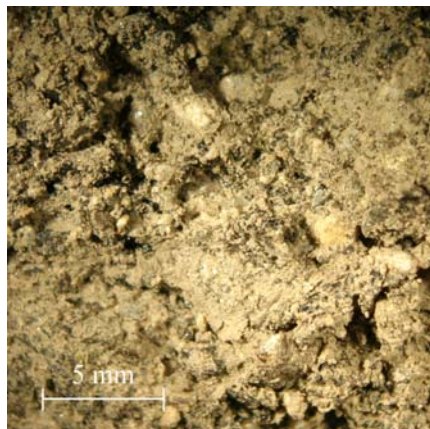
(c) Microscope image of the fracture face of Specimen A
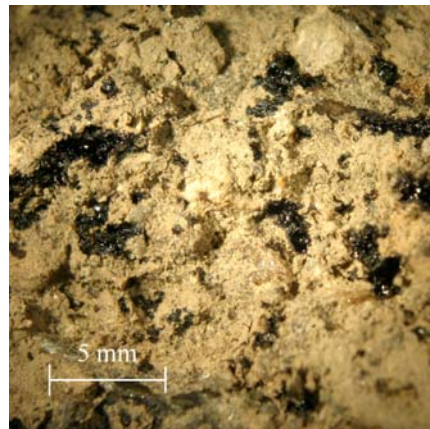
(d) Microscope image of the fracture face of Specimen B
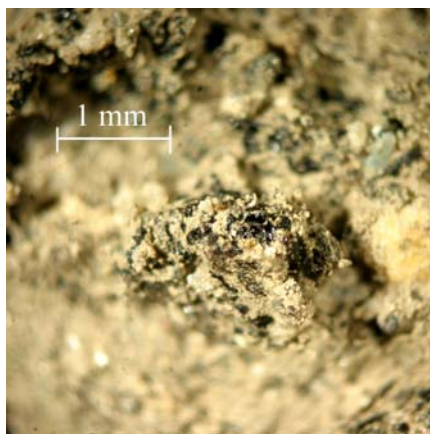
(e) Microscope image of the fracture face of Specimen A
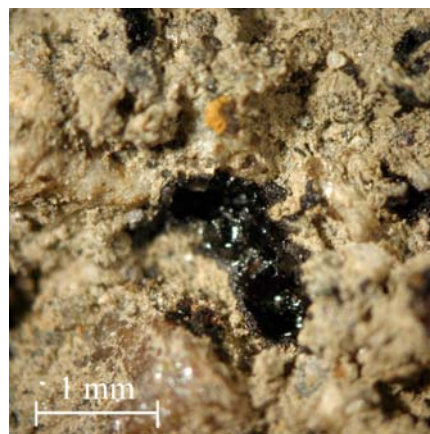
(f) Microscope image of the fracture face of Specimen B

Figure 5.5   Fracture face images of cured and uncured ITS specimens

Note: Both specimen contained 3% foamed asphalt and no portland cement.   Specimen A was subjected to Curing Condition A before the ITS test; Specimen B was subjected to Curing condition B and 1-day soaking before the ITS test.

5.6   A Long Term Curing Study

A small scale laboratory study was carried out to validate the proposed curing mechanism for a relatively long term with limited evaporation.   The specimens were fabricated in Phase I of the UCPRC study (Section 2.15).   The granular material used was RAP-3 as described in Section 2.2.   The asphalt binder was AR-4000 as described in Section 2.3, and the asphalt foam had an expansion ratio of 12 and a half-life of 10 seconds.   No active filler was added to the mixes.

After compaction, the triaxial specimens were left in the molds with the bottom tightly sealed, the top open to air, and placed on shelves in a room with no climate control for a period of six months. Local climate conditions in the room were mild with little diurnal temperature variation and moderate to high humidity.   Ambient temperatures varied between 10ºC and 25ºC during the cure.   Limited evaporation occurred after the six month period had elapsed.   Each specimen was subjected to multiple Tx RM tests with different preconditions.   Results for one representative specimen, containing 4.5 percent foamed asphalt, are discussed below.   Extensive laboratory testing performed during the UCPRC study (Jones et al. 2008) demonstrated that there was no fundamental difference between behavior of mixes of this material containing 4.5 percent foamed asphalt and that of mixes with 3 percent foamed asphalt.   Table 5.5 shows the preconditions that the specimen was consecutively subjected to before each test and the moisture content at the time each test was performed.

Table 5.5   Preconditions before each Tx RM test for the long term curing study

Sequence index	Conditions experienced before testing	Moisture content (%)
Test 0	Immediately after compaction (no test was performed)	5.2
Test 1	Six month cure in mold at ambient temperature and humidity	1.9
Test 2	Soaked in water for 72 hours	4.6
Test 3	Dried in a forced draft oven at 40⁰C for 5 days	0.7
Test 4	Soaked in water for 7 days	3.6

The test results are plotted against the confining stress in Figure 5.6.   The results for one pulse

loading duration of 0.1 second are shown.   The different deviator stress levels applied caused

data point scattering at each confining stress level.
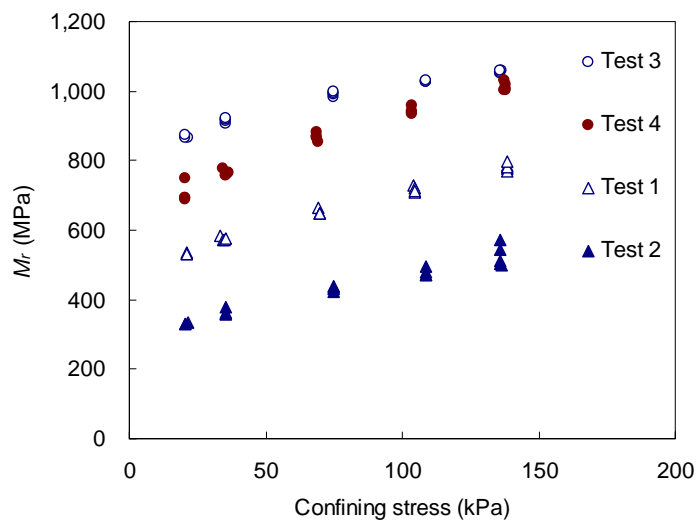
Figure 5.6   Tx RM test results for the long term curing study

When the specimen was extruded from the mold, there was 1.9 percent molding water remaining.

The moisture distribution in the mix should be similar to that depicted in Figure 5.3(c), with a large percentage of the original molding water that had been retained in the larger voids having evaporated, but water in smaller voids mostly still retained, especially at the interface between asphalt mastic droplets and aggregate particles. The specimen gained considerable stiffness during the six months of initial cure (Test 1, resilient modulus between 500 MPa and 700 MPa depending on the stress states). Similar specimens when tested immediately after compaction would have stiffnesses between 200 MPa and 400 MPa. This improvement was mostly attributed to suction provided by the residual water and to weak, natural cementation in the mineral filler phase.

When the specimen was soaked, it lost approximately 40 percent of this stiffness. Resilient moduli measured in this state (Test 2) were comparable to or only slightly higher than that would be measured in the fresh state (i.e. immediately after compaction). When the specimen was subjected to further oven drying (Test 3), significant stiffness improvement was observed, as expected, corresponding to the state shown in Figure 5.3(d). When the specimen was re-soaked, only minimal stiffness reduction occurred (10 to 20 percent depending on the stress state), similar to observations in Chapter 4. When comparing the results of Tests 2 and 4, it was evident that bonds between asphalt mastic and aggregate particles developed during the drying process (in oven) and not during the six months of initial curing when limited evaporation occurred. This asphalt-asphalt bonding, once formed, impedes re-introduced water from reentering some of the voids (moisture content for Test 4 was one percent lower than that for Test 2). This effect was

expected to be more apparent on this specimen, which had 4.5 percent foamed asphalt compared to specimens containing 3 percent asphalt.

Results from this study clearly supported the proposed curing mechanism, in which bonding between asphalt mastic and aggregate particles will not develop until most of the molding water retained at the interface evaporates. It appears that curing duration only has indirect effects on curing of foamed asphalt stabilized mixes by affecting the degree of water evaporation.

5.7   Conclusions and Recommendations

The observations made from the results presented in this chapter have important implications for full-depth reclamation of pavements. They indicate that the bonding provided by foamed asphalt develops as the mixing/compaction water evaporates, and only fully develops once this water is no longer present. If, under certain conditions, this water is retained after compaction (e.g. by early placement of the asphalt wearing course, or because of inadequate drainage) the bonds will not develop, even after a prolonged period of time (months or years). However, once the bonds have formed, occasional reintroduction of water into the treated layer will only partially damage the bonding, provided that extended soaking periods along with heavy repetitive loading do not occur.

It is therefore crucial to allow the initial mixing/compaction water to evaporate from the recycled layer before the HMA surface layer is placed, to ensure that the road is adequately drained, and to

ensure that roadside practices (e.g. irrigation) do not adversely affect the moisture condition of the pavement.

The laboratory curing strategy adopted in this study is recommended as the standard curing process for research and project level material evaluation.   Precisely duplicating or simulating the field curing conditions in a laboratory is extremely difficult, if not impossible.   It also creates problems for procedure standardization given the great variety of environments in which FDR-foamed asphalt can be implemented.   The two curing conditions adopted in this study, simulating conservative (by sealed curing for a short duration) and optimistic conditions (by unsealed curing for a long duration) for water evaporation respectively, are recommended to characterize the fundamental properties of foamed asphalt mixes specific to curing.   Site specific criteria should be noted during project assessments to determine whether the tested materials can meet the conditions of the site.

Portland cement was shown to be very effective in improving strength, stiffness and permanent deformation resistance of the foamed asphalt mixes tested in this task (weathered granite material), especially in the early stages when the foamed asphalt mastic has not cured.   Other active fillers may provide equal or better performance depending on the aggregate characteristics and chemistry.   Many foamed asphalt recycling projects, including those in California, typically require that the rehabilitated section of road is opened to traffic before darkness each day.   Early strength is therefore a key issue in the design, thereby supporting the use of appropriate active fillers in conjunction with foamed asphalt.   The results of this and other tasks in the UCPRC

study (Jones et al. 2008) have shown that the addition of foamed asphalt and active fillers (in this case portland cement) both serve the same purpose of bonding aggregate particles together, but that their roles are complementary rather than interchangeable. The bonds formed by hydrated cement are strong but brittle compared to those of foamed asphalt which are weaker, but more ductile. Portland cement reduces water susceptibility and increases early as well as long term strength. Meanwhile, foamed asphalt improves ductility or flexibility of the mixes, and also provides long-term strength after the more brittle active filler cementation breaks down under traffic. The effects of foamed asphalt and the selected active filler on a mix should be optimized separately in a project mix design procedure, since most conventional laboratory testing methods cannot differentiate the contributions of foamed asphalt treatment from contributions of active fillers.

Chapter 6 Micromechanics of the Effects of Mixing Moisture on Foamed Asphalt Mix Properties

6.1   Introduction

The mixing moisture content (MMC) of a foamed asphalt mix is defined as the moisture content in the granular material when foamed asphalt is injected.   In FDR practice, it is possible to reduce or increase moisture content in the time window between recycling/mixing and compaction.   The MMC and the compaction moisture content (CMC) might therefore be different.   Such practice has been reported in the literature (Acott, 1980) and also observed in California.   Researchers and practitioners have known that mixing moisture content is an important factor in mix design for decades (Csanyi, 1960, after Jenkins 2000).   Although conflicting conclusions were often drawn in different studies, there was general consensus that mixing moisture primarily affects foamed asphalt mix (final product, compacted and cured) properties by two mechanisms.

First, moisture in granular materials can potentially aid, or impede foamed asphalt dispersion.   It was suggested that moisture can help "break down lumpy agglomerations" during recycling (Ruckel et al., 1983).   This effect is intuitive but of little significance in current FDR practice, for example in California, since the recycled materials include mostly pulverized HMA and only

a small amount of the original aggregate base. Agglomerations, if they exist, are broken apart mainly by mechanical action of the recycler. It was also proposed by Csanyi (1960), that "water also separates the fine particles and suspends them in a liquid medium, making channels of moisture through which the foamed asphalt may penetrate to coat all the mineral particles." This is considered to be a hypothesis, rather than a conclusion supported by detailed laboratory or field testing.

Second, moisture content significantly affects compaction behavior of granular materials. This has been thoroughly studied in soil mechanics (Proctor, 1933; Seed & Chan, 1959). In addition to water, the asphalt binder itself may serve as a compaction aid in foamed asphalt mixes, especially at relative high temperature. Nevertheless, this mechanism is considerably simpler and better understood than the mechanism affecting asphalt dispersion. It can be assumed that higher mix densities (as a function of CMC) will result in improved engineering properties of the final product for a given asphalt dispersion pattern in a mix. Soils compacted at different moisture contents potentially have different microstructural characteristics (Seed & Chan, 1959), but this is less significant for coarser materials than for clays. Consequently this mechanism can be treated as a conventional moisture-density problem in this respect and all the principles for soil compaction still apply. It should be noted that the final mix (cured) properties are the main concern in this chapter, and that CMC will also influence early performance of the mix (i.e. wetter mix cures slower) before the curing process is fully completed.

The acronym OMC (Optimum Moisture Content) in soil mechanics and geotechnical engineering

is the moisture content optimized only for dry density. This thesis follows this convention (i.e. OMC means the optimum for compaction/density only) and use OMMC (Optimum Mixing Moisture Content) to represent the MMC optimized for foamed asphalt material properties. The properties of interest varied from one study to another in the literature. In this thesis work, soaked strength, stiffness, and asphalt dispersion as indicated by the FFAC are the primary considerations. Additionally, the MMC and CMC for each mix were generally different in the experiment study documented in this chapter,

6.2   Literature Review

Many studies reported in the literature have investigated the effects of mixing moisture on foamed asphalt mix properties. While informative and inspiring, a number of problems and limitations were identified that warrant additional study on this topic.

In most studies, the effects of moisture content on asphalt mastic dispersion and on compaction were not properly differentiated. Some studies determined the optimum mixing moisture content (OMMC) exclusively based on density criteria (Ruckel et at., 1983; Sakr & Manke 1985) while ignoring potential differences in asphalt dispersion. Other studies (Lee, 1981) investigated the effects of MMC on strength behavior, but the test plan did not permit identification of the contributions of asphalt dispersion and density. This problem has been addressed more appropriately in recent studies (Kim & Lee, 2006; Saleh, 2004) where both density and strength

were measured and reported.

A variety of materials and laboratory procedures were employed in previous studies. The granular materials to be treated with foamed asphalt ranged from sands in most of the early works (Accot, 1980; Sakr & Manke, 1985; Lee, 1981; Little et al., 1983; Roberts et al., 1984; Castedo & Wood, 1982), to coarse aggregates (Saleh, 2004), and to pulverized asphalt pavement (Kim & Lee, 2006; Roberts et al., 1984; Brennen et al., 1983). Most of the recent studies utilized pulverized asphalt pavement (PAP) as the granular material for treatment, and this reflects the evolution of foamed asphalt applications. At the same time, the test procedures, including mixing, compaction, curing and testing adopted by different research groups are far from standardized. These differences partially explain why contradictory conclusions were often reached. For example, in terms of the comparison between optimum MMC (OMMC) for asphalt dispersion and that for compaction (OMC), Little et al. (1983) reported that the OMMC for asphalt dispersion was higher than the OMC for the materials tested (mostly sands); Lee (1981) recommended that the OMMC be 65 to 85 percent of the OMC determined by the standard AASHTO (i.e. standard Proctor) procedure. In contrast, Roberts et al. (1984) reported that peak tensile strengths were achieved at a MMC as low as one percent.

Some researchers (Little et al., 1983) consciously made direct assessments of foamed asphalt dispersion with varying MMC, but no objective and quantitative description of the results was reported.

In terms of the strategies determining OMMC in project level design, three categories of solutions have been proposed as summarized below.

Relating OMMC to other mix design variables. Lee (1981) recommended using OMMC equivalent to 65 to 85 percent of OMC, while Sakr and Manke (1985) related the OMMC to OMC (by standard Proctor compaction), fines content (*PF*, percentage of mass passing a 0.075 mm sieve), and foamed asphalt content (*AC*) by linear regression and recommended the following relation:

$$OMMC = -8.92\% + 1.48OMC + 0.40PF - 0.39\,AC \qquad (6.1)$$

This work was based purely on density criteria, without considering asphalt dispersion or strength characteristics. (A typing error [i.e. a missing negative sign] in the original paper was identified by reexamining the raw data. The corrected equation is shown here).

Using the fluff point. A concept termed the "fluff point", which is the water content at which the untreated moist granular material occupies the maximum bulk volume per unit weight, was introduced (Brennen et al., 1983) as an ideal MMC for foamed asphalt treatment. This approach was rarely followed due to a lack of standard procedures and experience.

Sensitivity analysis. Ruckel et al. (1983) and the South African design guideline (Asphalt Academy, 2002) recommended a sensitivity analysis approach for choosing the OMMC value. Maximizing the dry bulk density was the only objective function, and asphalt dispersion was not

considered.

This chapter attempts to investigate the microstructural mechanisms of the effect of MMC on asphalt dispersion in foamed asphalt mixes. New techniques for characterizing the microstructure of loose moist granular materials and for quantifying asphalt dispersion in foamed asphalt mixes (final product) were developed and employed. The effects of MMC on asphalt dispersion and on mix properties were assessed through a variety of laboratory tests. This study was largely qualitative with a goal of understanding general trends, and consequently only two granular materials were tested in this study, one with a large percentage of fines and the other with less.

6.3 Laboratory Experiment Program

6.3.1 Experiment design

The experiment design for this study is summarized in Table 6.1. Details about this laboratory experiment study are provided in Sections 6.3.2 to 6.3.4.

6.3.2 Materials, mix preparation and specimen fabrication

Owing to the explorative and qualitative nature of this study, only two PAPs (88-C and 33-A as described in Section 2.2) and one asphalt cement type (PG64-16) were tested. The same materials were used in the studies documented in Chapter 3 and Chapter 4 of this thesis work.

The asphalt was foamed with a Wirtgen WLB10 laboratory plant at 165°C with 4% foaming water by mass added. The average expansion ratio and half-life were 23 and 19.5 seconds respectively.

Table 6.1   Experiment factorial design for the MMC study

Variable	Values
Granular material	- PAP 88-C - PAP 33-A
Target MMC	- PAP 88-C: 3%, 4%, 5%, 6%, and 7% - PAP 33-A: 3%, 4%, 5%, and 6%
Test methods	- Indirect tensile strength (ITS, 100 mm) - Triaxial resilient modulus (Tx RM) - Unconfined compressive strength (UCS) test
Water conditioning	- ITS: soaked and unsoaked - TxRM and UCS, soaked only
Replicates per mix	- 4×100 mm ITS specimens (2 unsoaked + 2 soaked) - 1× triaxial/UCS specimen
Binder type	- PG64-16, optimized foaming characteristics
Foamed asphalt content	- 3%
Target CMC	- PAP-88-C: 6% (unless MMC was higher) - PAP-33-A: 5% (unless MMC was higher)

[1]Additional water was added immediately after foamed asphalt injection for mixes with a higher target CMC than the target MMC

The mix preparation procedure was described in detail in Section 2.5. For each mix type, one batch of loose mix (20 kg total) was prepared to fabricate a cylindrical specimen for Tx RM tests and UCS tests, and a series of ITS specimens. The same specimen fabrication procedures and

test setups as described in Sections 2.6 and 2.8 were followed. All tests were carried out at 20ºC.

6.3.3 Moisture content measurements

There were some inevitable variations (as shown in Table 6.2) of the target moisture content planned (shown in Table 6.2) during execution of this work.

6.3.4 Curing, water conditioning and testing

All compacted specimens were cured in a forced draft oven at 40°C for 7 days for this chapter. Specimens subjected to water conditioning were soaked in a water bath at 20°C for 72 hours with the water level 100 mm above the surface of the specimen. The prolonged drying and soaking durations were designed to represent extreme and critical field conditions and to minimize the influence of different specimen sizes by obtaining complete drying or sufficient water infiltration through all specimens. The implications of soaked vs. unsoaked strength and stiffness tests, as well as the reasons why soaked tests were more preferable for evaluating mix performance in this study are discussed in detail in Section 3.6.2.

The Tx RM, ITS and UCS tests performed in this task are described in Sections 2.6, 2.8, and 2.10 respectively.

Table 6.2   Planned and measured moisture contents

PAP	Mix	Target MMC (%)	Measured MMC (%)	Target CMC (%)	Measured CMC (%)
PAP 88-C	I	3.0	2.6	6.0	5.9
	II	4.0	4.0	6.0	6.5
	III	5.0	4.6	6.0	6.0
	IV	6.0	6.3	6.0	6.3
	V	7.0	7.1	7.0	7.1
PAP 33-A	I	3.0	2.5	4.9	5.0
	II	4.0	3.7	5.1	5.0
	III	5.0	4.8	4.8	5.0
	IV	6.0	6.0	6.0	6.0

6.4   Microscopic Observation on Loose Mixes

6.4.1 Visual inspection of loose mixes

Samples of loose moist mixes were observed through a low power microscope.   Selected images of the PAP 88-C mixes at various mixing moisture contents are shown in Figure 6.1.   The microstructures formed by the moist aggregate particles and their evolution with increasing moisture content can be observed.   These mixes were prepared specifically for visual observation, and thus the moisture contents were similar but not identical to the values listed in Table 6.2.   No foamed asphalt was added to these mixes.

In a loose moist aggregate particle assembly, water bridges bond the particles primarily through capillary suction (Figure 6.2[a]), with the suction forces providing tensile strength to the bonds.

As the mixing moisture content increases from zero percent, the agglomeration state of the aggregate particles evolves through a series of states:

- •State-A: No water exists in the loose mix and the aggregate particles are not attached to each other in any way.

- •State-B: When the MMC is low, a few small aggregate particles are bonded together by water bridges to form a number of small clusters, with each cluster containing a few fine particles (Figure 6.1[a]).

- •State-C: As the MMC increases, a higher proportion of the aggregate particles and larger particles are bonded together and various spatial structures are formed (Figure 6.1[b] and Figure 6.2[b]).

- •State-D: When the MMC is high (i.e. close to or higher than the OMC [modified Proctor]), relatively large agglomerations are formed, in which fine particles form a paste like substance that coats bigger aggregate particles (Figure 6.1[c], [d] and Figure 6.2[c]).

If relatively large agglomerates are formed in the loose mixes (such as in state D), the finer aggregate particles are suspended in pore fluid, and the effective total surface area available for foamed asphalt coating is small.   This is likely to result in inferior asphalt dispersion characterized by concentrated asphalt distribution with thick asphalt film, when such mixes are treated with foamed asphalt.   This postulation will be validated by direct observations on foamed asphalt mix (cured and tested) fracture face features in the following sections.

(a)

MMC = 2.5%

(b)

MMC = 4.9%

(c)

MMC = 6.4%

(d)

MMC = 7.3%
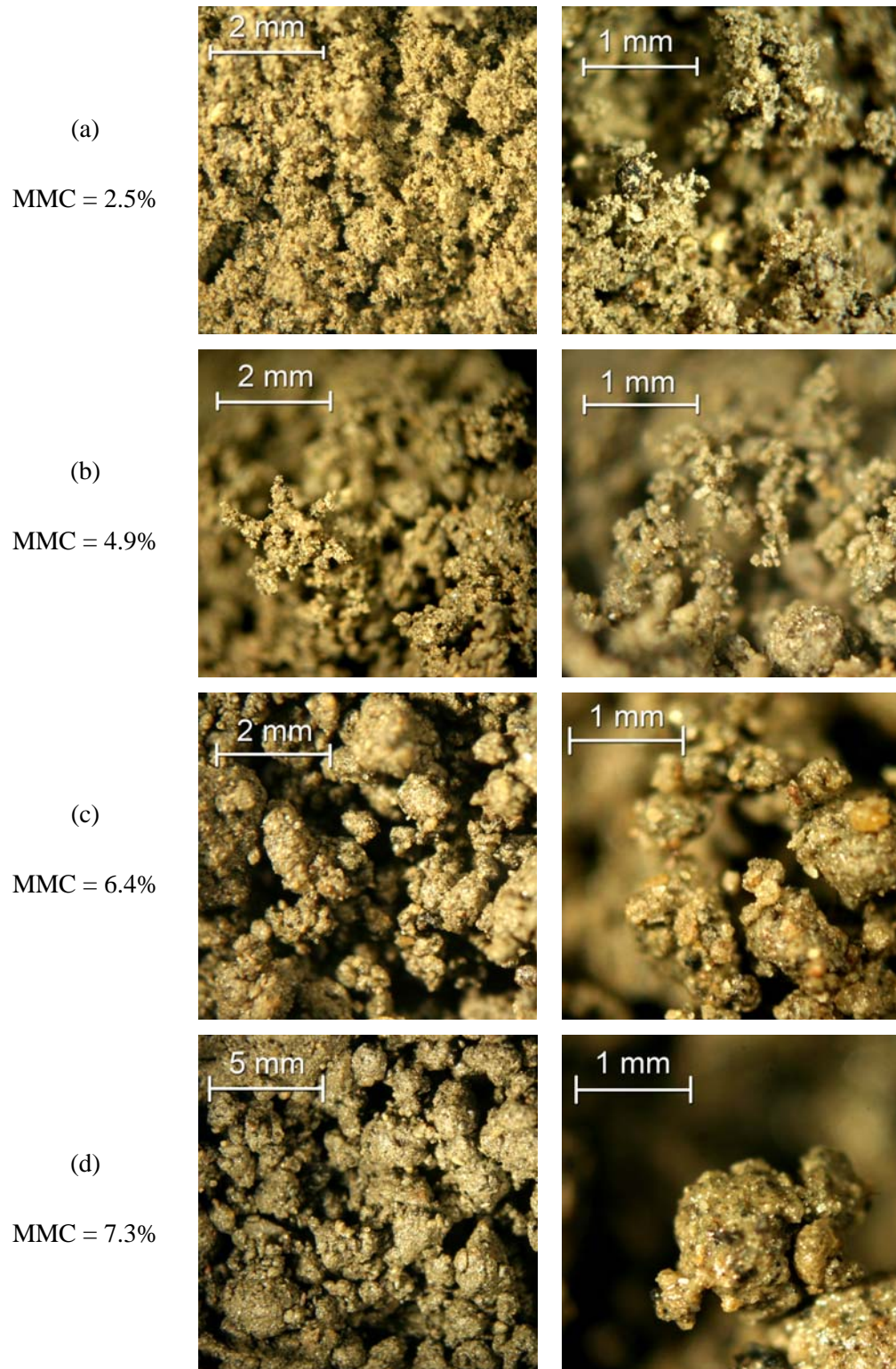
Figure 6.1   Microscope images of loose mixes at various mixing moisture contents
Note: Not all the figures are in the same scale.

These states form a spectrum with no clear boundaries between each other. Based on the microscope assessment of the PAP 88-C materials, it is proposed that mixes with mixing moisture contents lower than 3 percent should be in State B; mixes with moisture content in the vicinity of 5 percent should be in State C, while mixes with mixing moisture contents around 6.5 percent should be in State D. These values are only relevant to this particular material.

(a)   (b)   (c)
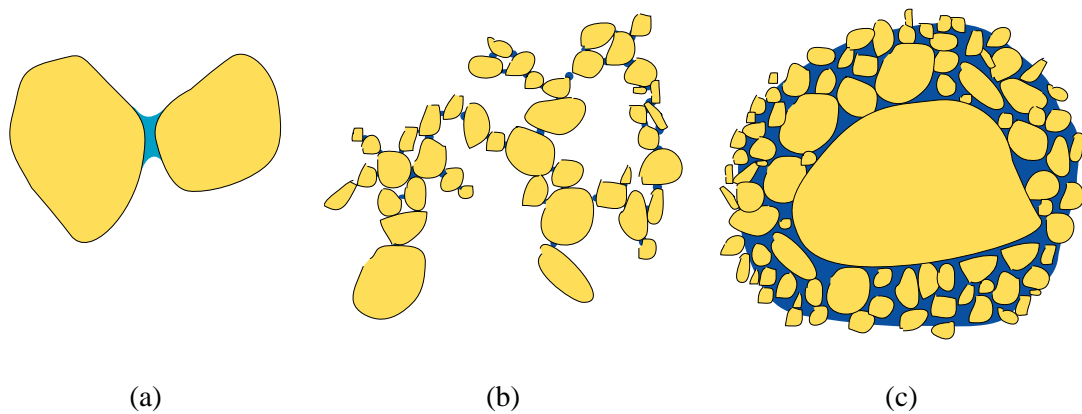
Figure 6.2   Various microstructures formed by water bridges and soil particles
(a) Two soil particles connected by a water bridge; (b) spatial structure foamed at low MMC,
state-C; and (c) particle agglomeration at high MMC, state-D.

6.4.2 Micromechanics for agglomeration evolution, a thermodynamic perspective

The observed evolution of the agglomeration (or clustering) states of moist aggregate particles can be semi-quantitatively explained by tracking pore water distribution characteristics in loose moist mixes. This investigation involved theories and principles pertaining to the thermodynamic potential of soil pore water.

Although similar topics are often considered in *unsaturated soil mechanics* (Fredlund & Rahardjo, 1993; Lu & Likos, 2004), a literature survey on the evolution of agglomeration states of moist

loose granular materials did not yield useful results, apparently because uncompacted loose moist granular materials are not considered as engineered materials. Numerous studies on the behavior of a pair of solid particles bonded by a liquid bridge have been reported in the last 30 years, mostly by researchers in chemical engineering. The calculation in this paper was based on the work by Mehrotra and Sastry (1980), which presented closed form approximations for the pendular bond strength between unequal-sized spherical particles. The notations also follow their work, although the equations are not repeated here.

During the mixing process, the system consisting of aggregate particles, pore water and pore air tends to approach thermodynamic equilibrium, namely in thermal equilibrium (pertaining to temperature), in mechanical equilibrium (pertaining to pressure), and in diffusive equilibrium (pertaining to chemical potential). The mechanical equilibrium dominates the phenomena discussed in this study, and is primarily affected by pressure difference between individual water bridges induced by the capillary effect. In a system in ideal equilibrium, pressure in all water bridges should be the same if the effects of gravity are ignored. Otherwise moisture transport will occur, either by mechanical actions of the mixer, or through the process of evaporation and condensation until thermodynamic equilibrium is reached.

A particle pair is shown in Figure 6.3, assuming all aggregate particles are spherical to allow quantitative calculation. Particles A and B are in tight contact and their radii are R_1 and R_2 respectively. The radius ratio is defined as $r=R_2/R_1$ and without losing generality, $R_2<R_1$. The contact angle at the water-soil particle interface is θ. Ψ_1 and Ψ_2 are the two filling angles. The

water bridge geometry is characterized by the two principal radii of curvature ρ_1 and ρ_2. Curvature ρ_2 is not a constant throughout the water bridge profile, and an approximate average value is used instead. Using the pore air pressure (atmospheric pressure) as the datum, the pressure in this water lens can be calculated based on the Young-Laplace equation (6.2).

$$P = \gamma(\frac{1}{\rho_2} - \frac{1}{\rho_1})$$

(6.2)

where γ is the air-water surface tension in N/m. If the water bridge is relatively small compared to the particle sizes (i.e. water content is low), then ρ_1 is generally smaller than ρ_2, and consequently $P<0$ indicating suction.
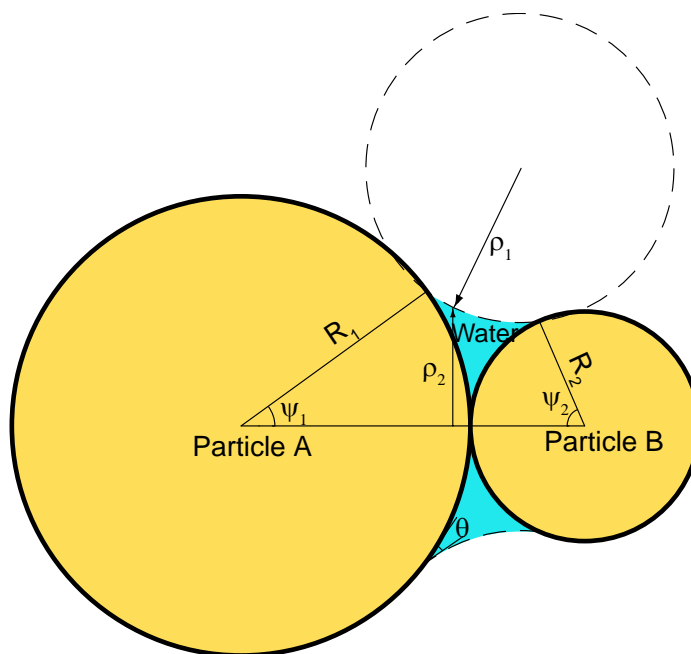

Figure 6.3   Geometrical representation of a pendular liquid bridge

The normalized volume of the water bridge V^* is defined as the ratio of the volume of the water

bridge (V_w) to the total volume of the two spherical particles (see equation [6.3]).

$$V* = \frac{V_w}{\frac{4}{3}\pi(R_1^3 + R_2^3)} \qquad\qquad (6.3)$$

The normalized water bridge volume is associated with the moisture content in the mix. For a simple face-centered cubic or hexagonal close-packed packing of equal sized spheres with uniform water distribution, the moisture content MC = $12V*/G_s$, noting that each particle has 12 water lenses attached, where G_s is the specific gravity of the soil solid. For a typical granular loose mix with any gradation and a random packing pattern, the description is much more complicated. Nevertheless, it is apparent that if normalized volumes of most water bridges increase, the moisture content in the mix increases accordingly.

To illustrate the water transport process between soil particle pairs of different sizes, the following ideal case was analyzed. A particle pair O is chosen as the reference. The basic geometrical characteristics as shown in Figure 5 are:

$R_1=R_{1O}$, $R_2=R_{2O}$, $\Psi_1=\Psi_{1O}$, $\Psi_2=\Psi_{2O}$, $\rho_1=\rho_{1O}$ and $\rho_2=\rho_{2O}$.

A second particle pair I is geometrically similar to the reference pair O, as:

$R_{1I}/R_{1O}=R_{2I}/R_{2O}=\rho_{1I}/\rho_{1O}=\rho_{2I}/\rho_{2O}=\eta$, $\Psi_{1I}=\Psi_{1O}$, $\Psi_{2I}=\Psi_{2O}$ and $V*_I=V*_O$

where η is the size ratio of the two particle pairs. If particle pair I is smaller than pair O ($\eta<1$), then according to equation (6.1), $P_I<P_O<0$. This indicates that the thermodynamic potential of

the water bridge in pair I is lower than that in pair O, and water will transport from O to I. As

the normalized water bridge volume of pair O decreases, the associated water pressure decreases

resulting in stronger suction. At the same time, the normalized water bridge volume of pair I

increases, associated with water pressure increasing (weaker suction). This process continues

until thermodynamic equilibrium is achieved, namely the two water bridges have equal pressure.

Based on this qualitative analysis, water bridges connecting smaller soil particles tend to have

higher normalized volumes in a system in thermodynamic equilibrium. More detailed

quantitative analysis is shown in the two following numerical examples, with the water-soil

particle contact angle θ assumed to be zero.

In the first case, the normalized water bridge volume (V_O*) for the reference soil particle pair O is

fixed at three levels (0.01, 0.001 and 0.0001). Three radius ratio levels ($r = 1$, 0.5 and 0.25) are

considered. The second soil particle pair I is geometrically similar to the first pair, and its size,

represented by the scaling factor $\eta = R_{1I}/R_{1O}$, is the main variable. As η decreases, or as the

particle size of pair I decreases, the normalized water bridge volume $V*_I$ needs to increase to

achieve the same pressure/thermodynamic potential as that for the first pair O. Figure 6.4(a)

shows the ratio ($V*_I/V*_O$) of the normalized water bridge volumes between the two particle pairs

as a function of V_O^*, r and η to ensure that these two pairs are in thermodynamic equilibrium.

In the second case (Figure 6.4[b]), the normalized water bridge volume of the first pair O (V_O*)

changes from 0.00001 to 0.1 continuously as the main variable. The results show the

normalized water bridge volume (V_I*) of the second pair that achieves thermodynamic

equilibrium.   The calculation was performed for four sizes of the second pair (η = 0.5, 0.2, 0.1 and 0.01).

The above analysis assumes water in the mix maintains a uniformly distributed temperature, which is not strictly true.   The evaporation and condensation procedures change the water temperature, which in turn changes the water-air surface tension.   However in the soil particle-water system concerned in this study, heat transfer with the ambient environment takes place much quicker than does internal moisture transfer, and water-air surface tension is only mildly influenced by temperature.   The effects of changing temperature can thus be reasonably ignored.   As long as the temperature distribution in the mix is assumed to be uniform, the above analysis does not depend on the specific value of water surface tension.

(a) $V_O{}^*$ fixed with η varying;   (b) η fixed with $V_O{}^*$ varying
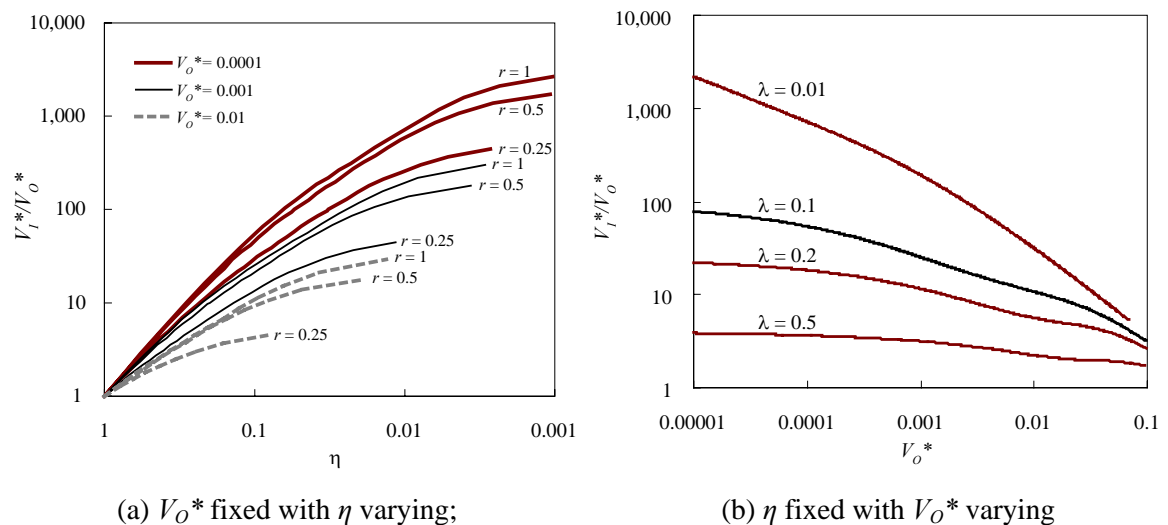
Figure 6.4   Ratio of normalized water bridge volumes of two particle pairs in thermodynamic equilibrium

(Note: η is the size ratio of the two particle pairs.)

These two quantitative analyses studied the same attribute from two different perspectives.   Both

of them show that the normalized water bridge volume of the smaller soil particle pair needs to be much higher to reach thermodynamic equilibrium with the larger particle pair. As a numerical illustration, for instance, in each pair the two particles are assumed to have the same sizes ($r = 1$), and $R_{1O}=R_{2O}=1$ mm, $R_{1I}=R_{2I}=0.01$ mm, $\eta=0.01$. Pair **O** consists of two sand particles and pair **I** consists of two silt particles. According to the calculation results, for a normalized water bridge volume of pair **O** $V_O{}^*=0.001$, the filling angles $\Psi_{1O} =\Psi_{2O}=15°$. To achieve thermodynamic equilibrium with pair **O**, the normalized water bridge volume for pair **I** needs to be 195 times greater ($V_I{}^*=0.195$) with corresponding filling angles $\Psi_{1I} =\Psi_{2I}=53°$.

In an actual aggregate assembly consisting of particles with radii ranging from 10 mm to 0.01 mm, water tends to be absorbed by the smaller soil particles first. When the MMC is low, such as in State-B discussed previously, both small soil particles and large particles are bonded together by water bridges at their contact points. This state was termed the "pendular state" (Figure 6.5[a]) by Newitt and Conway-Jones (1958) as one of the liquid saturation states of moist granular materials. As the water bridge volume grows and eventually saturates the voids in the particle assembly, another state, termed the "capillary state" (Figure 6.5[c]) is reached for some particle pairs.

According to the calculation results, the finer fraction of the granular material apparently always has a higher normalized water bridge volume. As the MMC increases, the fine fraction first reaches the capillary state, forming a paste like substance with a suspension of soil particles in a background fluid. A cut-off particle size can ideally be identified at each MMC level. For

particles smaller than this cut-off size the particle-water mixture is most likely in the capillary state, whereas larger particles should be in the pendular state. Particles with sizes similar to this cut-off size probably exist in the "funicular state" (Figure 6.5[b]), which is the transitional state between the pendular and capillary states. The cut-off size increases as the MMC increases, which implies that as the MMC increases, more and larger particles reach the funicular or capillary states. In State-C (Figure 6.1[b] and Figure 6.2[b]), a small portion of the granular particles are already in the capillary state. However, in State-D there is sufficient paste like substance to entirely coat the larger particles. This explains the observation in Figure 6.1(c) (d) and Figure 6.2(c).

(a) Pendular state   (b) Funicular state   (c) Capillary state

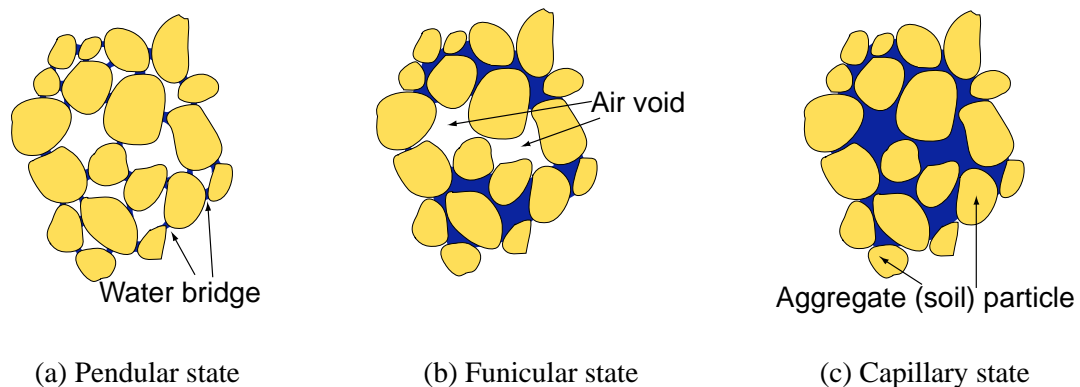Figure 6.5   Three liquid saturation states of moist granular particle assemblies with a narrow particle size spectrum.

6.5   Fracture Face Observations and Test Results

6.5.1 Fracture face observations

The fracture faces of the tested ITS specimens were assessed to evaluate asphalt dispersion characteristics at different MMC levels. The fracture faces of the PAP 88-C soaked ITS-100mm

specimens for all MMC levels tested are shown in Figure 6.6. The two figures for each MMC level were from the two replicates per mix, respectively. As the two fracture faces yielded by each specimen have generally similar appearances, only one of them is shown. The images have been cropped to facilitate comparison (approximately 80 percent of the fracture face [80 mm x 50 mm] is shown).

The fracture faces show a large number of small asphalt spots for low MMC mixes (2.6% to 4.6%, corresponding to loose mixes in States-B and -C). The visible asphalt mastic distribution features for each pair of fracture faces are generally the same for these mixes. When the MMC is close to or higher than the OMC (6.3% and higher, corresponding to loose mixes in State-D), the fracture faces show less asphalt spots and the size of these spots is generally larger. The overall asphalt coverage ratios (or FFAC) are lower for these mixes. At the same time, higher variance between replicate specimens was observed. Loose mixes in State-B and State-C, when treated with foamed asphalt, tend to produce a microstructure featuring a larger number of small asphalt mastic droplets uniformly dispersed in the mix, with a thin asphalt film.

Foamed asphalt mixes made of loose granular materials in State-D, result in relatively large asphalt globules with a concentrated distribution, and thick asphalt film, which is undesirable in foamed asphalt treated mixes.

The fracture faces of the PAP 33-A mixes are not shown because the asphalt dispersion patterns for different MMC levels were only marginally different. One possible reason is that the

spectrum of particle sizes for PAP 33-A is significantly narrower: PAP 88-C contains more fines

and the particle sizes of the fines (introduced baghouse dust) in PAP 88-C are much smaller than

those in PAP 33-A (fine sands).   The aforementioned mechanism should affect, but does not

dominate, behavior of PAP 33-A, and further investigations are required to identify other potential

mechanisms.   As discussed in the following sections, the FFAC values for PAP 33-A mixes were

insensitive to MMC values, which confirm the above observations.

## 6.5.2 Strength and stiffness test results

The strength and resilient modulus (stiffness) test results and the corresponding FFAC results are

summarized in Table 6.3.

Table 6.3   Strength and stiffness test results for different mixing moisture contents

Mix[1]		ITS-Unsoaked		ITS-Soaked			Tx RM-Soaked			
		ITS (kPa)	FFAC[2] (%)	ITS (kPa)	FFAC[2] (%)	UCS (kPa)	k_1	k_T	k_2	k_3
PAP 88-C	I	564	9.0	104	9.8	643	4,208	-0.106	0.39	-0.15
	II	596	9.0	98	9.2	639	4,042	-0.104	0.41	-0.17
	III	563	7.7	102	8.2	723	4,407	-0.102	0.40	-0.16
	IV	449	8.8	65	4.4	516	2,914	-0.088	0.50	-0.20
	V	481	5.8	79	5.6	483	3,604	-0.094	0.44	-0.18
PAP 33-A	I	752	29.8	162	25.3	703	5,827	-0.103	0.28	-0.11
	II	696	34.0	175	33.1	829	6,949	-0.120	0.23	-0.11
	III	780	34.2	146	27.7	790	6,650	-0.116	0.24	-0.10
	IV	773	32.9	153	28.3	924	7,216	-0.113	0.24	-0.10

[1]: Mixing and compaction moisture contents shown in Table 6.2   Mixing moisture content increases with mix number.

[2]: FFAC measured for soaked tested specimens (FFAC-ITS-Soaked) is preferable as explained in Section 3.6.2.
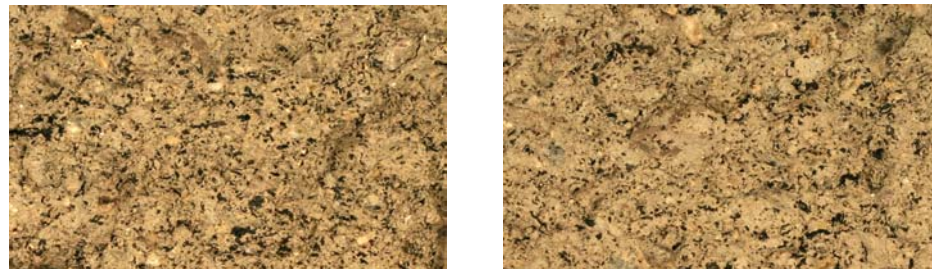
(a) PAP 88-C-I, MMC = 2.6%
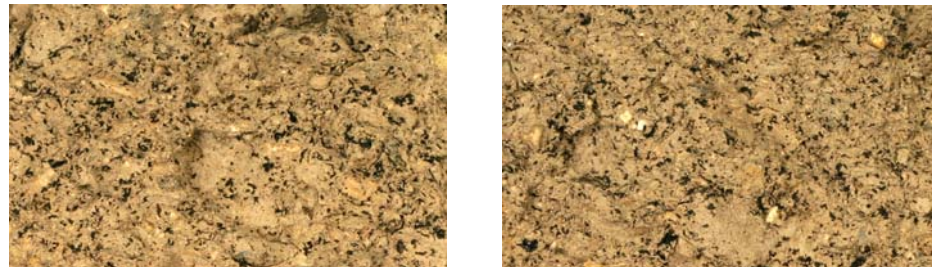
(b) PAP 88-C-II, MMC = 4.0%

(c) PAP 88-CIII, MMC = 4.6%

(d) PAP 88-CIV, MMC = 6.3%
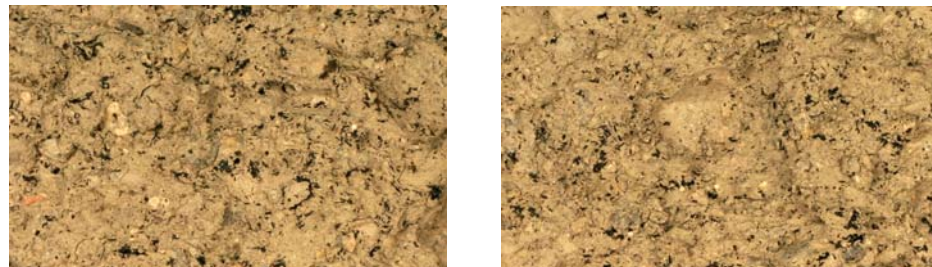
(e) PAP 88-CV, MMC = 7.1%

Figure 6.6   Fracture faces of specimens with different mixing moisture contents

Figure 6.7(a) illustrates the effect of MMC on the FFAC values. FFAC values can be used as an indicator of the degree of fo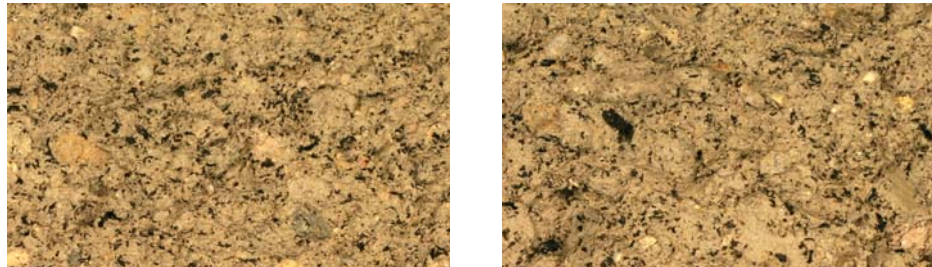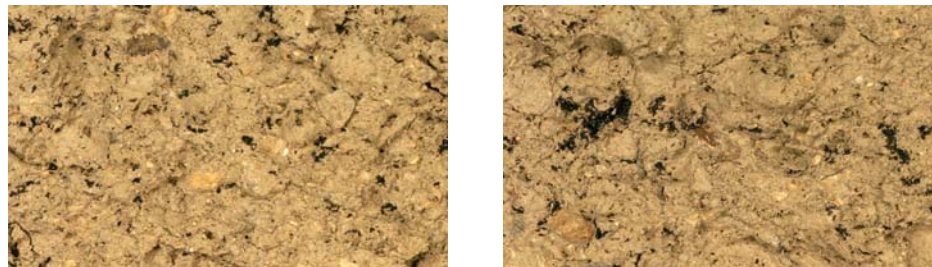amed asphalt dispersion in the mix (for materials with the same grading), with higher values representing better dispersion and hence better quality mixes. Although results for the two PAP types are plotted together in Figure 6.7 and Figure 6.8, direct comparisons between them are not intended because direct comparisons of mixes with significantly different gradations are considered inappropriate in the context of this study. Pulverized materials with coarser gradations, such as PAP 33-A, generally yield fracture faces with higher asphalt mastic coverage, however, does not necessarily indicate that foamed asphalt is dispersed better in these materials.

PAP 88-C mixes with lower mixing moisture contents have better asphalt dispersion characterized by higher FFAC values, while PAP 33-A mixes do not show an obvious trend, consistent with the direct observations in loose mixes and on fracture faces. Figure 6.7(b) through (d) show the correlation between FFAC values and the soaked ITS, unsoaked ITS and soaked UCS test results respectively. Mixes with better asphalt dispersion generally showed higher strengths. All these trends are more distinct for the PAP 88-C mixes than for the PAP 33-A mixes.
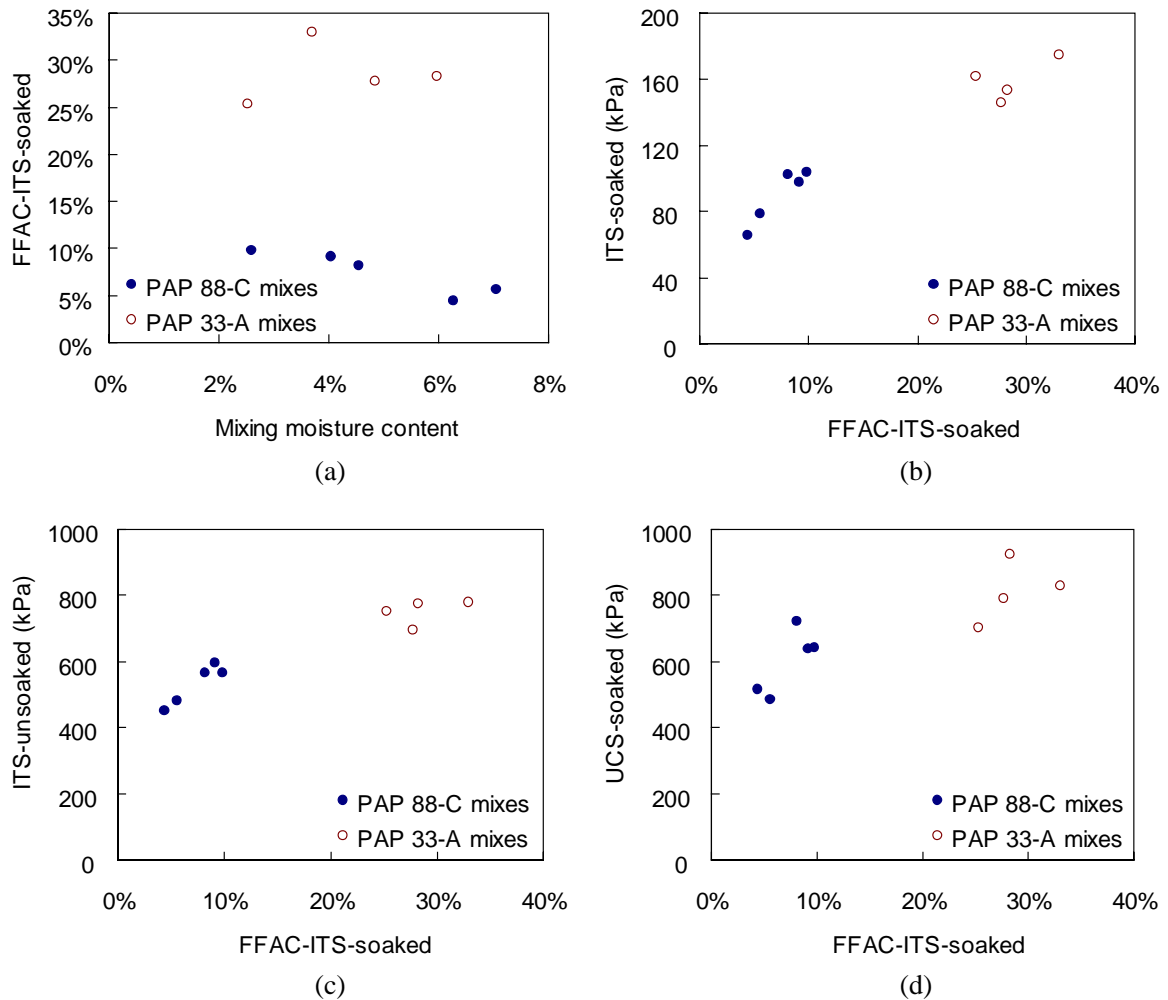
Figure 6.7   Strength test results and the effects of foamed asphalt dispersion
(a) Effect of MMC on asphalt dispersion; (b) effects of asphalt dispersion on soaked ITS; (c)
effects of asphalt dispersion on unsoaked ITS; (d) effects of asphalt dispersion on soaked UCS.

Figure 6.8(a) through (d) show correlations between the resilient modulus model fitting constants

(k_1, k_T, k_2, and k_3) and the FFAC values measured from soaked ITS specimens.   The constants k_T, k_2

and k_3 represent the sensitivity of the foamed asphalt mix resilient modulus to loading rates (or

equivalently load pulse durations), bulk stresses, and deviator stresses, respectively, as described in

Section 2.8.   For PAP 88-C, mixes with better asphalt dispersion (higher FFAC values) show

stiffness to be less sensitive to stress states (higher value of k_1; lower absolute values of k_2 and k_3)

and more sensitive to loading rates (higher absolute values of k_T). This indicates that mixes with

better asphalt dispersion show behavior similar to that of typical asphalt-bound materials.   These

correlations were less significant for the PAP 33-A mixes than for the PAP 88-C materials.

Figure 6.8   Correlations between resilient modulus parameters and FFAC values
(a) Correlation between FFAC and k_1; (b) correlation between FFAC and k_T; (c) correlation
between FFAC and k_2; (d) correlation between FFAC and k_3.

6.6 Summary and Discussions

Observations of the loose untreated mixes and ITS specimen fracture faces indicate that the MMC affects asphalt distribution in foamed asphalt mixes through its influence on the agglomeration states of aggregate particles, specifically the fine particles.
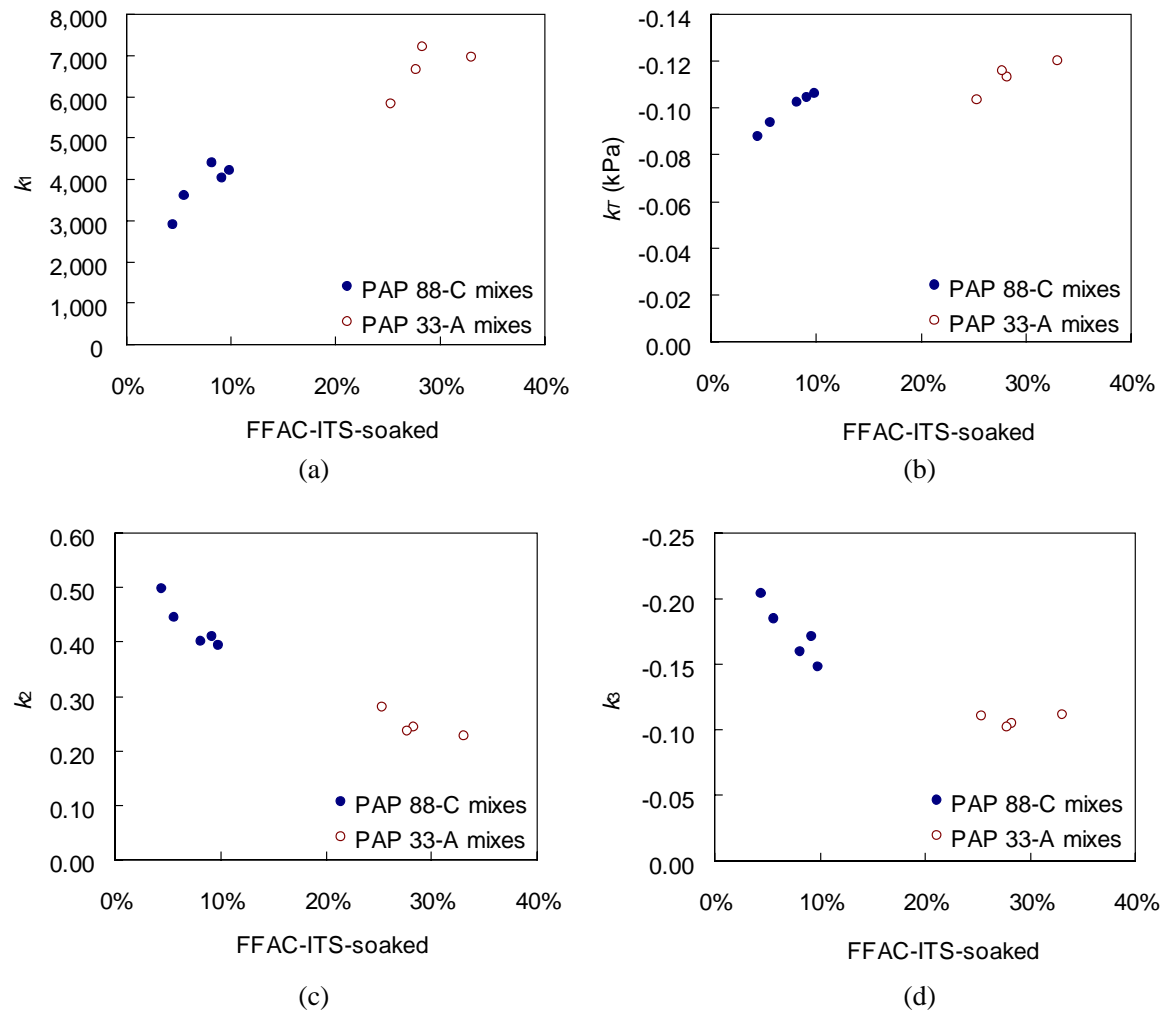
A series of agglomeration states, A through D, of moist aggregate particles are qualitatively identified.   Visual assessments of the ITS specimen fracture faces, supported by quantitative FFIA analysis, indicate the following:

- Poor dispersion of foamed asphalt is likely if the agglomeration state of a moist mix is in State-D, because the exposed surface area of the aggregate particles is small and the asphalt will have a concentrated distribution with a relatively high asphalt film thickness on a few particles.

- Mixes in State-B typically have good asphalt distribution, but in practice the mixes might be too dry to achieve adequate density.

- Mixes in State-C appear to have a good balance between mix workability (or compactability) and asphalt distribution, if the construction procedure does not allow changing moisture content between mixing and compaction.   Data collected during this thesis study were insufficient to determine clear upper and lower limits for the moisture content of this state, but 75 percent to 90 percent of the optimum compaction moisture content (modified Proctor) appears to be an appropriate starting point.   These limits should be established during the

mix design process for any specific material.

- If the construction procedure permits adding water to field foamed asphalt mixes between recycling/mixing and compaction, then low mixing moisture content is desired for asphalt dispersion considerations. However, in this situation, other construction requirements, such as dust control and the optimum moisture content for recycler operation (i.e. drier soils are generally harder to cut by the recycler teeth) may dictate the moisture content. Nevertheless, applying additional water to recycled materials might involve another pass of the recycler on the materials, which is costly and can negatively change the grading (by creating more fines) of the materials.

Identifying these agglomeration states can be achieved by experienced laboratory mixing operators and field construction inspectors, and does not require special equipment. Foamed asphalt dispersion in mixes with high fines contents (e.g. higher than 12% passing the 0.075 mm sieve) appears to be more sensitive to mixing moisture content. Although the evolution of agglomeration states applies to most granular materials with different aggregate gradations, other mechanisms might dominate behavior of certain materials.

The most important contribution of the study reported in this chapter is possibly to dismiss the postulation that high MMC in granular materials can aid foamed asphalt dispersion (Csanyi, 1960; Little et al., 1983). Both conventional laboratory testing (strength and stiffness) and direct microstructure observation in this study confirmed that an excess amount of water actually impedes

asphalt dispersion. Possible reasons for the discrepancy between the current study and some studies reported in the literature are discussed below.

Early research and implementation of full-depth reclamation with foamed asphalt were mainly on sandy materials with relatively small quantities of recycled asphalt pavement. However, in the United States, coarser PAP materials are more typical in recycling projects. Different granular materials might show different behaviors and the conclusions drawn in this study are not necessarily representative of all materials types and gradations.

Early laboratory investigations mostly used Hobart planetary mixers whereas in this thesis study a pugmill type mixer was used. Studies reported by Acott (1980), Sakr and Manke (1985), and Lee (1981) all used Hobart planetary mixers. Other studies in the 1980's to the 1990's possibly have used similar mixing equipment without explicitly mentioning it, owing to its ready availability.

The mixing efficiency of Hobart mixers could be impaired when the mix is relatively dry. When a Hobart mixer is used, the observed different asphalt dispersion patterns might have been more attributed to different mixing efficiencies associated with mixing moisture change rather than due to the different microstructures of the mix itself observed in this study. Efrem's study (2000, after Jenkins 2000) highlighted the fact that mixing techniques have substantial effects on properties of foamed asphalt mixes, and pugmill type mixers tend to produce better quality mixes. It is the author's opinion that pugmill mixers best simulate the action of modern pavement recyclers. Consequently the validity of conclusions drawn from studies utilizing Hobart planetary

mixers requires further investigation.

Most investigations reported in the literature did not have the necessary tools and techniques to directly quantify microstructures in loose untreated mixes and foamed asphalt dispersion patterns. The new techniques developed for this study provided greater insight, and it is believed have lead to more solid conclusions.

Chapter 7 Conclusions and Recommendations for Engineering Practice

7.1 Challenges to This Thesis Study

Full depth reclamation (FDR) of flexible pavement with foamed asphalt is a promising highway rehabilitation strategy. If designed and constructed properly, it has a lower life cycle cost and less environmental impact than do many other alternative strategies. However, a number of challenges are to be tackled before deeper understanding of foamed asphalt stabilized materials can be achieved, based on which more reliable design can be made.

The primary challenge is the intrinsic complexity of foamed asphalt treated materials. Compared to hot mix asphalt and unbound aggregate base materials, foamed asphalt mixes involve more mixing variables, the mixing procedure is of a less controllable nature, and the main constituent, namely recycled asphalt pavement materials, also introduces unpredictability.

As a result of the complexity in foamed asphalt mix behavior, many unique characteristics of this material were not adequately considered in some of the previous studies reported in the literature. The design philosophies, test methods and evaluation criteria for HMA and aggregate base materials have been presumed to be directly applicable to foamed asphalt mixes. This practice,

as revealed in this thesis, often yields suboptimum engineering solutions.

This thesis presents a micromechanical research framework to investigate a number of key properties of foamed asphalt mixes. Instead of directly seeking the connections between mix variable and material properties, this new framework investigates how mix variables affect the material microstructure and in turn how changes in microstructure influence material behavior. Such a framework is well suited for composite materials including foamed asphalt mixes, and was proven to provide useful insight into complex behavior of this material.

7.2   Quantifying the Microstructure of Foamed Asphalt Mixes

It was found that typical microstructures of foamed asphalt mixes consist of three major solid phases, namely the aggregate skeleton, the asphalt mastic phase which exists in the form of numerous droplets bonding the aggregate skeleton, and the mineral filler phase partially filling the voids in the aggregate skeleton. Due to the significant difference between the microstructure of hot mix asphalt (HMA) and that of foamed asphalt mixes, the existing methods for characterizing microstructure of HMA cannot be directly applied to foamed asphalt mixes.

For most research and engineering purposes, foamed asphalt mixes' most important microstructural characteristic is the quantity of asphalt mastic produced during mixing and its distribution in foamed asphalt mixes (cured and compacted). A Fracture Face Image Analysis (FFIA) method was developed in this study to quantify volumetric characteristics of the asphalt

mastic phase in foamed asphalt mixes. A series of mapping rules from the 2D distribution of visible asphalt mastic on fracture faces to the 3D asphalt mastic distribution in foamed asphalt mixes were established. A standard procedure to acquire fracture images and perform image analysis, as well as an image processing software package was developed. Recommended laboratory testing conditions for FFIA were suggested. A new parameter, Fracture Face Asphalt Coverage (FFAC) was proposed as a simple quantitative indicator of asphalt mastic distribution. Most of the examples presented in this thesis work involved Fracture Face Image Analysis, and it was found to provide great insight into the stabilizing mechanisms of foamed asphalt.

Apart from quantitative Fracture Face Image Analysis for research, empirical visual inspection on fracture faces can be performed by experienced design engineers to diagnose mix problems, for which guidelines were suggested.

7.3   Strength Behavior of Foamed Asphalt Mixes

The strength behavior of foamed asphalt mixes without the addition of active fillers was evaluated for a number of different mix designs, under different conditions with different test methods. Highlights of the findings include:

Soaked vs. unsoaked strength

The asphalt mastic phase and the mineral filler phase both contribute to the tensile strength of

foamed asphalt mixes, but the proportions of their contributions are different under the unsoaked and soaked conditions. Under the unsoaked conditions, the mineral filler phase may contribute most of the measured tensile strength, but its strength is extremely sensitive to water conditioning. On the other hand, under the soaked condition, the majority of the measured tensile strength is attributed to the bonding provided by the asphalt mastic phase. The soaked condition was recommended for mix evaluation because the main goal of mix design is to evaluate and optimize the stabilizing effects of foamed asphalt, and in the field soaked or partially soaked conditions are inevitable. This is significantly different from the prevailing practice, which primarily uses unsoaked strength tests, or the ratio of soaked to unsoaked strength which masks the actual soaked strength for mix design.

Relative density or compaction effort

High compaction effort was found to greatly enhance the tensile strength of foamed asphalt mixes. Fracture Face Image Analysis found that compaction improves bonding strength between asphalt mastic droplets and the aggregate skeleton. Applying high compaction effort in construction of FDR-foamed asphalt projects is highly encouraged.

Asphalt grade

Two asphalt binders from the same source, with similar foaming characteristics but different grades (or equivalently different viscosities) were evaluated. It was found that mixes treated with the softer (or less viscous) binder had higher tensile strength. Fracture Face Image

Analysis found that although the binder with higher viscosity itself might have higher strength, softer binder can disperse into and stabilize granular materials more effectively. The direct implication to engineering practice is that if different asphalt binders with similar foaming characteristics are available, the softer one should be chosen.

Effects of PAP gradation

It was found that if a PAP contains a high percentage of fines, a large proportion of the fines are not able to be bonded by foamed asphalt. A continuous mineral filler phase is formed, which makes foamed asphalt mixes very weak under soaked conditions. Consequently PAP materials with high fines contents are not desired.

7.4 Stiffness Behavior of Foamed Asphalt Mixes

The stiffness of foamed asphalt mixes is an important parameter for pavement design. This study found that stiffness, characterized by the resilient modulus of foamed asphalt mixes is highly dependent on the stress state. Many laboratory test methods have been employed to evaluate resilient modulus of foamed asphalt mixes as reported in the literature. Among these test methods, the indirect tensile resilient modulus test and the free-free resonant column test fail to yield stress states representative of the field stress states, and consequently the test results of these methods are of a minimal value. Because the resilient modulus values of these two test methods are usually unrealistically high, they might lead to unsafe designs.

On the other hand, the stress states yielded by the triaxial resilient modulus test and the flexural beam test are clearer, and each can partially represent the field stress state under traffic loading. The results of the triaxial resilient modulus tests indicate that foamed asphalt transforms material behavior from that of typical unbound granular materials towards that of partially asphalt-bound materials. Foamed asphalt treatment does not necessarily improve the absolute values of stiffness, but makes resilient modulus more loading rate dependent and less stress dependent. The flexural beam test results show that foamed asphalt mixes without active filler lose most of the tensile stiffness after soaking. However, typical triaxial resilient modulus tests ignore this problem, which may lead to nonconservative design. Field observations supporting this conclusion was documented in Fu et al. (2009b), but not recorded in this thesis.

7.5   Curing Mechanism of Foamed Asphalt Mixes

Multiple types of laboratory tests as well as direct fracture face inspection were employed to reveal the curing mechanisms of foamed asphalt mixes. It was found that bonding provided by the asphalt mastic phase develops as the mixing/compaction water evaporates, and only fully develops once this water is no longer present. This bonding of asphalt mastic, once formed, is only moderately sensitive to water conditioning. It is therefore crucial to allow the initial mixing/compaction water to evaporate from the recycled layer before the HMA surface layer is placed, and to ensure that the road has adequate drainage. Portland cement was shown to be very effective in improving early strength, stiffness and permanent deformation resistance

development.   It is advisable to use appropriate active fillers in conjunction with foamed asphalt

to allow the constructed road to be open to traffic early, but not so much to cause shrinkage

cracks.

Two standard curing conditions are recommended for project level mix design.   One of them

creates an optimistic environment for water evaporation, and is used to evaluate and optimize the

long term effectiveness of foamed asphalt stabilization.   Under this curing/test condition, active

fillers (e.g. portland cement) should be excluded from the mix design, to enable evaluating and

optimizing the stabilization effects of foamed asphalt.   The other curing condition creates a

conservative environment for evaporation to evaluate and optimize the effectiveness of active

fillers in improving early strength.   In a mix design procedure, the use of foamed asphalt (in

terms of the binder type, foaming parameters, asphalt content, etc.) should be determined under

the first curing/test condition, and the use of active fillers under the second condition.

7.6   Effects of Mixing Moisture Content on Foamed Asphalt Mix Microstructure and Properties

The study reported in Chapter 6 provides the first quantitative results regarding why and how

mixing moisture content influences the asphalt distribution pattern in foamed asphalt mixes,

which was made possible by the newly developed Fracture Face Image Analysis technique.   It

was found that loose (or uncompacted) aggregate materials transition between different

agglomeration states as the mixing moisture content increases. When the moisture content is high, fines in the capillary state are suspended in pore fluid and form a paste like substance coating larger aggregate particles. Granular materials in this agglomeration state cannot yield optimum asphalt dispersion due to the low surface area per mass exposed to asphalt coating. In engineering practice for FDR-foamed asphalt, a balance between compactability and asphalt dispersion should be sought. A very important contribution of this study was to dismiss the idea proposed by others that high moisture content in granular materials can aid foamed asphalt dispersion.

7.7   Recommendations for Future Research

The following recommendations are made for future research on full depth reclamation with foamed asphalt based on the conclusions and limitations of this thesis work.

This study used PAP materials from two sites in California. The validity of the conclusions drawn in this study should be tested with a wider range of materials.

Most laboratory testing in this study was performed on newly mixed and cured specimens. Foamed asphalt stabilized base layers in real pavements inevitably deteriorate under the action of traffic loading and the environment. The evolution of properties of field materials need to be studied and laboratory procedures to reproduce these field conditions and evaluate material performance under these conditions need to be developed.

Better performance models for foamed asphalt stabilized materials should be developed and calibrated with both laboratory and field data. These models will not only enable more reasonable design, they will also make life cycle cost analysis and comparison between different road rehabilitation strategies more accurate.

This thesis study primarily focused on the characteristics of the asphalt mastic phase and its contribution to material behavior. The effects of various available active filler types, especially their impact on long term pavement performance are important considerations, and need further investigation.

High variability in tested foamed asphalt stabilized material properties was observed during this study. This variability needs to be quantified and related to the variability in the parent materials and that in the mixing and specimen fabrication procedures.

Bibliography

Acott, S.M. (1980). *The Stabilisation of a Sand by Foamed Asphalt – a Laboratory and Field Performance Study.* Master's thesis, University of Natal, South Africa.

Al-Rousan, T., Masad, E., Tutumluer, E., and Pan, T. (2007). Evaluation of image analysis techniques for quantifying aggregate shape characteristics. *Construction and Building Materials*, 21(5): 978-990.

Asphalt Academy, South Africa. (2002). *The Design and Use of Foamed Bitumen Treated Materials (Interim Technical Guidelines, TG2)*. CSIR Transportek, Pretoria, South Africa.

Asphalt Institute. (1974). *Mix Design Methods for Asphalt Concrete and Other Hot-Mix Types* (*MS-2*). Lexington, Kentucky.

Bowering, R.H. (1970). Upgrading marginal road-building materials with foamed bitumen. *Highway Engineering in Australia*, Mobil Oil Australia, Melbourne South.

Bowering, R. H., and Martin, C. L. (1976). Foamed bitumen production and application of mixtures: evaluation and performance of pavements. Journal of the Association of Asphalt Paving Technologists, 45: 453-477.

Braz, D., da Motta, L.M.G., and Lopes, R.T. (1999). Computed tomography in the fatigue test analysis of a asphaltic mixture. *Applied Radiation and Isotopes*, 50: 661-671.

Brennen, M., Tia, M., Altschaefl, A., and Wood, L.E. (1983). Laboratory investigation of the use of foamed bitumen for recycled bituminous pavements. *Transportation Research Record*, 911: 80-87.

California Department of Transportation. (2008). *California State of the Pavement Report, 2007*. The California Department of Transportation, Division of Maintenance.

Castedo, F.L.H. and Wood, L.E. (1982). Stabilization with foamed asphalt of aggregates commonly used in low-volume road. *Transportation Research Record*, 898: 297-302.

Chiu, C.T. and Lewis, A.J.N. (2006). A study on properties of foamed-asphalt-treated mixes. *Journal of Testing and Evaluation*, 34(1): 5-10.

Collings, D., Lindsay, R., and Shunmugam, R. (2004). LTPP exercise on a foamed bitumen treated base - evaluation of almost 10 years of heavy trafficking on MR 504 in Kwazulu-Natal. *Proceedings of the 8th Conference on Asphalt Pavements for Southern Africa*: 468-499.

Csanyi, L.H. (1960). Bituminous mixes prepared with foamed asphalt. *Iowa Engineering Experiment Station Bulletin*, no.19, Ames, IA, Iowa State University.

Ebels, L.J. and Jenkins, K.J. (2006). Determination of material properties of bitumen stabilised materials using Tri-axial testing. *Proceedings of the 10th International Conference on Asphalt Pavements*, Quebec City, Canada.

Efrem, G.E. (2000). *Stabilisation of Cinder with Foamed Bitumen and Cement and Its Use as (Sub)base for Roads*. MSc thesis, International Institute for Infrastructural, Hydraulic and Environmental Engineering, Delft, Netherlands.

Elseifi, M.A., Al-Qadi, I.L., Yang, S.-H., and Carpenter, S.H. (2008). Validity of asphalt binder film thickness concept in hot-mix asphalt. *Transportation Research Record*, 2057: 37-45.

Eriksen, K. and Wegan, V. (1993). Optical methods for the evaluation of asphalt concrete and polymer-modified bituminous binders. *5th Eurobitume Congress*, Stockholm, pp 705-708.

Fredlund, D.G. and Rahardjo, H. (1993). *Soil Mechanics for Unsaturated Soils*. Wiley, New York.

Fu, P. and Harvey, J.T. (2007). Temperature sensitivity of foamed asphalt mix stiffness: field and lab study. *International Journal of Pavement Engineering*, 8(2): 137-145.

Fu, P., Steven, B.D., Harvey, J.T., and Jones, D. (2009). Relating laboratory foamed asphalt mix resilient modulus tests and field measurements. *Road Materials and Pavement Design*, 10(1): 155-185.

Harvey, J.T., Chong, A., and Roesler, J.R. (2000). *Climate Regions for Mechanistic-Empirical*

Pavement Design in California and Expected Effects on Performance. Report prepared for California Department of Transportation, Pavement Research Center, CAL/APT Program, Institute of Transportation Studies, University of California, Berkeley, UCPRC-RR-2000-07.

Hodgkinson, A. and Visser, A.T. (2004). The role of fillers and cementitious binders when recycling with foamed bitumen or bitumen emulsion. *Proceedings of the 8th Conference on Asphalt Pavements for Southern Africa*, Sun City, South Africa, p. 512-521.

Jenkins, K.J. (2000). *Mix Design Considerations for Cold and Half-Cold Bituminous Mixes with Emphasis on Foamed Bitumen*. Ph.D. thesis, University of Stellenbosch, South Africa.

Jenkins, K.J., Van de Ven, M.F.C, Molenaar, A.A.A., and de Groot, J.L.A. (2002). Performance prediction of cold foamed bitumen mixes. *Proceedings of the 9th International Conference on Asphalt Pavements*, Copenhagen, Denmark, 2002.

Jenkins, K.J., Robroch, S., Henderson, M.G, Wilkinson, J., and Molenaar, A.A.A. (2004). Advanced testing for cold recycling treatment selection on N7 near Cape Town. *Proceedings 8th Conference on Asphalt pavements for Southern Africa*: 537-552.

Jenkins, K.J., Long, F.M., and Ebels, L.J. (2007). Foamed bitumen mixes = shear performance? *International Journal of Pavement Engineering*, 8(2): 85-98.

Jones, D., Fu, P., and Harvey, J.T. (2008). *Full-Depth Recycling with Foamed Asphalt*. Research Report RR-2008-07, University of California Pavement Research Center, Davis and Berkeley, California.

Khweir, K. (2007). Performance of foamed bitumen-stabilised mixtures. *Proceedings of the Institution of Civil Engineers: Transport*, 160(2): 67-72.

Kim, Y. and Lee, H.D. (2006). Development of mix design procedure for cold in-place recycling with foamed asphalt. *Journal of Materials in Civil Engineering*, 18(1): 116-124.

Kose, S., Guler, M., Bahia, H.U., and Masad, E. (2000). Distribution of Strains Within Hot-Mix Asphalt Binders: Applying Imaging and Finite-Element Techniques. *Transportation Research Record*, 1728: 21-27.

Lancaster, J., McArthur, L., and Warwick, R. (1994). VICROADS experience with foamed bitumen stabilisation. *Proceedings of the 17th ARRB Conference*, Vol. 17, Part 3. Gold Coast,

Australia, p.193-211.

Lane, B. and Kazmierowski, T. (2005). Implementation of cold in-place recycling with expanded asphalt technology in Canada. *Transportation Research Record,* 1905: 17-24.

Lee, D.Y. (1981). Testing marginal aggregates and soils with foamed asphalt. *Journal of the Association of Asphalt Paving Technologists*, 50: 211-250.

Li, S. and Wang, G. (2008). *Introduction to Micromechanics and Nanomechanics*. World Scientific Publishing Co. Pte. Ltd., Singapore.

Little, D.N., Button, J.W., and Epps, J.A. (1983). Structural properties of laboratory mixtures containing foamed asphalt and marginal aggregates. *Transportation Research Record*, 911: 104-113.

Long, F.M. and Brink, A.C. (2004). *2nd Level Analysis on the HVS Data for the Southbound Carriageway of the N7 (TR11/1)*. Contract Report CR-2004/12, Transportek, CSIR, South Africa.

Long, F.M. and Theyse, H.L. (2002a). *Second Level Analysis of HVS Data from Road P243/1*. Contract Report CR-2002/23, Transportek, CSIR, South Africa.

Long, F.M. and Theyse, H.L. (2002b). *Laboratory Testing for the HVS Sections on Road P243/1*. Contract Report CR-2001/22, Transportek, CSIR, South Africa.

Long, F.M. and Theyse H.L. (2004). Mechanistic Empirical Structural Design Models for Foamed and Emulsified Bitumen Treated Materials. *Proceedings of the 8th Conference on Asphalt pavements for Southern Africa*, Sun City, South Africa, p. 553-568.

Long, F.M. and Ventura D.F.C. (2004). *Laboratory Testing for the HVS Sections on the N7 (TR11/1)*. Contract Report CR-2003/56, Transportek, CSIR, South Africa.

Lu, N., Wu, B.L., and Tan, C.P. (2007). Tensile strength characteristics of unsaturated sands. *Journal of Geotechnical and Geoenvironmental Engineering*, 133(2): 144-154.

Lu, N. and Likos, W.J. (2004). *Unsaturated Soil Mechanics*, New York, NY: Wiley.

Maccarrone, S., Holleran, G., Leonard, D.J. and Dip, S.H. (1994). Pavement recycling using foamed bitumen. *Proceedings 17th Australian Road Research Board Conference*, Vol. 17,

Part 3, Gold Coast, Australia, p. 349-365.

Marquis, B., Bradbury, R. L., Colson, S., Malick, R. B., Nanagiri, Y. V., Gould, J.S., O'Brien, S. and Marshall, M. (2003). Design, construction and early performance of foamed asphalt full depth reclaimed (FDR) pavement in Maine. *Compendium of Papers CD-ROM the 82th Annual Meeting of Transportation Research Board*.

Masad, E., Muhunthan, B., Shashidhar, N., and Harman, T. (1999). Internal structure characterization of asphalt concrete using image analysis. *Journal of Computing in Civil Engineering*, 13(2): 88-95.

Masad, E. (2004). X-ray computed tomography of aggregates and asphalt mixes. *Materials Evaluation*, 62(7): 775-783.

Mehrotra, V.P. and Sastry K.V.S. (1980). Pendular bond strength between unequal sized spherical particles. *Powder Technology*, 25: 203–214.

Mitchell, J.K. and Soga, K. (2005). *Fundamentals of Soil Behavior* (3rd Edition). Hoboken, N.J. : John Wiley & Sons.

Muthen, K.M. (1998). *Foamed Asphalt Mixes, Mix Design Procedure*. Report CR-98/077, CSIR Transportek, South Africa.

Nataatmadja, A. (2001). Some characteristics of foamed bitumen mixes. *Transportation Research Record*, 1767: 120-125.

Newitt, D.M. and Conway-Jones, J.M. (1958). A contribution to the theory and practice of granulation. *Transactions of the Institution of Chemical Engineers*, 36: 422-441.

Pan, T., Tutumluer, E., and Anochie J. (2006). Aggregate morphology affecting resilient behavior of unbound granular materials. *Transportation Research Record*, 1952: 12-20.

Proctor, R.R. (1933). Fundamental principles of soil compaction. *Engineering News Record*, 111: 245-248, 286-289 and 348-351.

Raffaelli, D. (2004). *Foamed Asphalt Base Stabilization*. Technology transfer program, Institute of Transportation Studies, University of California, Berkeley.

Ramanujam, J.M. and Jones, J.D. (2007). Characterization of foamed-bitumen stabilization.

International Journal of Pavement Engineering, 8(2): 111-122.

Roberts, F.L., Engelbrecht, J.C., and Kennedy, T.W. (1984). Evaluation of recycled mixtures using foamed asphalt. *Transportation Research Record*, 968: 78-85.

Romanoschi, S.A., Hossain, M., Gisi, A., and Heitzman M. (2004) .Accelerated pavement testing evaluation of the structural contribution of full-depth reclamation material stabilized with foamed asphalt. *Transportation Research Record*, 1896: 199-207.

Ruckel, P.J., Acott, S.M., and Bowering, R.H. (1983). Foamed-asphalt paving mixtures: preparation of design mixes and treatment of test specimens. *Transportation Research Record*, 911:88-95.

Sakr, H.A. and Manke, P.G. (1985). Innovations in Oklahoma foam mix design procedures. *Transportation Research Record*, 1034: 26-34.

Saleh, M. (2004). New Zealand experience with foam bitumen stabilization. *Transportation Research Record*, 1868: 40-49.

Saleh, M.F. and Herrington P. (2003). *Foamed Bitumen Stabilisation for New Zealand Roads.* Transfund New Zealand Research Report No. 250.

Seed, H.B. and Chan, C.K. (1959). Structure and strength characteristics of compacted clays. *ASCE Journal of Soil Mechanics and Foundation Engineering*, 85(5): 87-128.

Taylor, M.A., Garboczi, E.J., Erdogan, S.T., and Fowler, D.W. (2006). Some properties of irregular 3-D particles. *Powder Technology*, 162(1):1-15.

Theyse, H.L. and Mancotywa, W.S. (2003). *First Level Analysis Report: Second Phase HVS Testing of the Emulsion and Foamed Bitumen-Treated Sections on Road P243/1 Near Vereeniging*. Contract Report CR-2001/53, Transportek, CSIR, South Africa.

Theyse, H.L. (2004). *First-Level Analysis Report: HVS Testing of the Foamed-Bitumen-Treated Crushed Stone Base on the Slow Lane of the Southbound Carriageway of the N7 Near Cape Town*. Contract Report CR-2003/23, Transportek, CSIR, South Africa.

Twagira, M.E., Jenkins, K.J., and Ebels, L.J. (2006). Characterisation of fatigue performance of selected cold bituminous mixes. *Proceedings of the 10th International Conference on Asphalt*

Pavements, Quebec City, Canada.

Ullidtz, P. (2001). Distinct element method for study of failure in cohesive particulate media. *Transportation Research Record*, 1757: 127-133.

Uzan, J. (1985). Characterization of granular material. *Transportation Research Record*, 1022: 52-59.

Wang, L.B., Frost J.D., and Lai, J.S. (2004). Three-dimensional digital representation of granular material microstructure from X-ray tomography imaging. *Journal of Computing in Civil Engineering*, 18(1): 28-35.

Wirtgen GmbH. (2004). *Wirtgen Cold Recycling Manual*. Windhagen, Germany.

Yue, Z.Q., Bekking, W., and Morin, I. (1996). Application of digital image processing to quantitative study of asphalt concrete microstructure. *Transportation Research Record*, 1492: 53-60.